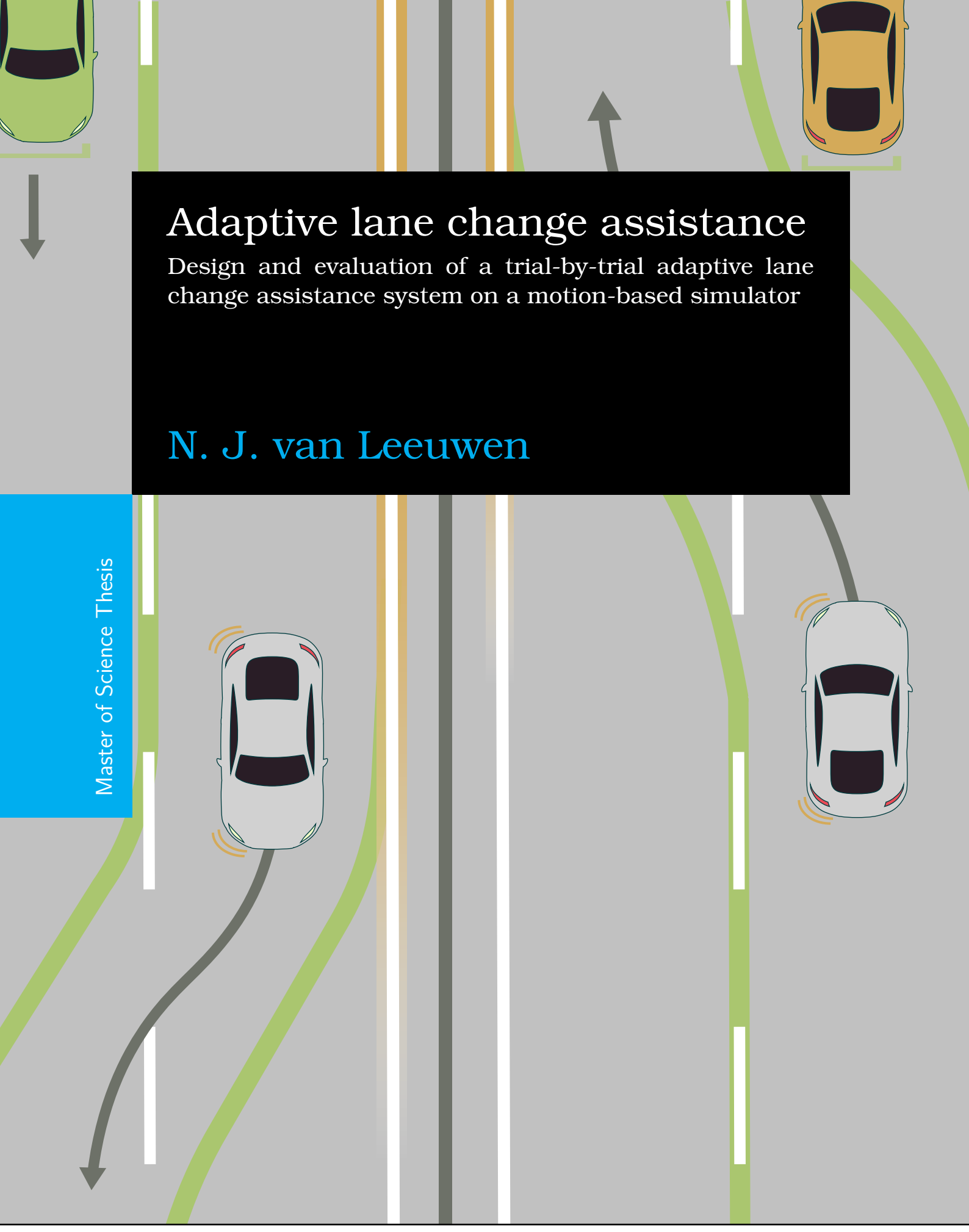

Adaptive lane change assistance

Design and evaluation of a trial-by-trial adaptive lane change assistance system on a motion-based simulator

N. J. van Leeuwen

Master of Science Thesis

TU Delft Delft University of Technology

Faculty of Mechanical, Maritime and Materials Engineering

Adaptive lane change assistance

Design and evaluation of a trial-by-trial adaptive lane change assistance system on a motion-based simulator

Master of Science Thesis

For the degree of Master of Science in Vehicle Engineering at Delft University of Technology

N. J. van Leeuwen

May 24, 2021

Faculty of Mechanical, Maritime and Materials Engineering (3mE)
.
Delft University of Technology

This thesis is supported by Cruden B.V. Their cooperation is hereby gratefully acknowledged.

Abstract

This study proposes a Lane Change Assistance (LCA) system that provides haptic guidance during lane changes. This system is fully integrated with Lane Keeping Assistance (LKA) functionality to provide continuous lateral support during highway driving. Two different system configurations of this LCA are investigated. One is a generalized LCA that provides lane change reference trajectories based on a fixed lane change duration value of 4 seconds. The other is an adaptive LCA that provides personalized lane change reference trajectories through trial-by-trial adaptation to lane change duration of previously driven lane changes. The effects of these systems with respect to mental workload, lateral control performance and user acceptance are investigated. This is observed in an experiment with three different driving sessions for each participant. A manual driving session, a driving session in which the generalized LCA is active and a driving session in which the adaptive LCA is active. The experiments are conducted on a 6 Degrees of Freedom (DoF) motion-based simulator with 34 participants, driving in a three-lane highway simulation environment with a scripted traffic scenario. To measure mental workload, an auditory cognitive secondary N-back task is introduced. The results show that the introduction of a generalized LCA or adaptive LCA does not have significant influence on mental workload compared to the manual driving session. When the adaptive LCA is introduced, lateral control performance is enhanced compared to the generalized LCA and manual driving. Additionally, user acceptance expressed as subjective usefulness is increased by introducing the adaptive LCA compared to the generalized LCA. Furthermore, inter-driver variability of the lateral control performance during lane changes is reduced by the proposed trial-by-trial adaptive LCA system compared to the generalized LCA system and manual driving.

Glossary

List of Acronyms

ACC	Adaptive Cruise Control
ADAS	Advanced Driver Assistance Systems
ANOVA	Analysis Of Variance
ASM	Automotive Simulation Model
CC	Cruise Control
DoF	Degrees of Freedom
DI	Discrimination Index
HSC	Haptic Shared Control
IQR	Interquartile Range
LC	Lane Change
LCA	Lane Change Assistance
LKA	Lane Keeping Assistance
LQR	Linear Quadratic Regulator
SAE	Society of Automotive Engineers
SAT	Satisfaction Score
SRR	Steering Reversal Rate
TLC	Time to Lane Crossing
TTC	Time to Collision
USE	Usefulness Score

List of Symbols

α	[-]	Cronbach's coefficient of reliability
$\boldsymbol{x}$	[-]	State vector used for state-feedback
ΔY	$[m]$	Lateral error
ΔY_p	$[m]$	Lateral preview error
τ	$[s]$	Lane change duration
τ_{avg}	$[s]$	Moving average lane change duration
θ	$[deg]$	Steering wheel angle
θ_c	$[deg]$	Steering wheel angle desired by the controller
θ_d	$[deg]$	Steering wheel angle desired by the driver
θ_{er}	$[deg]$	Steering wheel angle error between controller and driver
θ_{filt}	$[deg]$	Steering wheel angle filtered by second order Butterworth filter
θ_{gap}	$[deg]$	Steering wheel angle gap value for SRR
a_{max}	$[m/s^2]$	Maximum desired lateral acceleration
i_{st}	[-]	Steering ratio
j_{max}	$[m/s^3]$	Maximum desired lateral jerk
k_{hsc}	$[deg/Nm]$	Haptic Shared Control stiffness
t_b	$[s]$	One-sided blending time hyperbolic tangent blending function
T_{lca}	$[Nm]$	Steering wheel torque applied by lane change assistance
T_{mod}	$[Nm]$	Steering wheel torque applied from the multibody vehicle model
T_{tot}	$[Nm]$	Steering wheel torque applied to the simulator's steering column
w	$[m]$	Lane width
δ_{fc}	$[deg]$	Front wheel steering angle demanded by the LQR controller

Table of Contents

List of Figures

List of Tables

Acknowledgements

This thesis marks the end of my time as a student of the TU Delft. In these years I have been privileged with many enriching experiences, both inside and outside the academic field. This thesis and the steps leading up to it would not have been possible without the support of the people surrounding me, therefore I would like use this section to express my gratitude.

First of all, I would like to thank my supervisors Barys Shyrokau and David Abbink for guiding me through the process. Barys, thank you for supporting me in every phase of this research. I could always rely on your foreseeing advice, pragmatic feedback and encouraging words. David, thank you for all our fruitful discussions, providing me with self-reflection and inspiring me with new ideas. I am fortunate to have received guidance from two professors with different fields of expertise, narrowing down or broadening my perspective when needed.

Furthermore, I would like to thank my daily supervisor Christiaan Koppel, who always made time free whenever I needed a critical reflection on my work or reasoning. It was great having you as a sparring partner, providing valuable feedback in an informal manner. In addition to this, I would like to thank all the colleagues at Cruden for welcoming me, sharing insights and providing good company and laughter. In specific, thank you Edwin de Vries for helping me parametrize the vehicle model and writing a scientific paper. Thank you Frank Drop for helping to create a secondary task to measure workload. Thank you Omar Hassanain and Robbert van Hassel for helping me understand functionalities of the Panthera and dSpace software, enabling me to integrate my system and run simulations. Finally, thank you Bas Everts and Tim van Wees for assisting me in understanding and configuring the simulation hardware, ensuring a working setup during the experiments and the preparations thereof.

I would like to thank my loving family and all my dear friends who have provided an incredible amount of support throughout all the years of my studies. Celebrating good times together and providing a listening ear when needed has been essential for me to complete this academic trajectory. A special thanks to all the family, friends and colleagues who have taken the time and effort to participate in my experiment. This research would not have been as valuable without experimental validation, so I am very grateful for your contribution.

Finally, I would like to thank my girlfriend Annelot who has been my tower of strength and has enabled me to persist. Without her I would not be where I am right now and I am forever grateful for the faith and patience she has given to me. The last mile is the longest one and the past year has not been easy, but together we have made the best of it. It proves once again how resilient our relationship is and that after ten years I still love you more every day.

"Intelligence is the ability to adapt to change." — *Stephen Hawking*

Chapter 1

Conference Paper

This conference paper is submitted for publication at the Driving Simulator Conference 2021. The version that is submitted to the DSC 2021 can be found in Appendix E.

1-1 Introduction

To enable a transition from automation level 2 to level 3, as defined by the Society of Automotive Engineers (SAE), it is important to consider integration of Advanced Driver Assistance Systems (ADAS). Level 2 is defined as partial automation, in which the driver is supported by several automated functions. Level 3 is defined as conditional automation, in which the full driving task is automated under certain conditions [6]. Most currently available vehicles are partially automated and have Lane Keeping Assistance (LKA) systems installed that do not provide support during lane changes. Instead, lane keeping functionality is switched off when the indicator light is engaged.

Furthermore, mental workload is found to increase significantly during a Lane Change (LC) maneuver [1], as shown in Figure 1-1. Therefore, the goal of this research is to design a system that can mitigate this increase of mental workload, thus enhancing safety and comfort during lane changes. To achieve this goal, this study proposes a Lane Change Assistance (LCA) system that provides haptic support during lane changes. This system is completely integrated with an LKA system to enable continuous lateral support during highway driving.

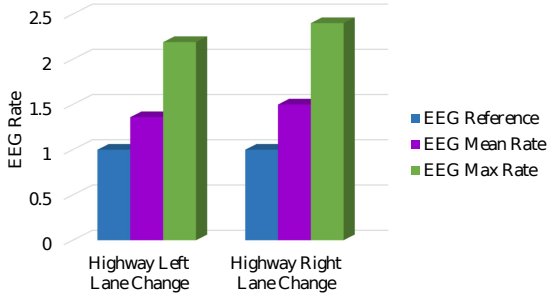

Figure 1-1: Mental workload measured by EEG, expressed as reference value 1 second prior to- and as mean and maximum value during lane changes, adapted from Kim et al. [1]

The increasing amount of installed ADAS in modern vehicles require an effective collaboration between these systems and the driver. Haptic Shared Control (HSC) is a commonly encountered solution to balance the control authority between ADAS and drivers [7]. To enhance smooth collaboration [8] and increase user acceptance [9] of such an HSC system, adaptation to a driver's personal preferences is desirable. Furthermore, adaptation to individual driving style can enhance usability and comfort, hence preventing disuse of the system [10]. This can be done by implicit or explicit personalization, adapting either to observed user data or explicitly stated preference settings, respectively.

Implicit personalization is expected to be more effective, since up to 67% of drivers have been shown to incorrectly identify their own driving style when explicitly stating their preferred driving style [11]. Driving behaviour varies widely between drivers, known as inter-driver variability, but also within a driver, known as intra-driver variability [12]. Since it is shown that there is a significant intra-driver modeling uncertainty when observing driving behaviour during two hours of lane keeping [13], continuous adaptation is expected to be more effective than implicit or explicit personalization.

In this study, an LCA system is designed that adapts its reference trajectory to the moving average of previous lane change durations. This is implemented by means of trial-by-trial adaptation, which has successfully personalized trajectories for haptic assistance during a non-driving task [14]. The effect of this adaptive LCA system is investigated by comparing it to manual driving and driving with a generalized LCA, which is based on a fixed value for average lane change duration. The research question is formulated as follows:

Does trial-by-trial adaptation to lane change duration of a haptic lane change assistance system reduce mental workload and increase control performance during highway driving?

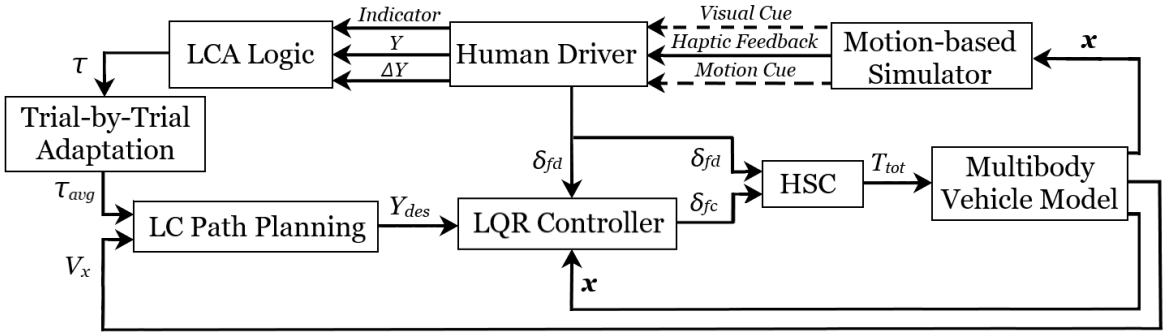

Figure 1-2: Schematic of the designed Lane Change Assistance system

This leads to the following hypotheses:

I. A trial-by-trial adaptive lane change assistance system reduces mental workload of drivers during highway driving.

II. A trial-by-trial adaptive lane change assistance system increases lateral control performance during highway driving.

To test these hypotheses, the following research objectives have been set:

1. Design a reference path planning algorithm that enables adaptation to individual preferences.
2. Design a path-following control algorithm that minimizes mental workload, lateral error and control effort.
3. Design a suitable LCA logic to switch from lane keeping to lane changing functionality and vice-versa.
4. Determine a definition of lane change duration that can capture the lane change behaviour of individual drivers, such that the trial-by-trial adaptation can be applied to it.
5. Design an experiment and choose corresponding metrics to assess the effect of the LCA system and the effect of the trial-by-trial adaptation.

1-2 LCA System Design

The novel adaptive LCA system is designed by integrating the concept of trial-by-trial adaptation in an LCA system. The planned reference path is adapted to the duration of previous LC maneuvers. The reference path is generated by a double fifth order polynomial path planning algorithm and subsequently fed to a path-following Linear Quadratic Regulator (LQR) controller. The state-space equations of the lateral controller are formulated using a bicycle model and driver model, the resulting gains are scheduled with longitudinal velocity. All subsystems are schematically shown in Figure 1-2.

Trial-by-Trial Adaptation

Intra-driver variability has been shown to be greater than inter-driver variability during long driving sessions [13]. Therefore, a learning-based adaptive system using current driving information is preferred rather than a personalized system that statically characterizes ones driving style based on historical data. It is shown that trial-by-trial adaptation reduces control effort and torque conflict without degrading the performance in a non-driving task [14]. Therefore, this method is chosen for implementation in the proposed LCA to reduce mental workload during an LC maneuver, increase user acceptance and enhance lateral control performance. The trial-by-trial adaption is based on the duration

of previous LC maneuvers and is applied to the planned reference path of the LCA system. The LC maneuver duration resulting from the collaborative steering behaviour on the HSC interface are registered by the LCA logic, stored and used to compute a moving average over 10 trials. This computed value is subsequently used to determine the desired duration for the reference path planning of the next LC maneuver. The registration of an LC maneuver in the LCA logic is initiated by the trigger of the indicator light and is considered completed when the absolute value of both the lateral error $\Delta Y = Y - Y_{des}$ and lateral preview error ΔY_p, shown in Equation 1-9, are within the lateral margin of 1 meter from the target lane center. The lane change is aborted when the indicator light is switched off before crossing the lane boundary, after which the lane keeping functionality is continued in the original lane.

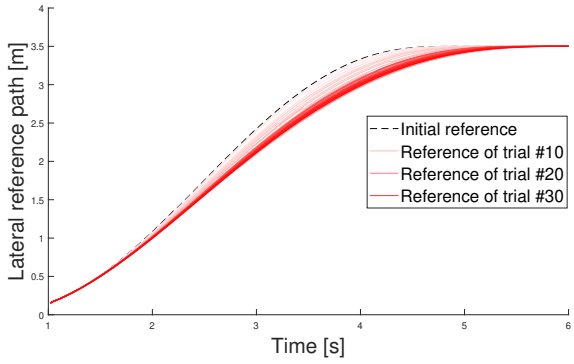

Figure 1-3: Reference path planning of the trial-by-trial adaptive LCA for the 37 trials of participant 25

Haptic Shared Control

The HSC algorithm is designed according to the virtual spring model [15], which is expressed in Equation 1-2. The HSC stiffness k_{hsc} is tuned for lateral control performance and user acceptance to a value of $k_{hsc} = 0.25$. The HSC interface of the steering wheel is used to combine the inputs of the driver and the LCA system as follows. First, the front wheel steering angle δ_{fc} resulting from the LQR controller is multiplied by the steering ratio i_{st} to obtain the steering wheel angle desired by the controller θ_c, shown in Equation 1-1. Subsequently, the measured steering input of the driver θ_d is subtracted to determine the steering wheel angle error θ_{er}. This angle is multiplied by the HSC stiffness to obtain the assistance torque T_{lca}. This assistance torque is added to the torque from the multi-body vehicle model T_{mod} to obtain the total torque T_{tot}, shown in Equation 1-3. The total torque is sent to the servomotor that provides torque to the simulator's steering column.

$$\theta_c = \delta_{fc} \cdot i_{st} \tag{1-1}$$

$$T_{lca} = k_{hsc} \cdot \theta_{er} = k_{hsc}(\theta_c - \theta_d) \tag{1-2}$$

$$T_{tot} = T_{mod} + T_{lca} \tag{1-3}$$

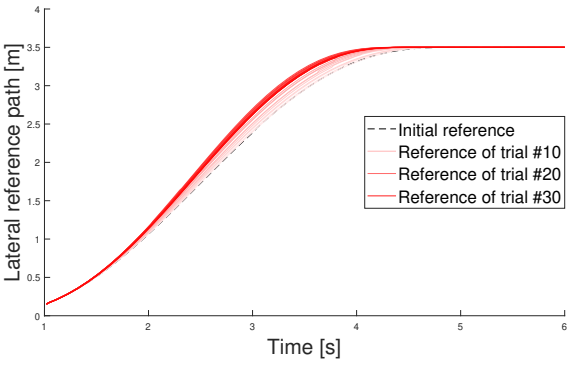

Figure 1-4: Reference path planning of the trial-by-trial adaptive LCA for the 34 trials of participant 34

Path Planning

The most commonly used method to plan the path of an LC maneuver is a fifth order polynomial. However, with a conventional fifth order polynomial replanning of the path is not possible. This could potentially lead to unsafe situations, therefore an adjustment is needed to enable the possibility to abort an

LC maneuver after initiation [16]. Furthermore, a human driver uses a higher lateral acceleration for steering out of the initial lane than for steering back into the target lane [17]. This asymmetric human steering behavior cannot be replicated by using a single quintic polynomial. By combining two different quintic polynomials, the asymmetric path can be generated to represent human LC maneuvers more accurately. Therefore, a double quintic polynomial [18] is implemented to determine the reference path for the path following controller.

$$\begin{aligned} s_1(t) &= c_0 + c_1\ t + c_2\ t^2 + c_3\ t^3 + c_4\ t^4 + c_5\ t^5 \\ s_2(t) &= c_6 + c_7\ t + c_8\ t^2 + c_9\ t^3 + c_{10}\ t^4 + c_{11}\ t^5 \end{aligned} \tag{1-4}$$

By defining the maximum desired lateral acceleration as $a_{max} = 1\ m/s^2$, the maximum desired lateral jerk as j_{max}= 1.5 m/s^3 and the lane width of w= 3.5 m, the two polynomials are solved with the symbolic toolbox of Matlab.

$$\begin{aligned} t_{a_{max}}(s_1) &= -\frac{2 \cdot c_4 \pm \sqrt{4 \cdot c_4^2 - 10 \cdot c_3 \cdot c_5}}{10 \cdot c_5} \\ t_{j_{max}}(s_1) &= -\frac{c_4}{5 \cdot c_5} \end{aligned} \tag{1-5}$$

The coefficients can be solved using Equation 1-5 for s_1 and s_2, under assumption that the maneuver is initiated without lateral acceleration, velocity or deviation from the lane center. Continuity is guaranteed by enforcing that the initial values of the second polynomial s_2 are equal to the final values of the first polynomial s_1. Since the LCA is integrated with an LKA, lane position metrics such as Time to Lane Crossing (TLC) are expected to cause conflict between the functionalities of these systems. Furthermore, most lane change intent prediction algorithms require eye-tracking or head movement tracking to accurately predict lane changes in real-time [19], which were not available for this study. Therefore, the manual trigger of the indicator light is used to switch from lane keeping to lane changing functionality.

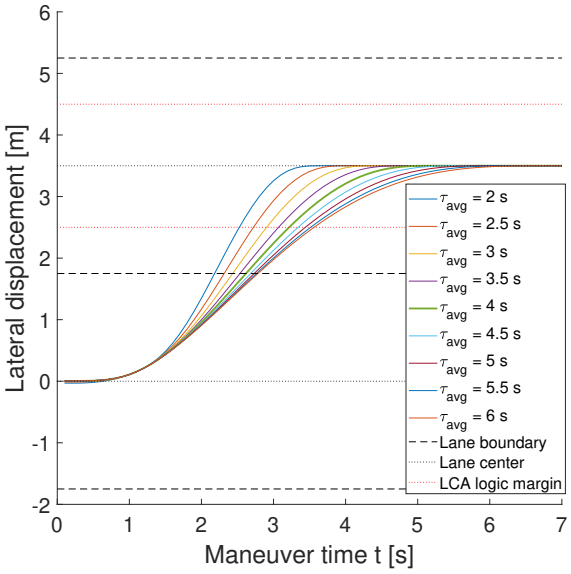

Figure 1-5: LC maneuver path planning for values of lane change duration τ_{avg} that were observed from 27 participants

To ensure smooth transition between the two polynomials, especially in the case of replanning, a hyperbolic tangent blending function with a one-sided blending time t_b= 0.5 seconds is used, as expressed in Equation 1-6. LC maneuver paths are computed for lane change duration values between τ= 1 and τ = 10 seconds and stored in a lookup table. This lookup table enables interpolation for the exact value for τ_{avg} whilst minimizing computational power during simulation. The computed reference paths are visualised in Figure 1-5 for the range of values between τ_{avg}= 2 and τ_{avg} = 6 seconds that were encountered during the experiment. The fixed value τ_{avg} = 4 that is used as lane change duration for the generalized LCA is highlighted. This value is based on the average lane change duration of 4.6 seconds and distribution found in literature [2], as can be seen in Figure 1-6.

$$\begin{aligned} s(t) = &\frac{1 - tanh(\frac{(t-\tau_{s_1})}{t_b})}{2} \cdot s_1(t) + \\ &\frac{1 + tanh(\frac{(t-\tau_{s_1})}{t_b})}{2} \cdot s_2(t) \end{aligned} \tag{1-6}$$

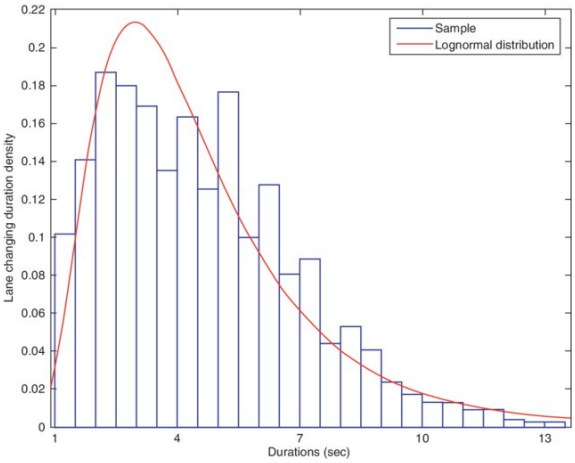

Figure 1-6: Distribution of lane change duration according to Toledo & Zohar [2]

Controller Design

A state feedback controller was selected as path-following controller, since it shows similar performance to state-of-the-art path-following algorithms in highway driving conditions [20]. The selected state feedback controller is a gain-scheduling LQR controller. State vector $\boldsymbol{x}$ containing 7 states is used to determine the additional steering angle δ_{fc} that the controller should provide to the front wheels of the vehicle, which is shown in Equation 1-7 to 1-9.

$$\delta_{fc} = \boldsymbol{k}(V_x) \cdot \boldsymbol{x} \tag{1-7}$$

$$\boldsymbol{x} = [V_y \quad \dot{\psi} \quad \psi \quad Y \quad \delta_{fd} \quad \dot{\delta}_{fd} \quad \Delta Y_p] \tag{1-8}$$

$$\Delta Y_p = Y_p - Y - t_p \cdot V_x \cdot \psi \tag{1-9}$$

The definition of lateral preview error ΔY_p is visualized by the schematic in Figure 1-7.

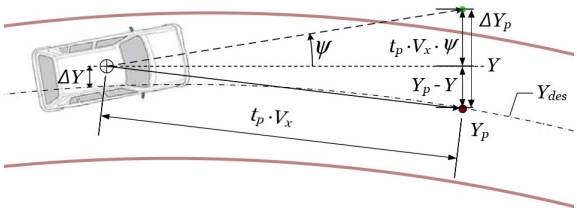

Figure 1-7: Schematic of the lateral preview error adapted from Wang et al. [3]

By considering multiple objectives including path-tracking error, driver's physical and mental workloads and control effort in the LQR controller, the cost function described in Equation 1-10 is minimized. J_1 represents the cost for lateral preview error, J_2 and J_3 represent the driver's mental and physical workload, respectively, and J_4 represents the control effort of the LCA system. To minimize computational power during simulation, the closed-loop control gains are calculated offline for a range of longitudinal velocities and integrated in the model by means of a lookup table. The control equations are formulated to schedule the gain based on longitudinal velocity. These control equations and the corresponding simplified vehicle and driver model are formulated in section A-1 of the Appendix.

$$J = \int_0^\infty (J_1 + J_2 + J_3 + J_4)\, dt \tag{1-10}$$

1-3 Experiment Design

Figure 1-8: A lane change maneuver during an experiment in the highway scenario of the 6 DoF motion-based simulator

To determine the effect of the adaptive and generalized LCA on mental workload, control performance and user acceptance, experiments with human participants in the loop are executed on a motion-based driving simulator. This 6 Degrees of Freedom (DoF) driving simulator utilizes a projected view of 210 degrees horizontally and 50 degrees vertically, two exterior rear-view mirrors, one interior rear-view mirror and a dashboard depicting all relevant dials.

The vehicle model used for the simulation in the experiment is a 13 DoF dSpace multibody Automotive Simulation Model (ASM) with the parametrization of a generic sedan. The selected signals of the vehicle model are recorded at a frequency of 100 Hz. The vehicle is equipped with Cruise Control (CC), which is set at 100 km/h and can be adjusted by the driver when necessary. A traffic scenario with 30 recurring entities is scripted such that the vehicles in the right lane drive at 90 km/h, 95 km/h in the center lane and 105 km/h in the left lane. The participants are instructed to adjust the longitudinal velocity as infrequently as possible and return to the right lane after overtaking, such that a high amount of LC maneuvers is encouraged.

Group	Session 1	Session 2	Session 3
A	Manual	Generalized	Adaptive
B	Generalized	Adaptive	Manual
C	Adaptive	Manual	Generalized

Table 1-1: Participant groups and corresponding sequence of system configuration in the different driving sessions

The experiment consists of 3 different sessions of 10 minutes on the driving simulator. A baseline measurement is recorded in a manual driving session, in which the driver has full lateral control and receives no assistance. Another session is driven with the generalized LCA system, for which the average value of a lane change duration τ was determined to be 4 seconds. A third session is driven with the adaptive LCA system, in which the lane change duration is determined by the LCA logic and implemented in the assistance by means of trial-by-trial adaptation. These three sessions are shuffled in sequence by using the Latin squares method to mitigate both learning effect and fatigue of the participants. The resulting three groups are classified as group A, group B and group C, which are shown in Table 1-1. The drivers are only informed if the driving session will be manual or with haptic assistance. They receive no prior information about the difference in LCA systems or which one is active.

Parameter	Mean	σ	Unit
Participant age	36.8	15.6	years
Driver's license	17.8	16.2	years
Average driving	4.52	3.90	hours/week
CC driving	2.18	3.22	hours/week
LKA driving	0.50	1.95	hours/week
Simulator driving	0.29	0.57	hours/week

Table 1-2: Demographic parameters and corresponding distribution of the 27 participants included in the results

The experiments were executed with 34 participants in total, of which five measurements contained corrupted signals. To ensure equal distribution over the three groups described in Table 1-1, two participants were eliminated randomly to obtain 9 participants per group, thus 27 in total. The demographics parameters of the 27 participants that are used for the analysis of the results are shown in Table 1-2. The measurements were rearranged such that the results can be presented per system configuration.

Metrics

Mental workload is measured during the complete duration of the experiment by means of an auditory N-back task [21], which is introduced as a cognitive secondary task.

In this task participants are asked to respond by tapping a touchscreen when the audio fragment of a recorded letter is identical to the letter played N trials before. N is chosen to be one, considering the substantial workload required for the driving task. Furthermore, it is shown that the 1-back auditory task results in lower variability of lateral position compared to the 0-back, 2-back and baseline measurement [22]. The resulting score is expressed as Discrimination Index (DI), which is calculated by using the hit rate H and false-positive rate F, as shown in Equation 1-11.

$$DI = \frac{1}{2} + sign(H-F) \cdot \frac{(H-F)^2 + abs(H-F)}{4 \cdot max(H,F) - 4HF}$$
$$H = \frac{\#hits}{\#signal\ trials} \qquad F = \frac{\#false\ positives}{\#noise\ trials} \tag{1-11}$$

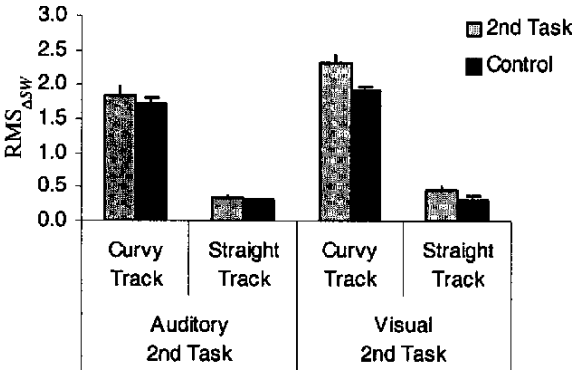

Figure 1-9: Secondary task influence on the variability of steering wheel angle [4]

Steering Reversal Rate (SRR) can be used as complement or alternative to lane position metrics to quantify lateral control performance [23]. It is easier to measure in real-world scenarios compared to lane position metrics, therefore SRR is often used as driving performance metric in field studies [24] [25]. Furthermore, the introduction of an auditory secondary task does not influence steering wheel angle variability, as is shown in 1-9, although it might influence mental workload [4]. Since a cognitive secondary task is introduced in this study, the corresponding parameters [23] are used to obtain the highest sensitivity for this scenario.

The steering wheel angle signal θ is filtered with a second order Butterworth filter with a 3dB cut-off frequency of 0.6 Hz to obtain θ_{filt}. If the difference in θ_{filt} of the current and previous time step is larger than the gap value θ_{gap}= 0.1 deg, it is registered as a reversal. These are expressed in SRR as reversals per minute. The SRR metric is also computed for the LC maneuvers only, by extracting the lane change sections of the steering wheel angle signal, shown in Appendix B-1.

To express user acceptance of the participants, a subjective van der Laan [26] questionnaire is used, in which the generalized and adaptive LCA system configurations are rated with respect to the manual driving session. The participants are requested to score the system configurations on 9 different aspects of the system, leading to a Usefulness Score (USE) and a Satisfaction Score (SAT). It is stated that Cronbach's coefficient of reliability α should be higher than 0.65 for the results to be valid. No prior knowledge about the LCA systems is provided to the participants to ensure unbiased results.

For all presented mean results, a linear mixed-effect model regression analysis is applied to obtain the statistical significance of the metrics. In this way, the individual participants were regarded as a random effect with no a-priori expectations. Since the data is obtained with repeated measurements of one individual participant and different system configurations, repeated-measures Analysis Of Variance (ANOVA) is more suitable than a one-way or two-way ANOVA. However, mixed-effect modeling is more robust against systematic inter-driver variability than repeated-measures ANOVA [27]. Since inter-driver variability is expected to be an important influence, linear mixed-effect model regression analysis is used to determine the statistical significance of results.

For all presented variance results, Levene's test of homoscedacity is applied to investigate the homogeneity of variances across system configurations. It is chosen over the two-sample F-test of equality of variance due to its robustness against non-normality in the data and the possibility to compare the variance of three system configurations. For both the linear-mixed regression analysis and Levene's test of homoscedacity a 95% confidence interval is applied, resulting in a significance level of 0.05.

1-4 Results

The means and statistical significance of the objective metrics for each system configuration are presented in Table 1-3. The variances of the objective metrics and corresponding statistical significance are presented in Table 1-4. The means, statistical significance and Cronbach's coefficient of reliability α for the subjective metrics are shown in Table 1-5. The results are displayed graphically in Figure 1-10 to Figure 1-13 by means of boxplots. These show the median of participants in red, the Interquartile Range (IQR) in blue and the whiskers in black, of which the maximum length is defined as 1.5 times the IQR. Furthermore, the mean results of individual participants are shown in different colours, connected by dotted lines between the different system configurations.

Metric	Man	Gen	Ada	F	p
DI	0.808	0.810	0.810	0.216	0.806
SRR	34.67	33.22	32.34	9.390	<0.001
LC-SRR	56.48	54.03	53.55	2.961	0.058

Table 1-3: Resulting means of objective metrics and statistical significance obtained by mixed-effect linear regression

Metric	MAN	GEN	ADA	F	p
DI	$4{\cdot}10^{-4}$	$2{\cdot}10^{-4}$	$1{\cdot}10^{-4}$	3.57	0.033
SRR	28.93	29.37	28.28	0.021	0.980
LC-SRR	48.70	91.57	31.22	3.59	0.032

Table 1-4: Resulting variances of objective metrics and statistical significance obtained by Levene's test of homoscedacity

Metric	GEN	ADA	α	F	p
USE	3.444	4.407	0.901	7.773	0.007
SAT	1.889	2.667	0.765	2.338	0.132

Table 1-5: Resulting means of subjective metrics and statistical significance obtained by mixed-effect linear regression

Mental Workload

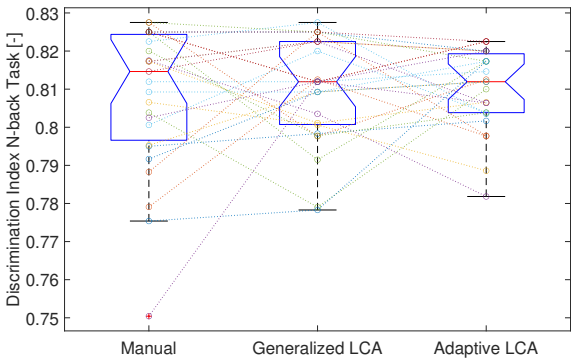

Figure 1-10: Mental workload measured by the cognitive N-back task per system configuration for 27 participants

In Table 1-3 it is shown that the small change of mean DI after introducing an LCA system compared to the manual driving session is regarded insignificant by the mixed-effect linear regression analysis. The variance of mean DI decreases across the three system configurations, as can be seen in Figure 1-10. This is regarded as a significant change in variance according to Levene's test with an associated p-value of 0.032, as shown in Table 1-4.

Lateral Control Performance

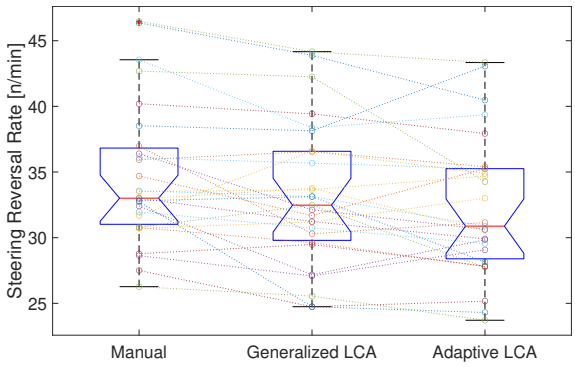

Figure 1-11: Steering reversal rate during complete driving sessions per system configuration for 27 participants

As can be seen in Figure 1-11 and in Table 1-3, the mean value of SRR decreases when the adaptive LCA is introduced compared to the generalized LCA and manual driving. In Table 1-4 it can be seen that the variance of SRR remains unchanged across the system configurations with a p-value of 0.98. Therefore, it passes Levene's test for equality of variances.

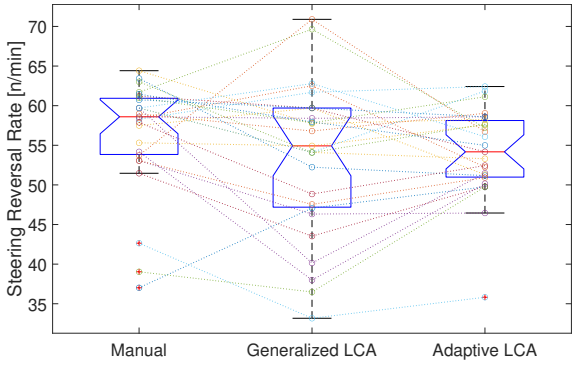

Figure 1-12: Steering reversal rate during lane change maneuvers per system configuration for 27 participants

It can be seen in Figure 1-12 that the variance of SRR during LC maneuvers increases from manual to generalized LCA. The variance of SRR during LC maneuvers of the adaptive LCA decreases compared to both the generalized LCA and the manual driving session. In Table 1-4 it is shown that this reduction of variance is significant according to Levene's test, with a p-value of 0.032.

User Acceptance

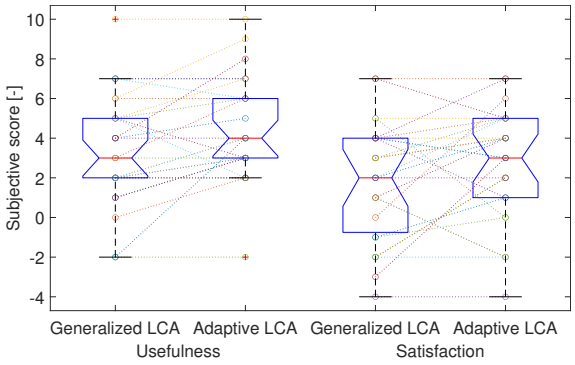

Figure 1-13: Subjective usefulness score and satisfaction score per system configuration for 27 participants

In Figure 1-13 it is shown that both the subjective usefulness score and the subjective satisfaction score increase with the introduction of the adaptive LCA system compared to the generalized LCA system. However, in Table 1-5 it is shown that this increase is only significant for the subjective usefulness score USE with a p-value of 0.007. Furthermore, it can be seen in Figure 1-13 that the usefulness score for both the generalized and the adaptive LCA are higher than the respective satisfaction score values. The subjective results are regarded as valid since Cronbach's coefficient of reliability α is higher than 0.65 for both system configurations, as is shown in Table 1-5.

1-5 Discussion

The unchanged mental workload measured by DI after introduction of the trial-by-trial adaptive LCA system does not agree with the expectations expressed in hypothesis I, thus the hypothesis is rejected. The negligible change in mean DI might be explained by the fact that the N-back task was executed continuously with random hits to prevent an expectation pattern. Therefore workload was

measured during both lane keeping and lane changing, possibly reducing visibility of the effect during LC maneuvers. Additionally, it could be explained by the low error rate measured for the auditory 1-back task [5] in a lane keeping task, as shown in Figure 1-14. Alternatively, the small change in measured mental workload across system configurations could be explained by the large dependence on traffic environment complexity [28]. This is in agreement with observations made during the experiment, in which it seemed that secondary task performance degraded in situations with high traffic complexity.

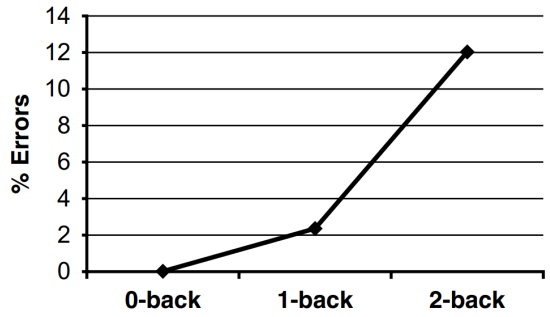

Figure 1-14: Error rate of the N-back task according to Mehler et al. [5]

Lateral control performance and SRR are inversely related, since the performance is considered to be reduced when many steering corrections have to be made. Therefore, the lateral control performance is increased by introducing the adaptive LCA system compared to manual driving and the generalized LCA system. This in agreement with hypothesis II, which is therefore accepted. The the validity of SRR as metric representing absolute steering performance can be questioned, since it is affected by the steering task difficulty. However, it is found that the metric is a valid representation of driving performance and can therefore be used to compare different drivers or conditions [29].

The increased steering wheel activity may be associated with both increased cognitive load and reduced lateral control performance [23]. However, literature shows that SRR is no significantly affected by a cognitive secondary task [30] [4], indicating that the change in SRR is more probable to be an effect of the different system configurations or traffic complexity rather than the introduced secondary task.

The reduction in variance of SRR during lane changes indicates that the inter-driver variability of performance is reduced by introducing the trial-by-trial adaptation. This could result from the fact that the adaptive LCA accommodates to the personal preferences of different drivers, thus increasing the lateral control performance resulting from the HSC interface of the steering wheel. This is in agreement with previous studies that applied a personalized driver model to both an LKA and an Adaptive Cruise Control (ACC) system [31] and a personalized LCA system based on identification of cautious, normal and aggressive driving style [32]. These studies also show that the differences in driving behaviour were accommodated and thus inter-driver variability could be reduced.

The significantly increased user acceptance expressed as usefulness score of the adaptive LCA compared to the generalized LCA system is in agreement with results from a previous study that applied continuous adaptation to personal preference of the longitudinal assistance system ACC to Time to Collision (TTC). This study also showed a higher user acceptance compared to a standard ACC [33]. The unchanged user acceptance expressed as satisfaction score is not in agreement with the expectations, this might be explained by conflicts of lane change intention caused by the limitations of the LCA logic.

Limitations

For the purpose of this study, longitudinal control is supported by means of a CC instead of an ACC system. This was done to stimulate lane changing rather than car-following

behaviour. However, it was observed during the experiments that the longitudinal control task required a lot of additional mental workload capacity in situations with high traffic density. Therefore it is expected that this has distorted the measurements of multiple metrics, which could have been mitigated by integration of the LCA system with an ACC system.

In this study it was chosen to embed a safety feature in the LCA logic, by aborting a lane change if the indicator light is switched off before crossing the lane boundary. However, aborted LC maneuvers were almost never encountered during the experiments, whereas many people switched off the indicator light before crossing the lane boundary during an intentional LC maneuver. This led to a relatively large number of conflicts between the LCA logic and the participants. These conflicts could have been mitigated by enlarging the time duration in which the lane boundary has to be crossed.

Furthermore, two subsequent left or right LC maneuvers could not be identified as such if the indicator light was not switched off between the maneuvers. The conflicts resulting from this could have be prevented by executing the simulation on a two-lane highway. More preferably, the LCA logic should be able to detect the intention of two subsequent lane changes.

1-6 Conclusion

The hypotheses of this study were stated as follows:

I. A trial-by-trial adaptive lane change assistance system reduces mental workload of drivers during highway driving.

II. A trial-by-trial adaptive lane change assistance system increases lateral control performance during highway driving.

The first hypothesis is rejected, since there is no significant change in mental workload, measured by the mean discrimination index of the cognitive secondary N-back task, when the generalized or adaptive LCA system is introduced.

The second hypothesis is accepted, since the lateral control performance, measured by the mean steering reversal rate, is increased significantly when introducing trial-by-trial adaptation to lane change duration in the adaptive LCA when compared to the generalized LCA and manual system configuration.

Furthermore, inter-driver variability of lateral control performance during lane changes is reduced significantly by introducing trial-by-trial adaptation to lane change duration in the adaptive LCA compared to the generalized LCA and manual driving. In addition to this, user acceptance expressed as subjective usefulness is increased significantly by introducing the adaptive LCA system.

1-7 Future Work

During this study, several observations are made of aspects that could be improved upon and topics to be researched in future studies. First of all, to achieve fully integrated longitudinal and lateral functionality of lane change assistance, implementation of HSC on a longitudinal control interface such as the acceleration or brake pedal would be preferable. By doing this, excessive braking or acceleration to complete a safe lane change could be made redundant. By integrating longitudinal control as proposed in [34], the functionalities of these systems could be optimized to complement one another and thus lead to more consistent results with reduced effect of traffic complexity.

Furthermore it is recommended to adjust the LCA logic to enable a more universal detection of lane change intention. It is expected that this will further enhance user acceptance and driving performance, whilst ensuring safe

driving behaviour. For example, the lateral margins defining the end of an LC maneuver could be reduced to a smaller value to capture more of both the intra-driver and inter-driver variability. Alternatively, different metrics could be chosen to define the start and end of an LC maneuver.

To improve upon the learning speed of the adaptive LCA system, naturalistic driving data of participants could be used to obtain initial values for the adaptive LCA, opposed to the generalized value for lane change duration of 4 seconds. Additionally, the effect of different values for the moving average window length could be investigated. Alternatively, other learning algorithms could be applied to obtain the desired value of lane change duration. Also, further research could be done to investigate the effect of adaptation to driver parameters other than lane change duration, such as preferred lateral acceleration [35].

Appendix A

System Design

The Lane Change Assistance system was designed within a Matlab-Simulink model that is used as I/O interface of the dSpace Automotive Simulation Model (ASM). In Figure A-3 to A-5 the model and specific elements of this model are highlighted. The LQR controller equations are presented in section A-1 and the LCA Logic is explained in more detail in section A-2.

A-1 LQR Controller Design

In this section the equations of the LQR controller are displayed more elaborately. The State-Space equations of the LQR controller are formulated in Equation A-1 to A-8. The cost function is formulated in Equation A-9 and the corresponding weights are shown in Table A-1.

$$A = \begin{bmatrix} 2\frac{(C_f+C_r)}{m\cdot V_x} & -\frac{V_x+(2\cdot(C_r\cdot l_r - Cf\cdot l_f))}{m\cdot V_x} & 0 & 0 & 2\frac{C_f}{m} & 0 & 0 \\ 2\frac{C_r\cdot l_r - C_f\cdot l_f}{I_z\cdot V_x} & -2\frac{C_f\cdot l_f^2 + C_r\cdot l_r^2}{I_z\cdot V_x} & 0 & 0 & 2\frac{C_f\cdot l_f}{I_z} & 0 & 0 \\ 0 & 1 & 0 & 0 & 0 & 0 & 0 \\ 1 & 0 & V_x & 0 & 0 & 0 & 0 \\ 0 & 0 & 0 & 0 & 0 & 1 & 0 \\ 0 & 0 & -\frac{R_g\cdot G_h\cdot t_p\cdot V_x}{a_0\cdot T_d^2} & -\frac{R_g\cdot G_h}{a_0\cdot T_d^2} & -\frac{1}{a_0\cdot T_d^2} & -\frac{1}{a_0\cdot T_d} & 0 \\ 0 & 0 & -t_p\cdot V_x & -1 & 0 & 0 & 0 \end{bmatrix} \tag{A-1}$$

$$B = \begin{bmatrix} 0 & 0 & 0 & 0 & 0 & \frac{R_g\cdot G_h}{a_0\cdot T_d^2} & 0 \end{bmatrix} \tag{A-2}$$

$$C = \begin{bmatrix} 0 & 0 & -t_p\cdot V_x & -1 & 0 & 0 & 0 \\ 0 & 0 & 0 & 0 & 1 & 0 & 0 \\ 0 & 0 & 0 & 0 & 0 & 1 & 0 \end{bmatrix} \tag{A-3}$$

$$D = \begin{bmatrix} 1 & 0 & 0 \end{bmatrix}^T \tag{A-4}$$

$$Q_d = \begin{bmatrix} q_1 & 0 & 0 \\ 0 & q_2 & 0 \\ 0 & 0 & q_3 \end{bmatrix} \tag{A-5}$$

$$Q = (C^T \cdot Q_d \cdot C) + (D^T \cdot Q_d \cdot D) \tag{A-6}$$

$$a_0 = \frac{\tau_{lag}\cdot\tau_{delay}}{T_d^2} \tag{A-7}$$

$$T_d = (\tau_{lag} + \tau_{delay}) \tag{A-8}$$

The cost function of the LQR controller is formulated in Equation A-9

$$\begin{aligned} J &= \int_0^\infty (J_1 + J_2 + J_3 + J_4)\ dt \\ J &= (q_1\cdot\Delta Y_p^2 + q_2\cdot\delta_{fd}^2 + q_3\cdot\dot{\delta}_{fd}^2 + R\cdot\delta_{fc}^2)\ dt \end{aligned} \tag{A-9}$$

The values of the control weighting factors and the state weight factors are obtained by tuning the controller in a digital simulation with a simplified vehicle model. The resulting values are shown in Table A-1.

Table A-1: Weighting factors for LQR Controller

Symbol	Parameter	Value
q_1	Path-tracking weight	5
q_2	Physical workload weight	52.96
q_3	Mental workload weight	61.7
R	Control effort weight	5296

A-2 LCA Logic

The definition of the start and end of an LC maneuver as used by the LCA Logic is graphically shown in Figure A-1 and Figure A-2. The start of an LC maneuver is defined as the moment that the indicator light is engaged. The end is defined as the moment that both the lateral error ΔY and the lateral preview error ΔY_p are within the defined margins of the LCA Logic.

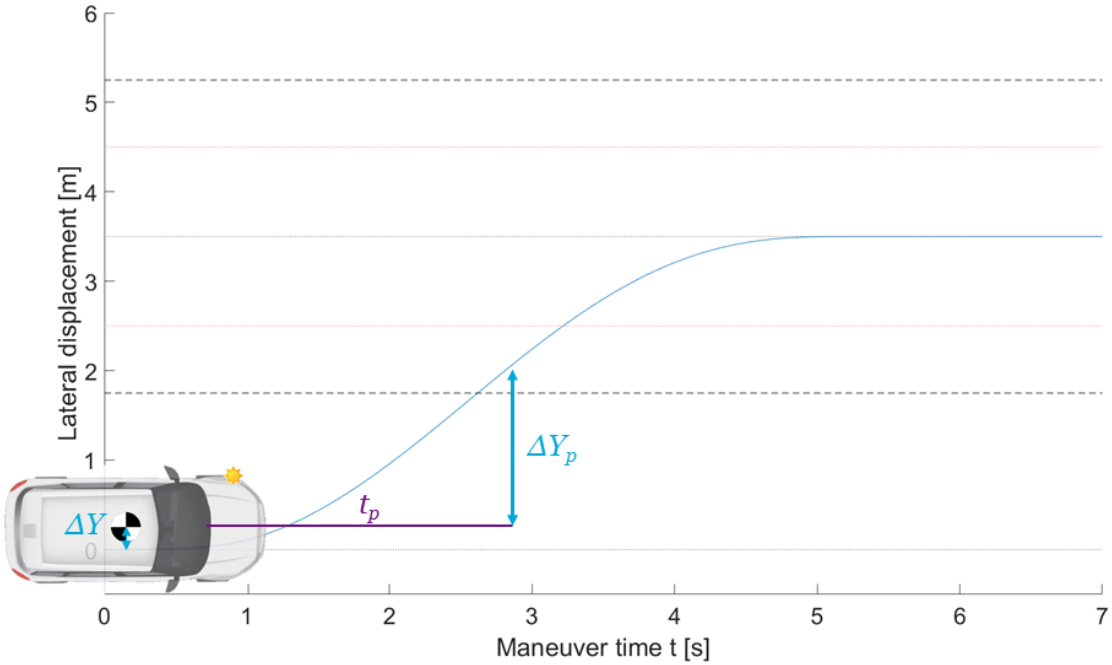

Figure A-1: Schematic showing the definition of the start of an LC maneuver

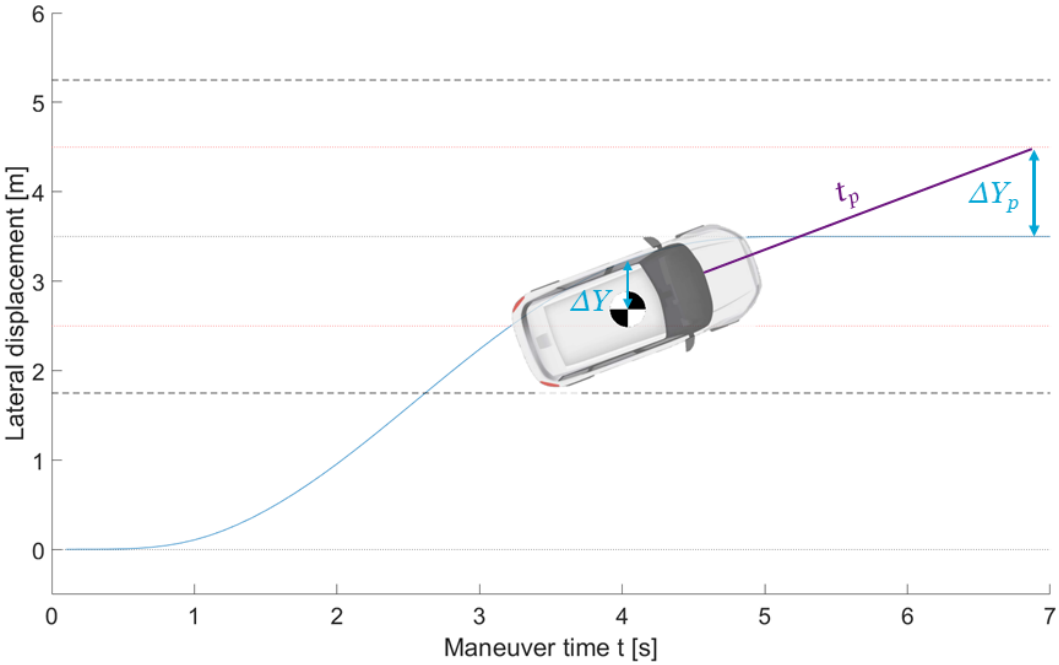

Figure A-2: Schematic showing the definition of the end of an LC maneuver

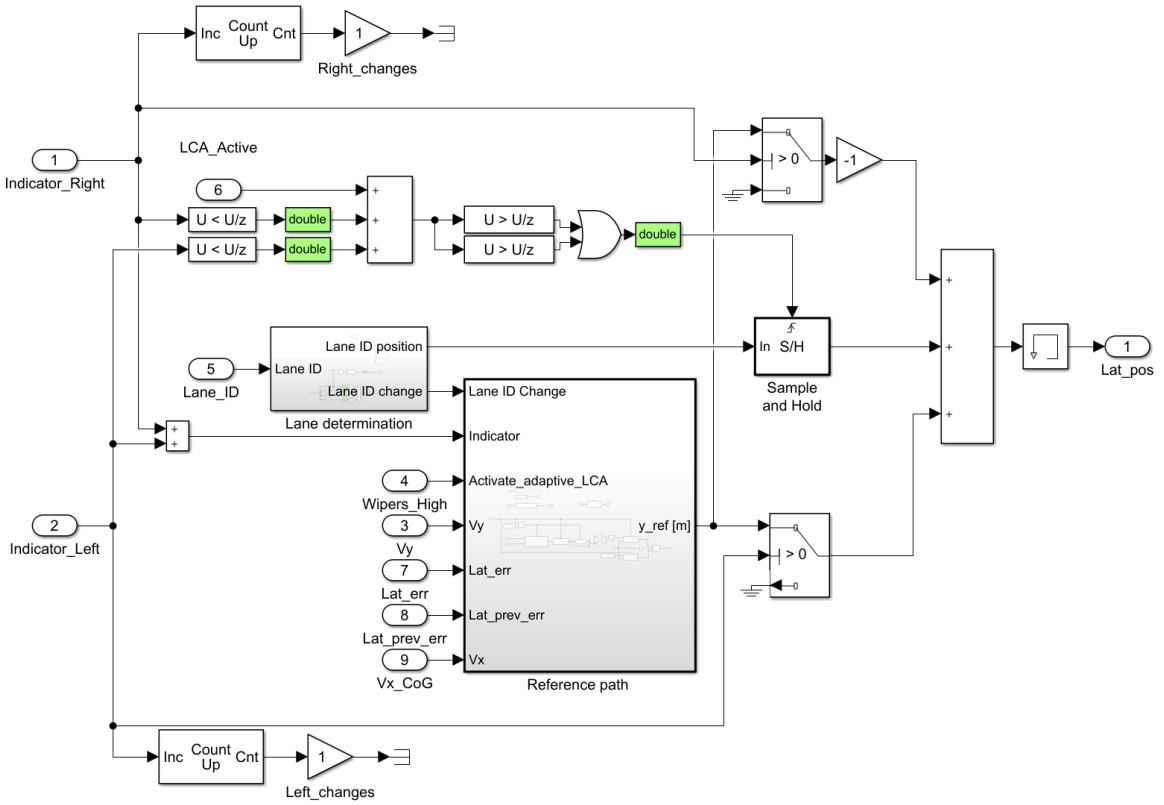

Figure A-3: Simulink model containing the computation of the desired lateral position, which is used to determine the reference error for the LQR controller

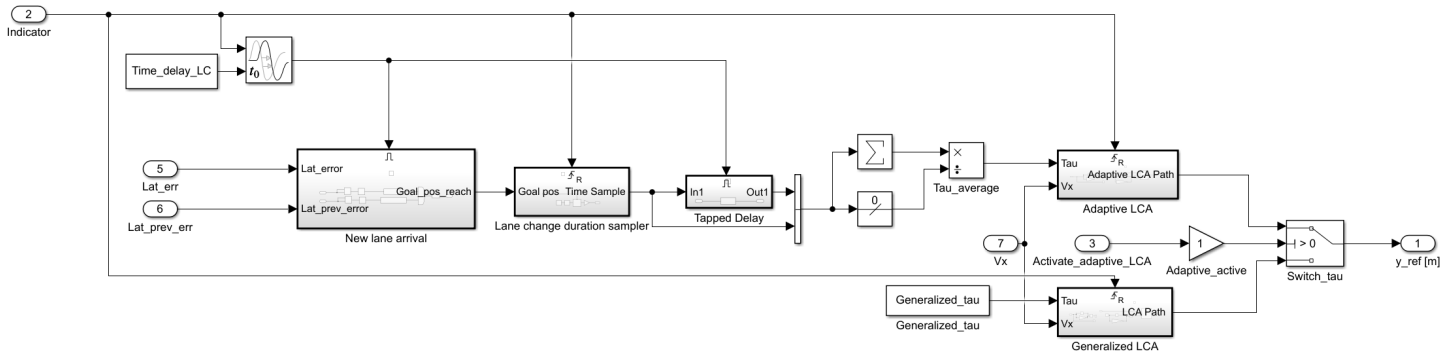

Figure A-4: Simulink Model containing the generation of the generalized and adaptive lane change reference trajectories

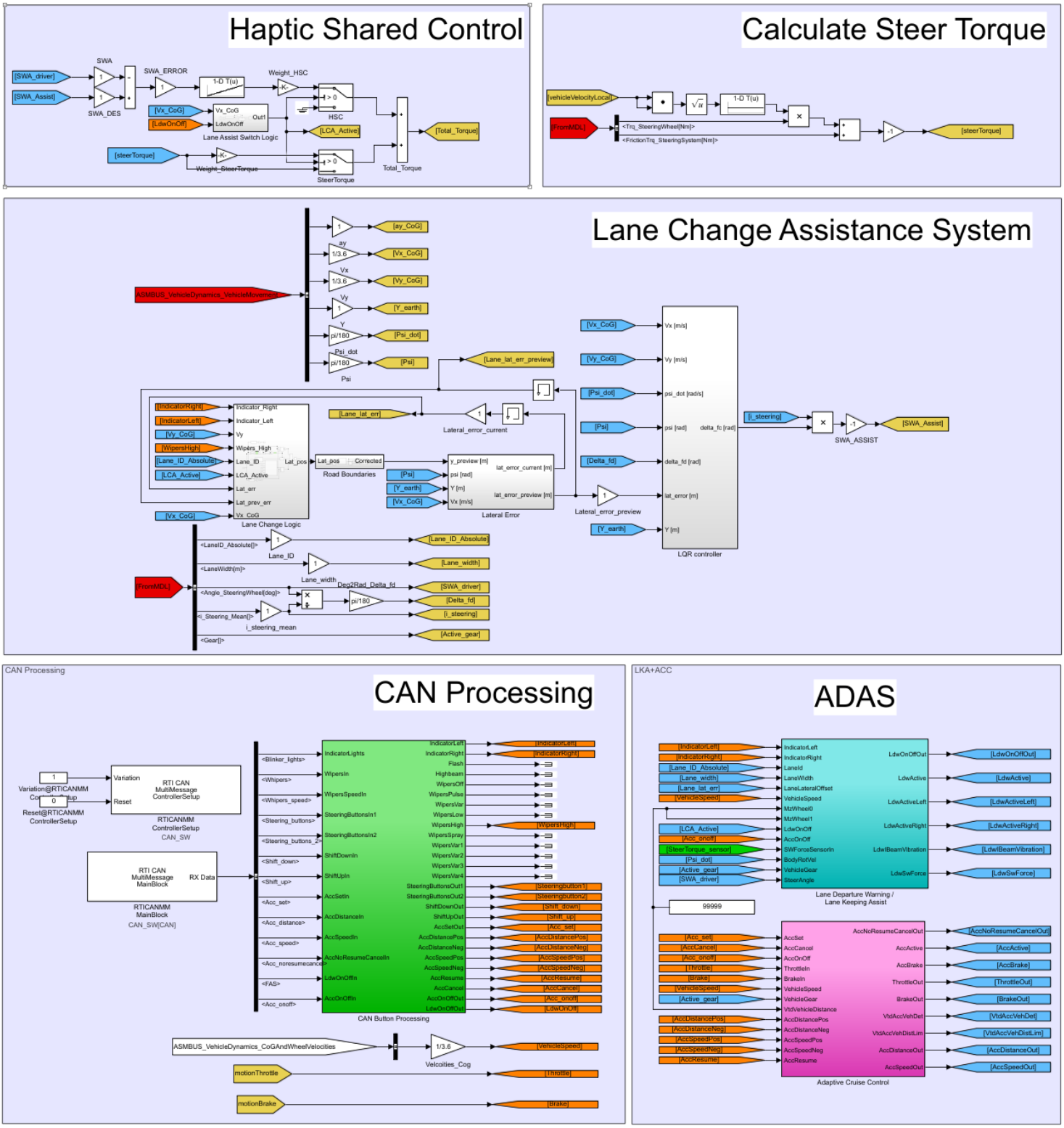

Figure A-5: Simulink Model containing the proposed Lane Change Assistance system

Appendix B

Additional results

B-1 Lane Change Sections

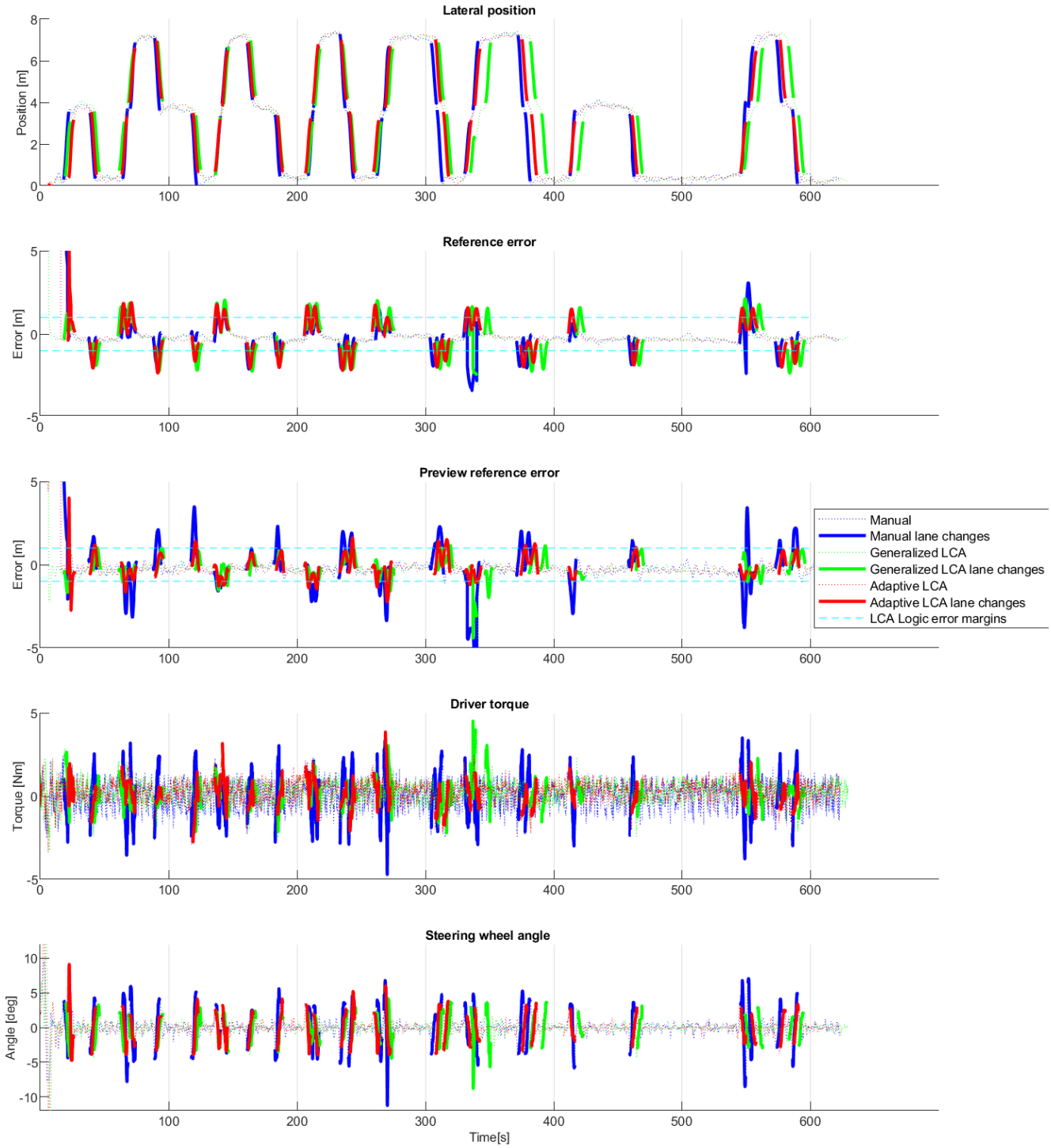

B-2 Torque Conflict Ratios

To express collaborative performance of the human driver and the LCA system, torque conflict is measured during the driving session. This torque conflict is expressed in different ratios, based on the amount of time in which the assistance was in in accordance with the drivers intention [36]. All the collaborative rates were not changed significantly due to the larger variance compared to the change in mean. The rates are shown both for complete driving sessions and for during the lane change maneuvers in Figure B-1 to Figure B-8.

The consistency ratio is formulated as follows:

$$r_{consist} = \frac{1}{T}\int_0^T \text{sign}\left(\mathbf{T}_{dr} \cdot \mathbf{T}_c\right) dt \quad |\mathbf{T}_{dr} \cdot \mathbf{T}_c \geq 0 \tag{B-1}$$

The intrusiveness ratio is formulated as follows:

$$r_{intru} = \frac{1}{T}\int_0^T \text{sign}\left(\mathbf{T}_{dr} \cdot \mathbf{T}_c\right) dt \text{ if } \mathbf{T}_{dr} \cdot \mathbf{T}_c < 0 \tag{B-2}$$

The resistance ratio is formulated as follows:

$$r_{resist} = \frac{1}{T}\int_0^T \text{sign}\left(\mathbf{T}_{dr} \cdot \mathbf{T}_c\right) dt \quad \begin{matrix} |\mathbf{T}_{dr} \cdot \mathbf{T}_c < 0 \\ |\mathbf{T}_{dr} > \mathbf{T}_c \end{matrix} \tag{B-3}$$

The contradiction ratio is formulated as follows:

$$r_{contra} = \frac{1}{T}\int_0^T \text{sign}\left(\mathbf{T}_{dr} \cdot \mathbf{T}_c\right) dt \quad \begin{matrix} |\mathbf{T}_{dr} \cdot \mathbf{T}_c < 0 \\ |\mathbf{T}_{dr} < \mathbf{T}_c \end{matrix} \tag{B-4}$$

B-3 Raw Data

Here the measured data is presented of the 27 participants who were included in the results of the research. For the first 16 participants, no lateral position plots are shown. This is due to an error in the measurement setup, causing the measurement of z position instead of y position. The different trials in each driving session are plotted over another by using measured parameters of the LCA Logic.

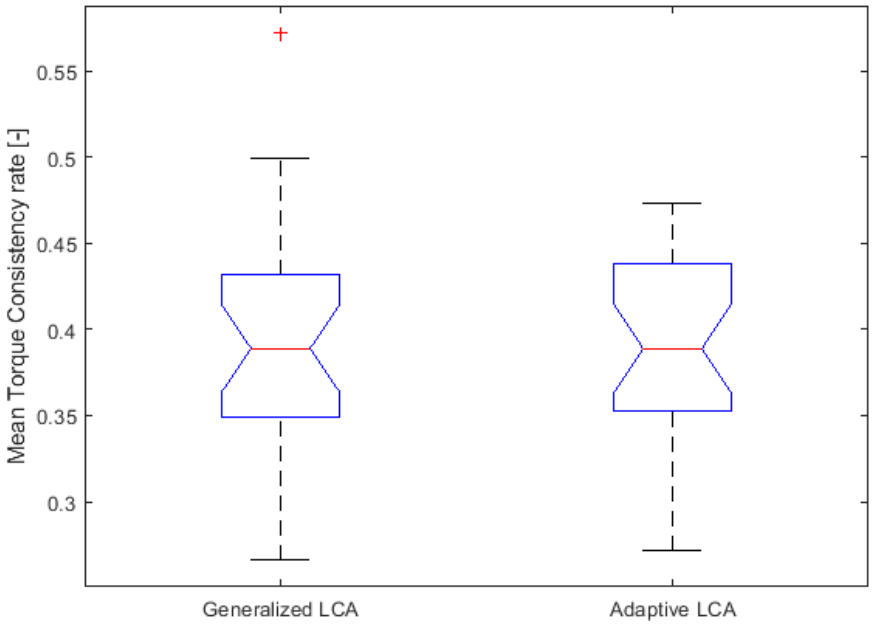

Figure B-1: Mean consistency rate during complete driving sessions of 27 participants

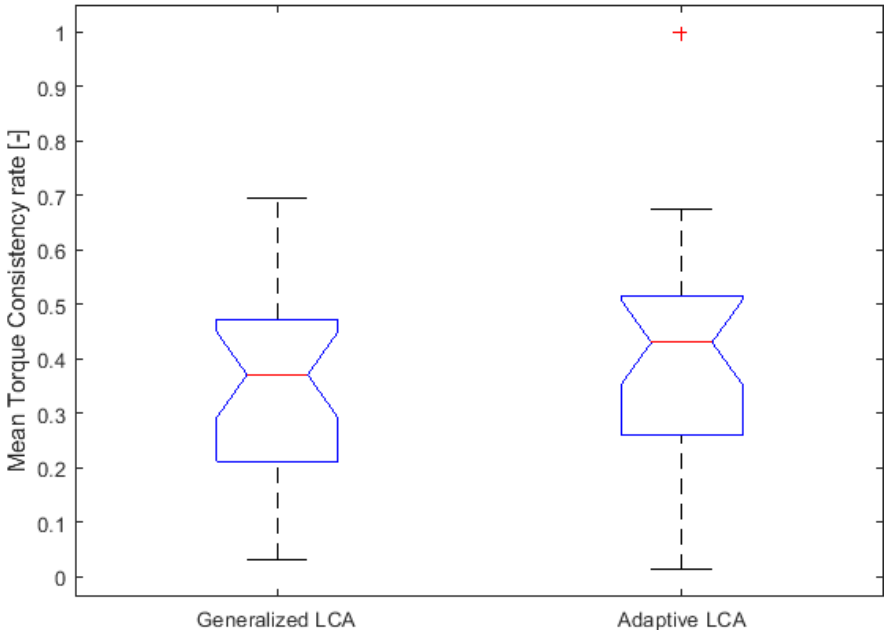

Figure B-2: Mean consistency rate during lane changes of 27 participants

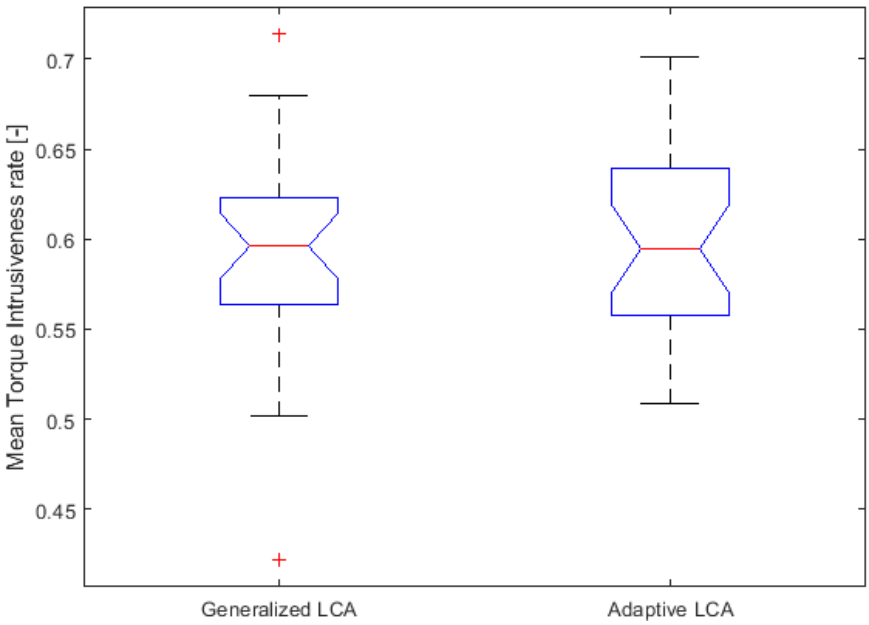

Figure B-3: Mean intrusiveness rate during complete driving sessions of 27 participants

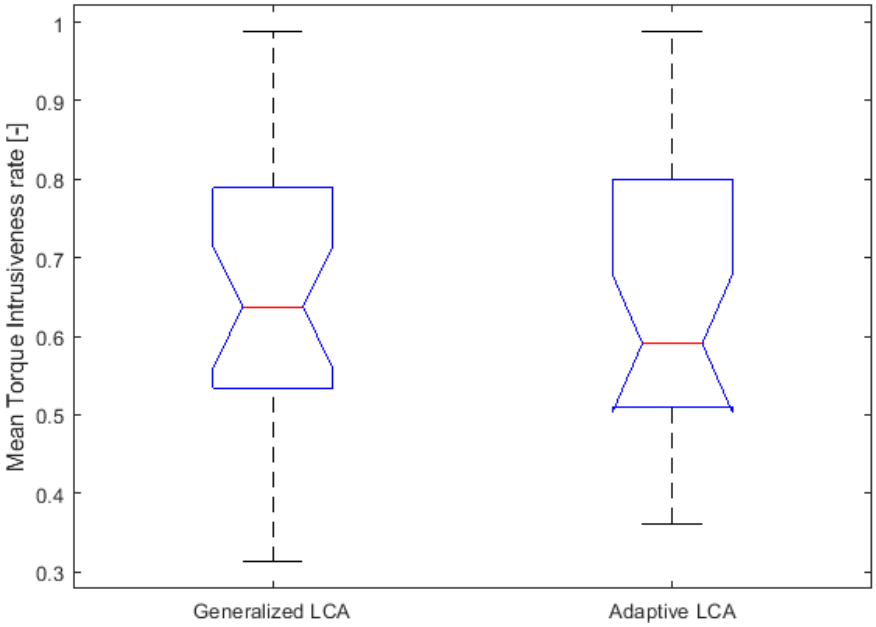

Figure B-4: Mean intrusiveness rate during lane changes of 27 participants

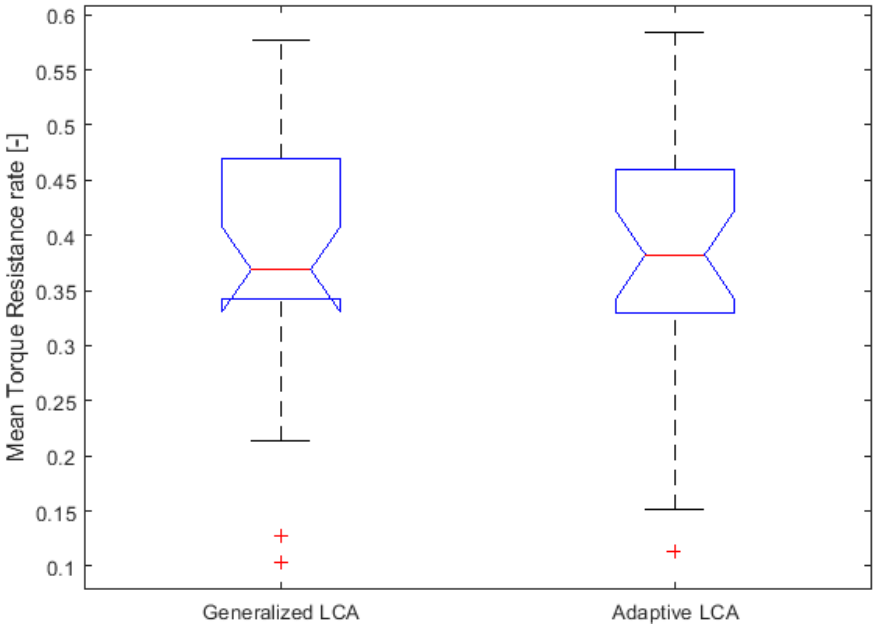

Figure B-5: Mean resistance rate during complete driving sessions of 27 participants

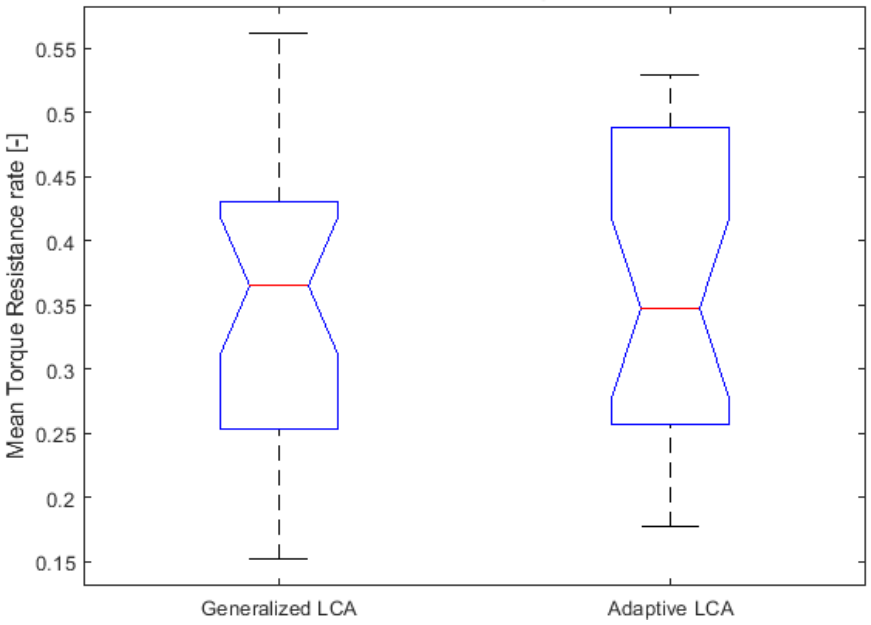

Figure B-6: Mean resistance rate during lane changes of 27 participants

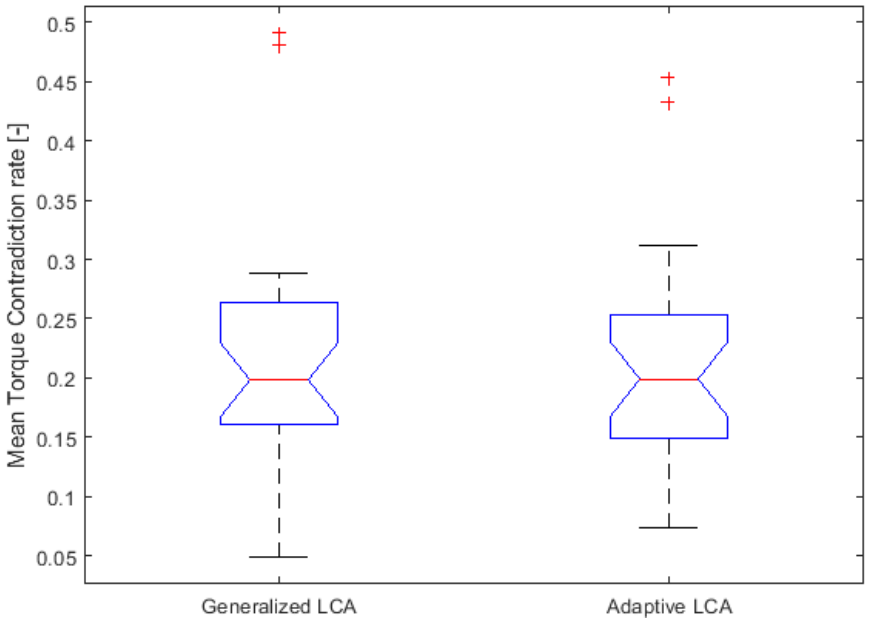

Figure B-7: Mean contradiction rate during complete driving sessions of 27 participants

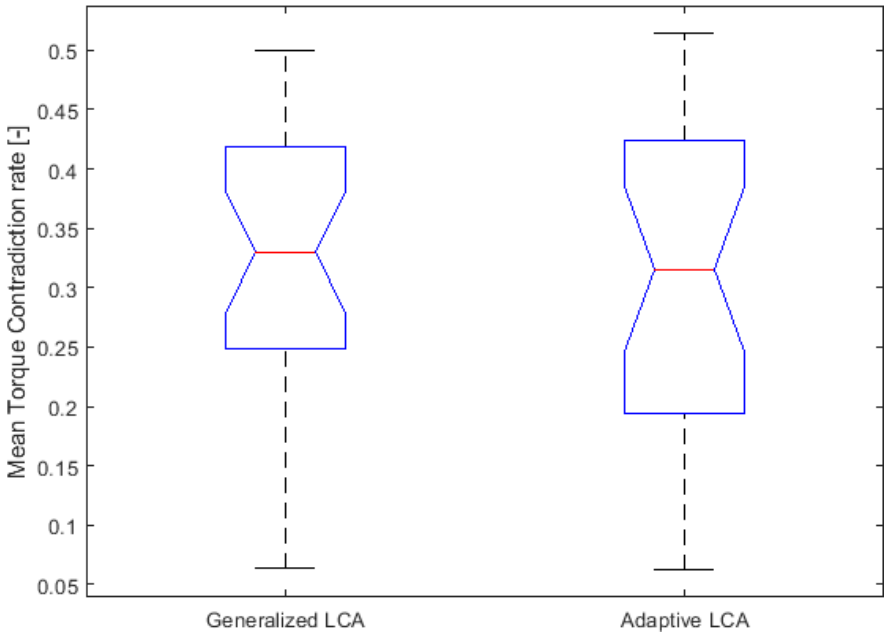

Figure B-8: Mean contradiction rate during lane changes of 27 participants

Raw data plots of participant 1

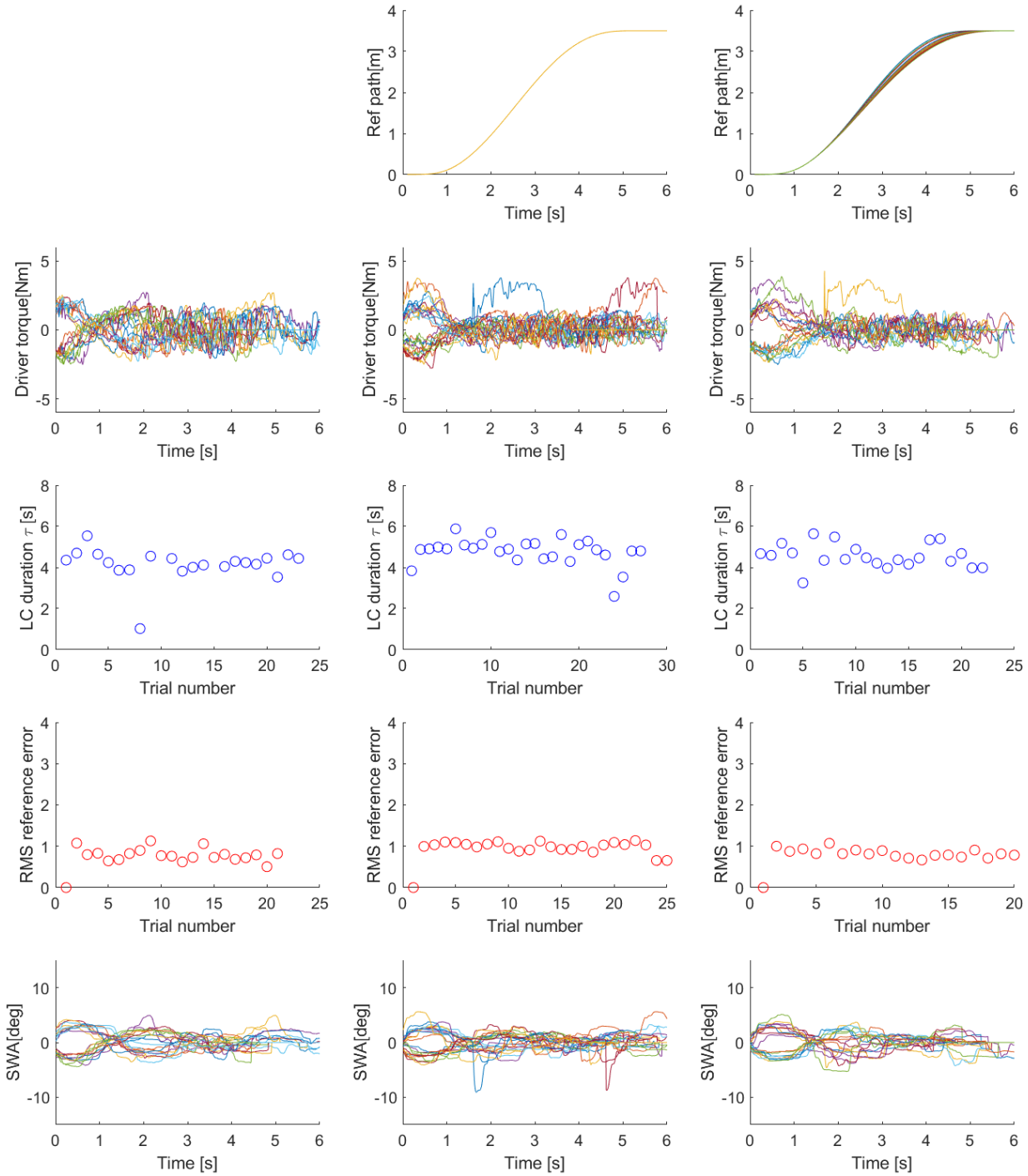

Raw data plots of participant 4

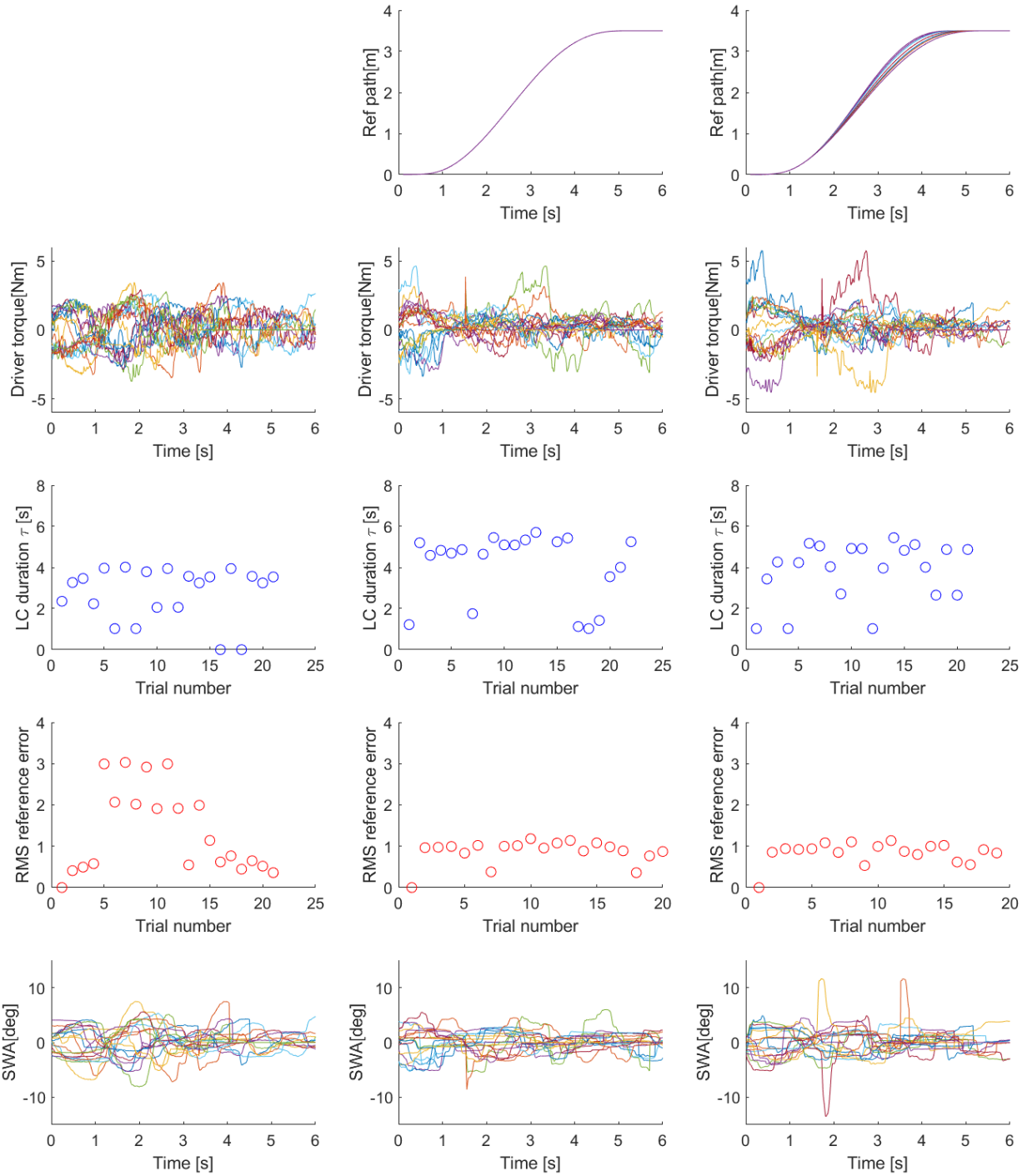

Raw data plots of participant 5

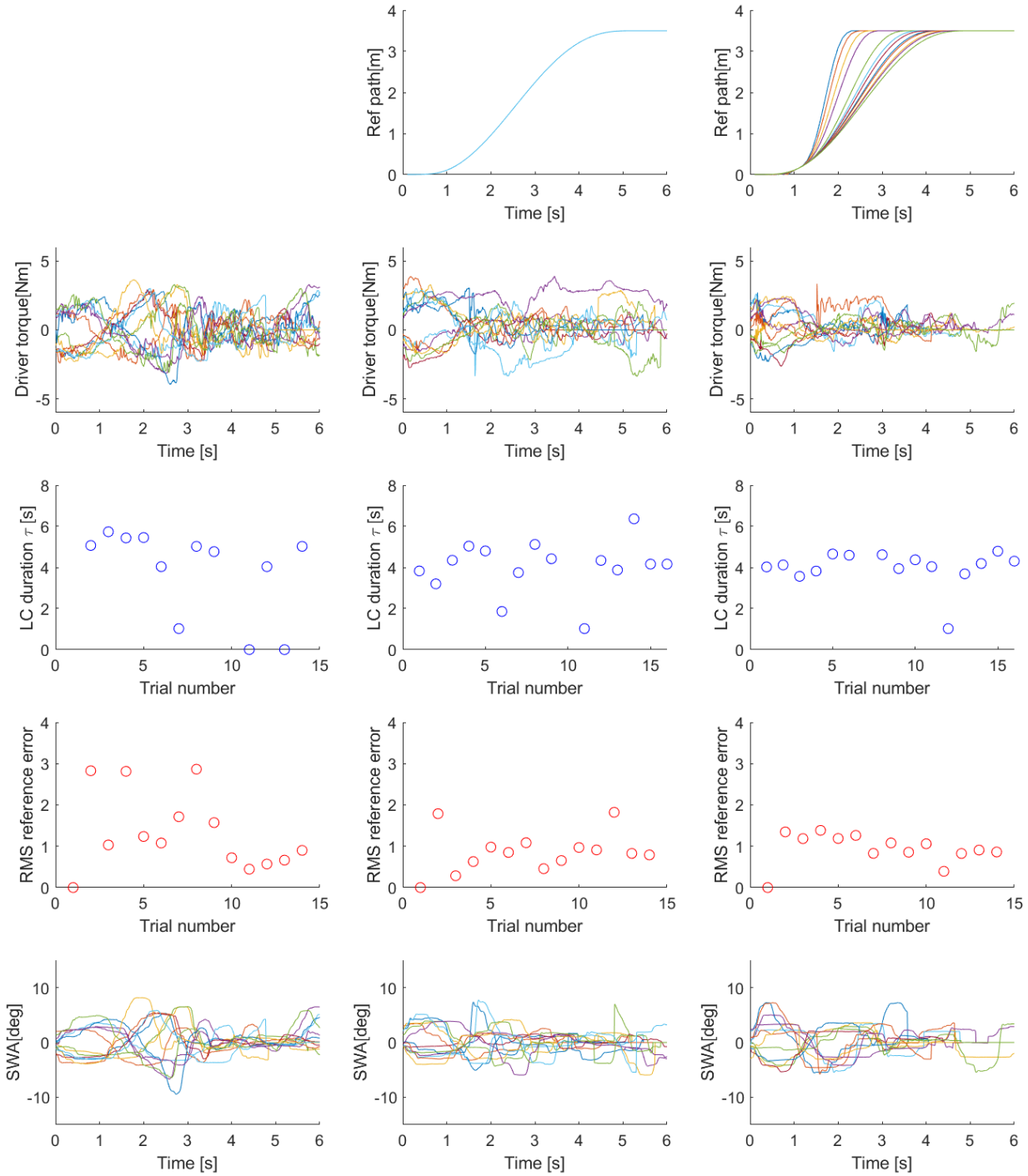

Raw data plots of participant 6

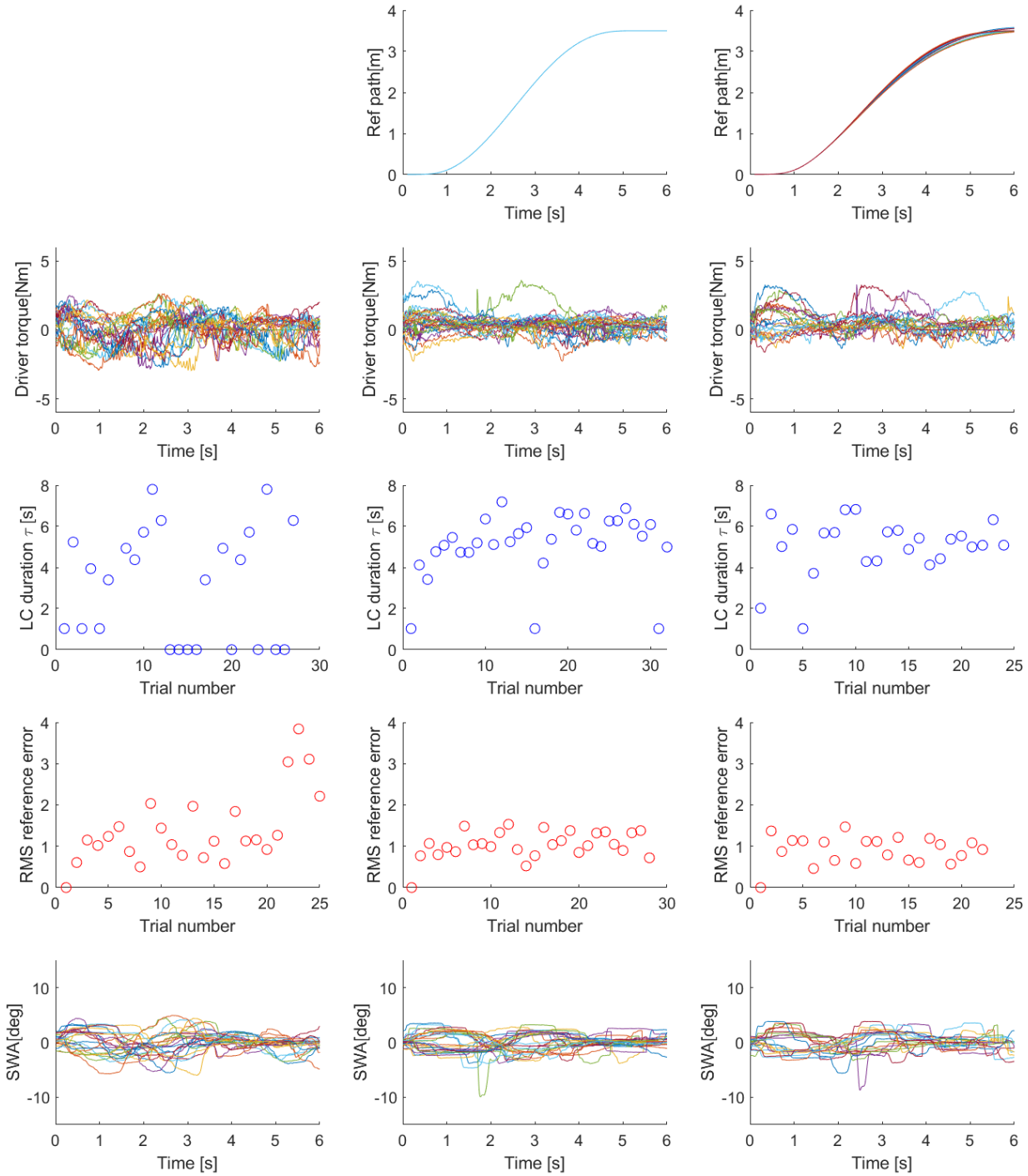

Raw data plots of participant 8

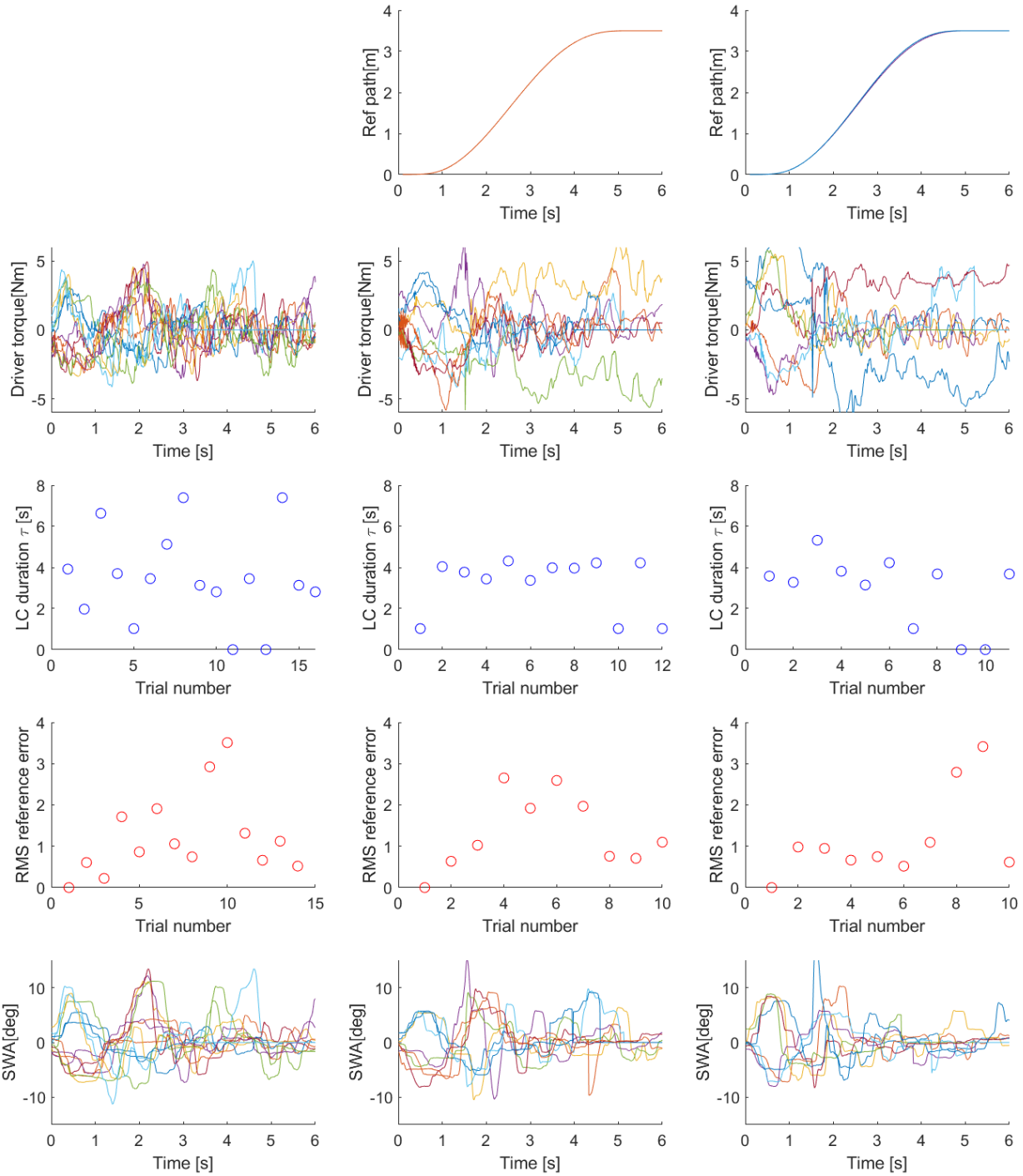

Raw data plots of participant 9

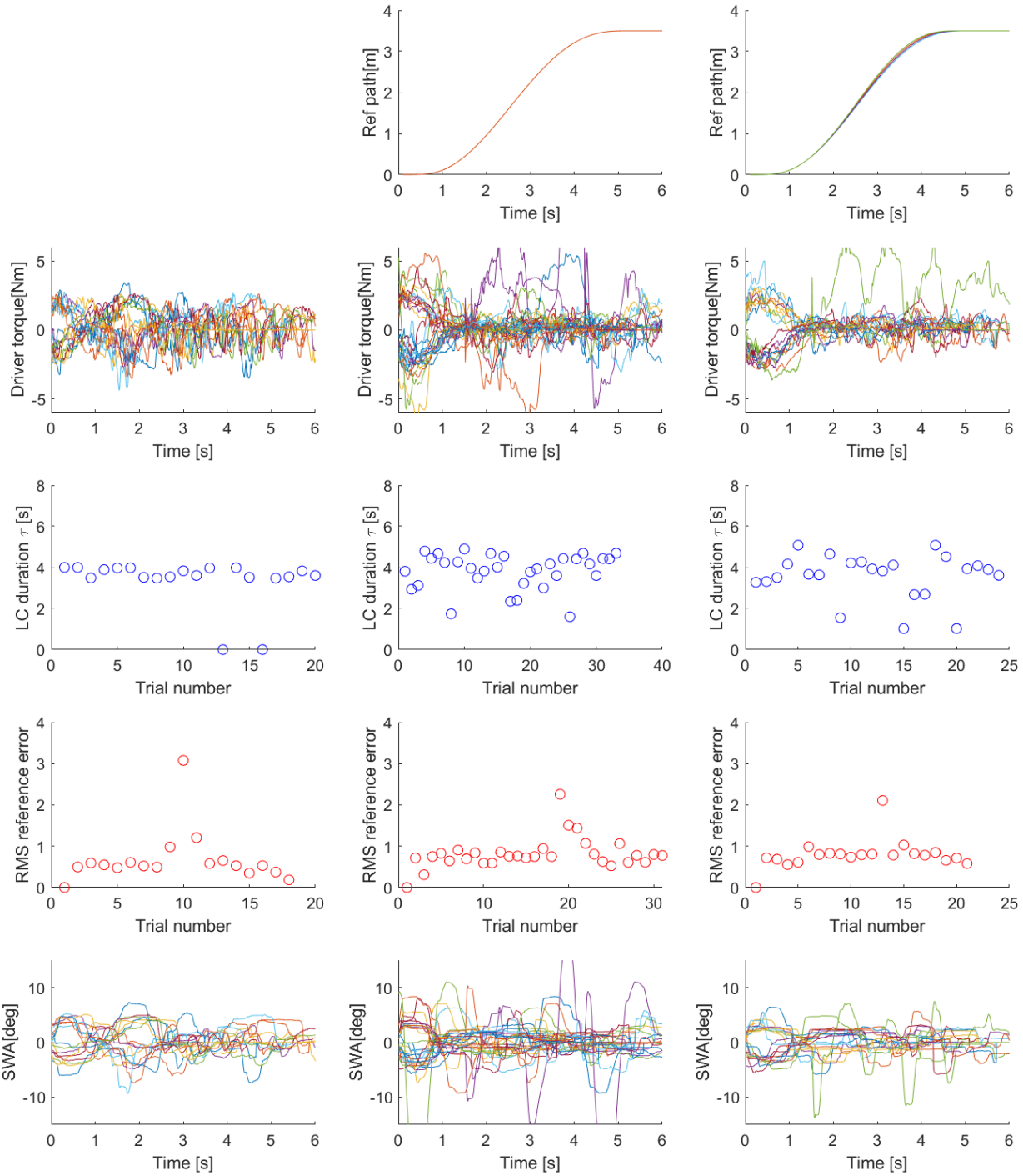

Raw data plots of participant 11

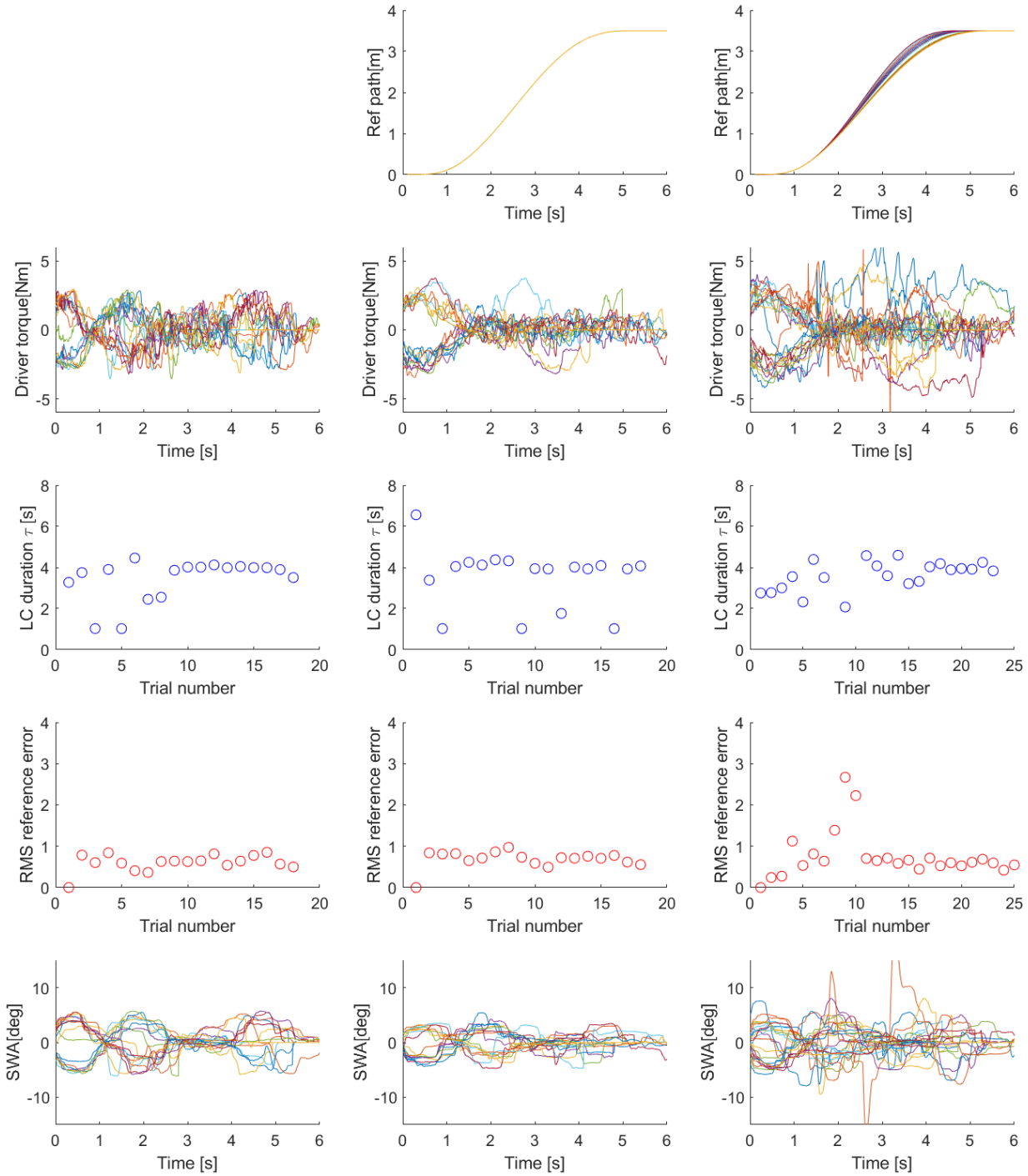

Raw data plots of participant 12

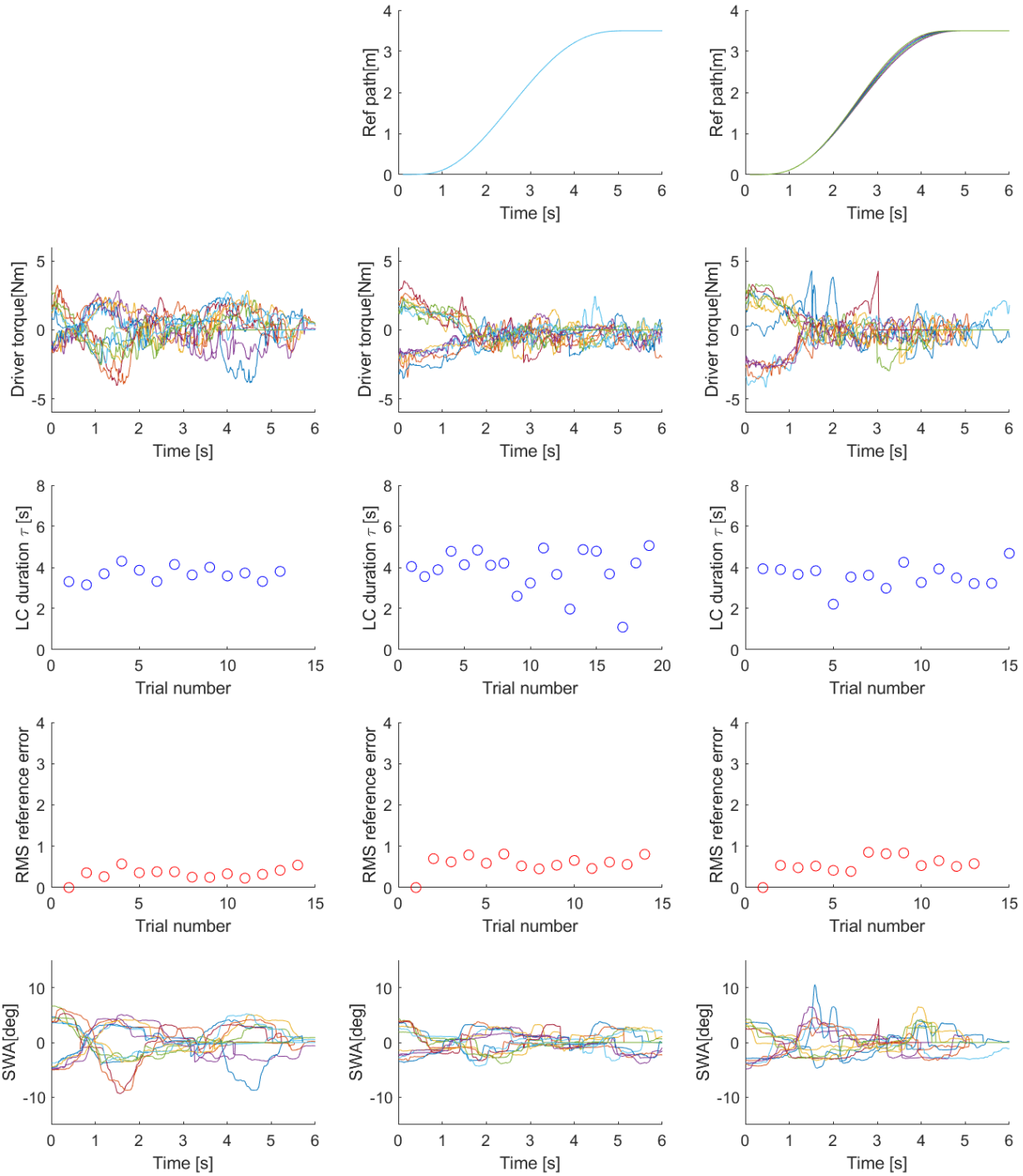

Raw data plots of participant 13

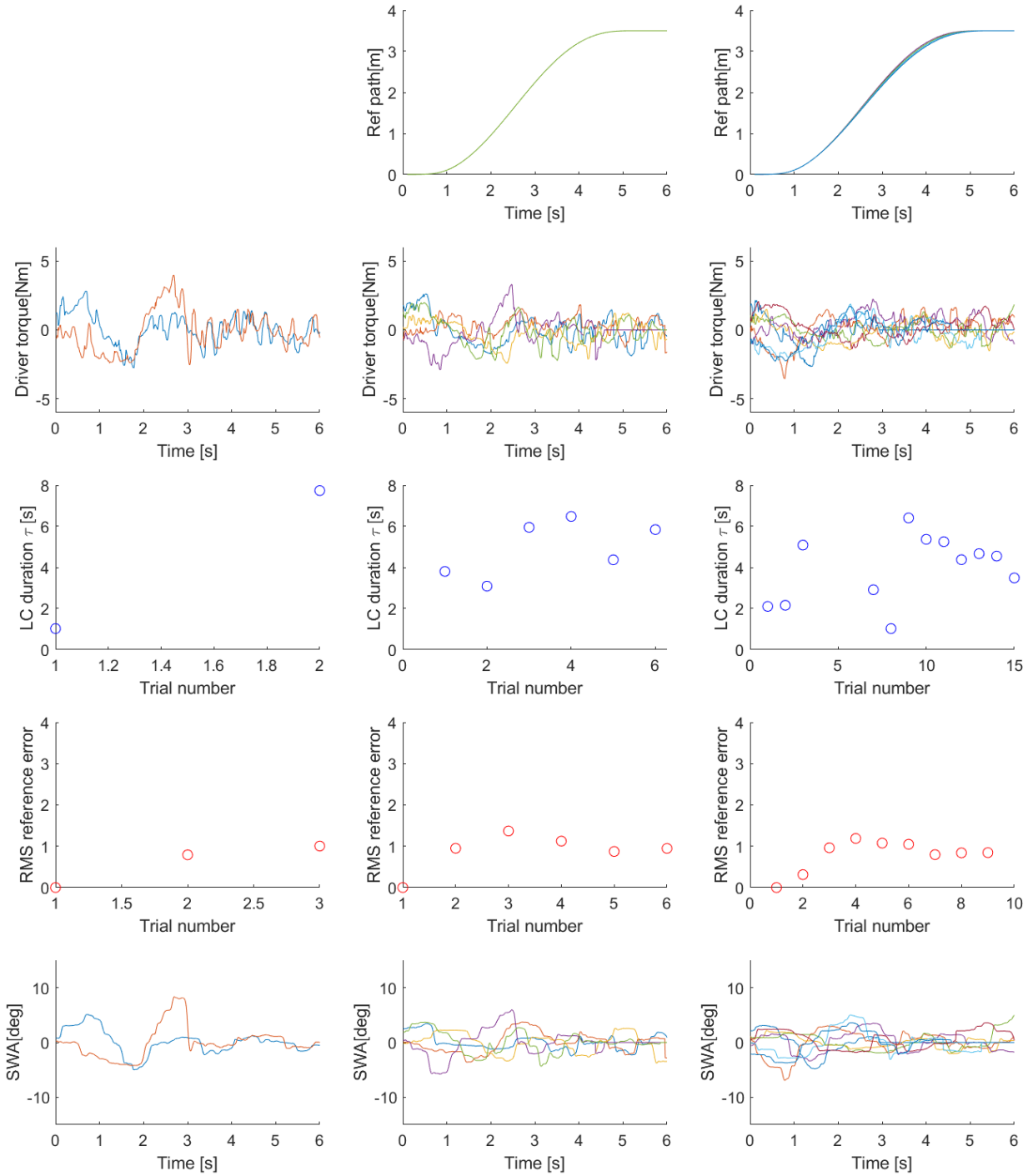

Raw data plots of participant 14

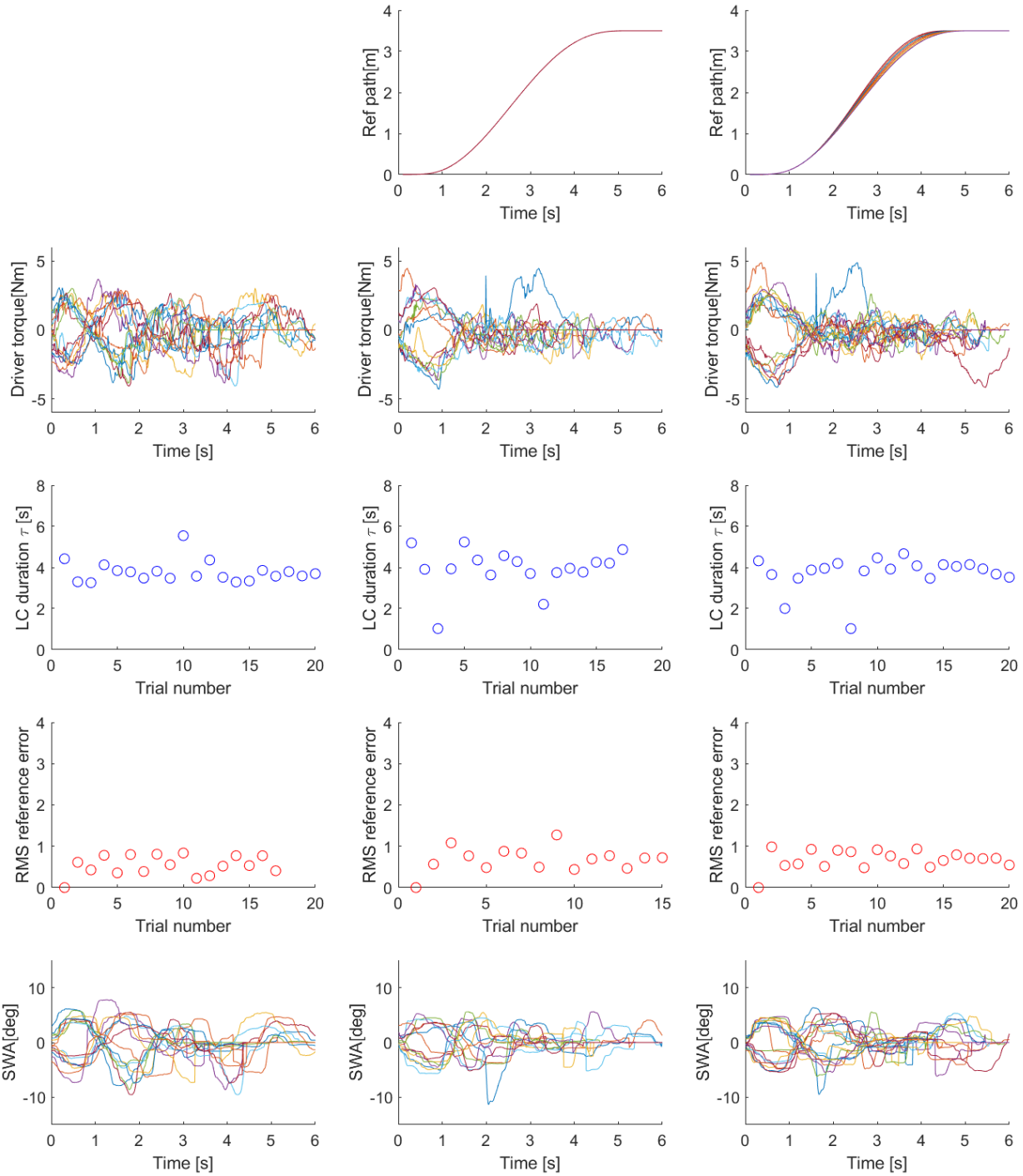

Raw data plots of participant 15

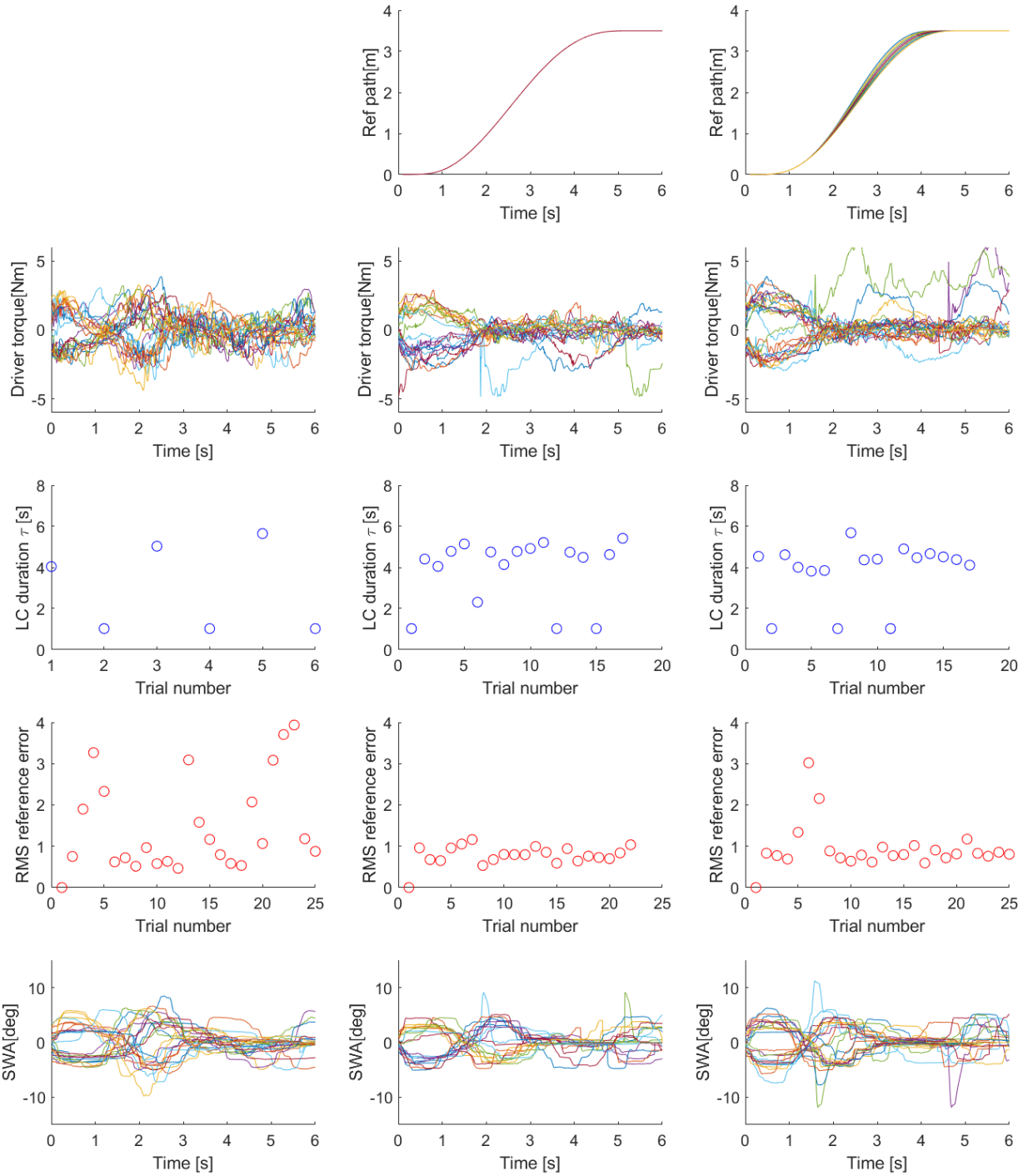

Raw data plots of participant 16

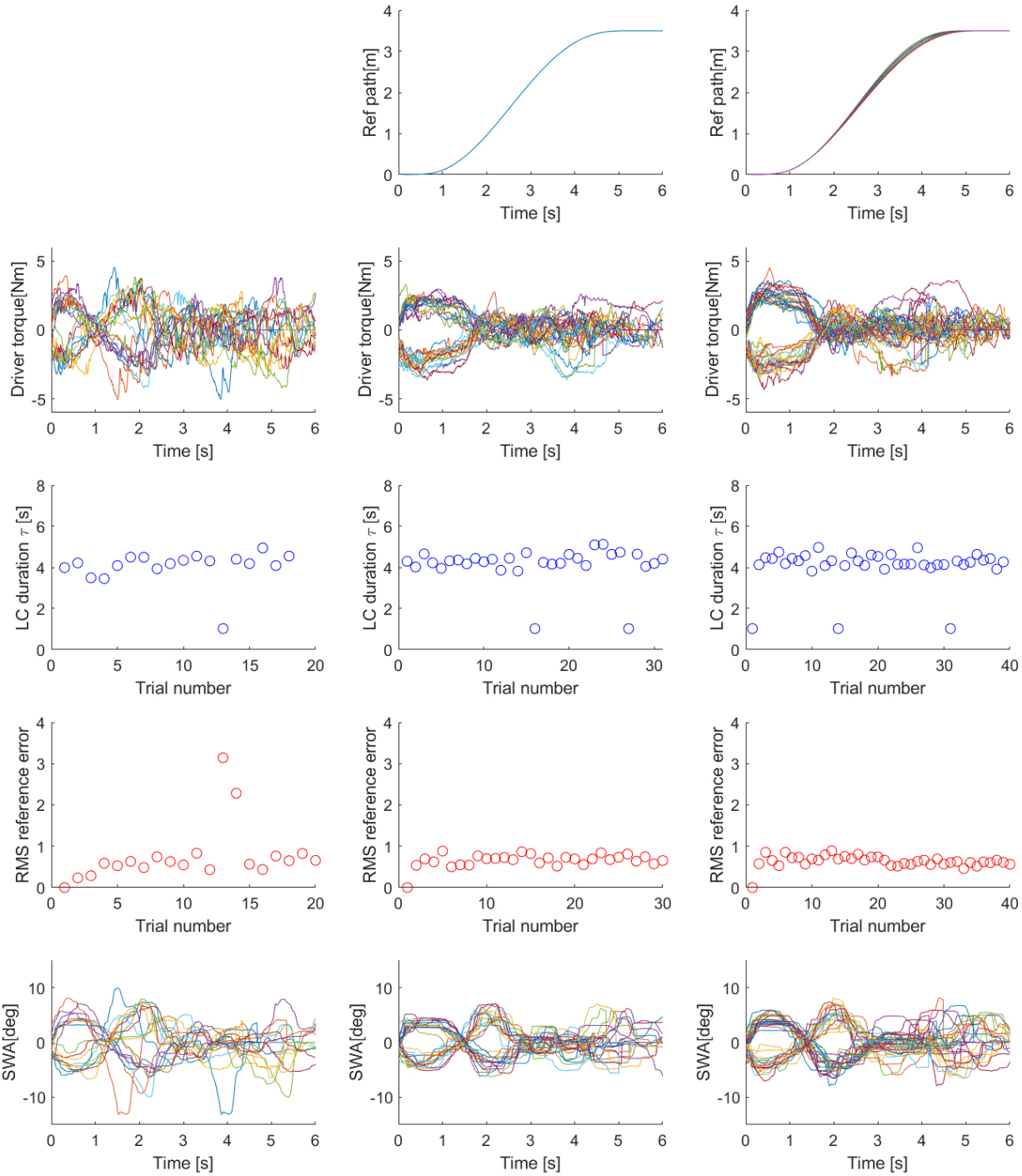

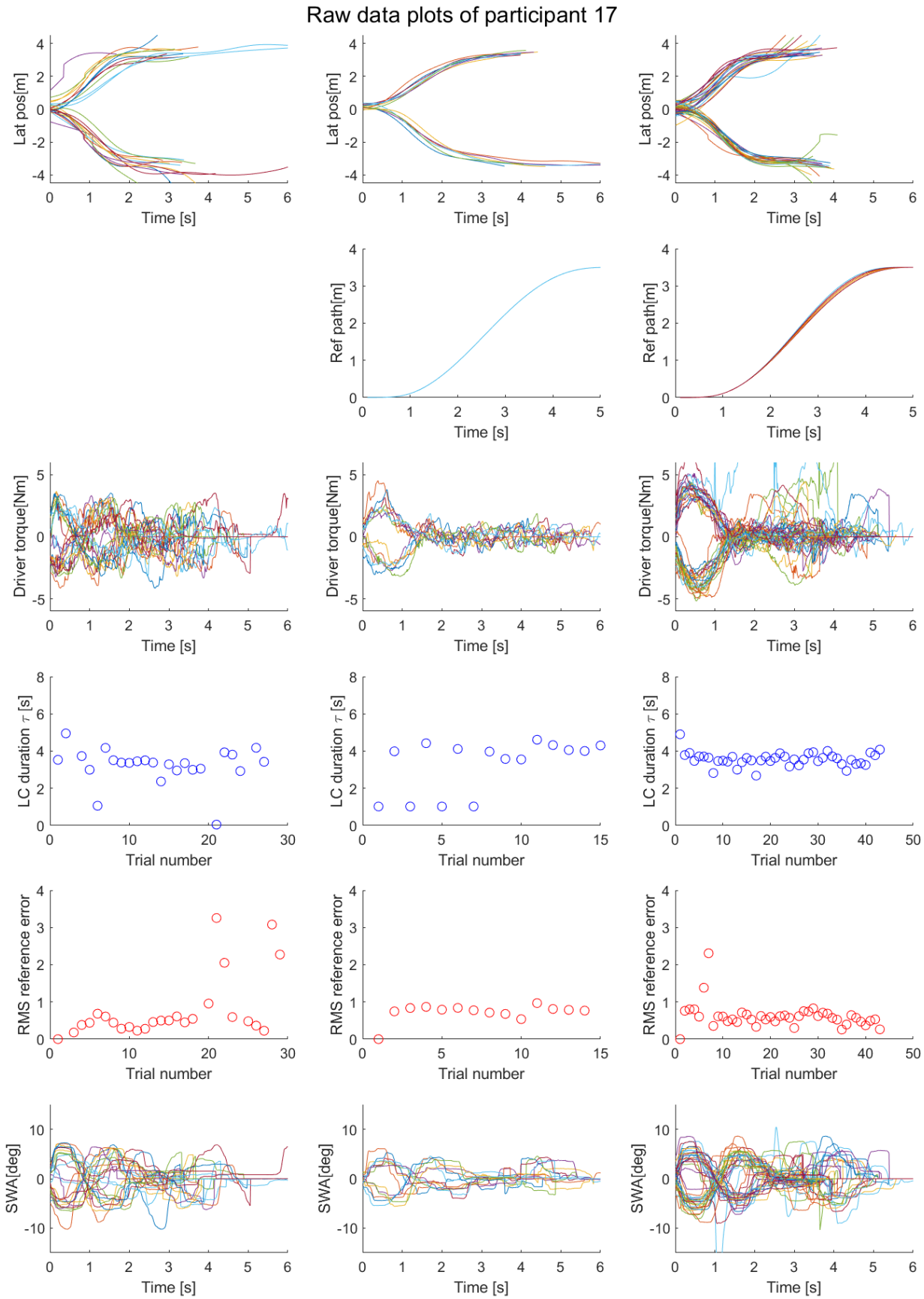
Raw data plots of participant 17
Lat pos[m]
Time [s]
Ref path[m]
Driver torque[Nm]
LC duration τ [s]
Trial number
RMS reference error
SWA[deg]

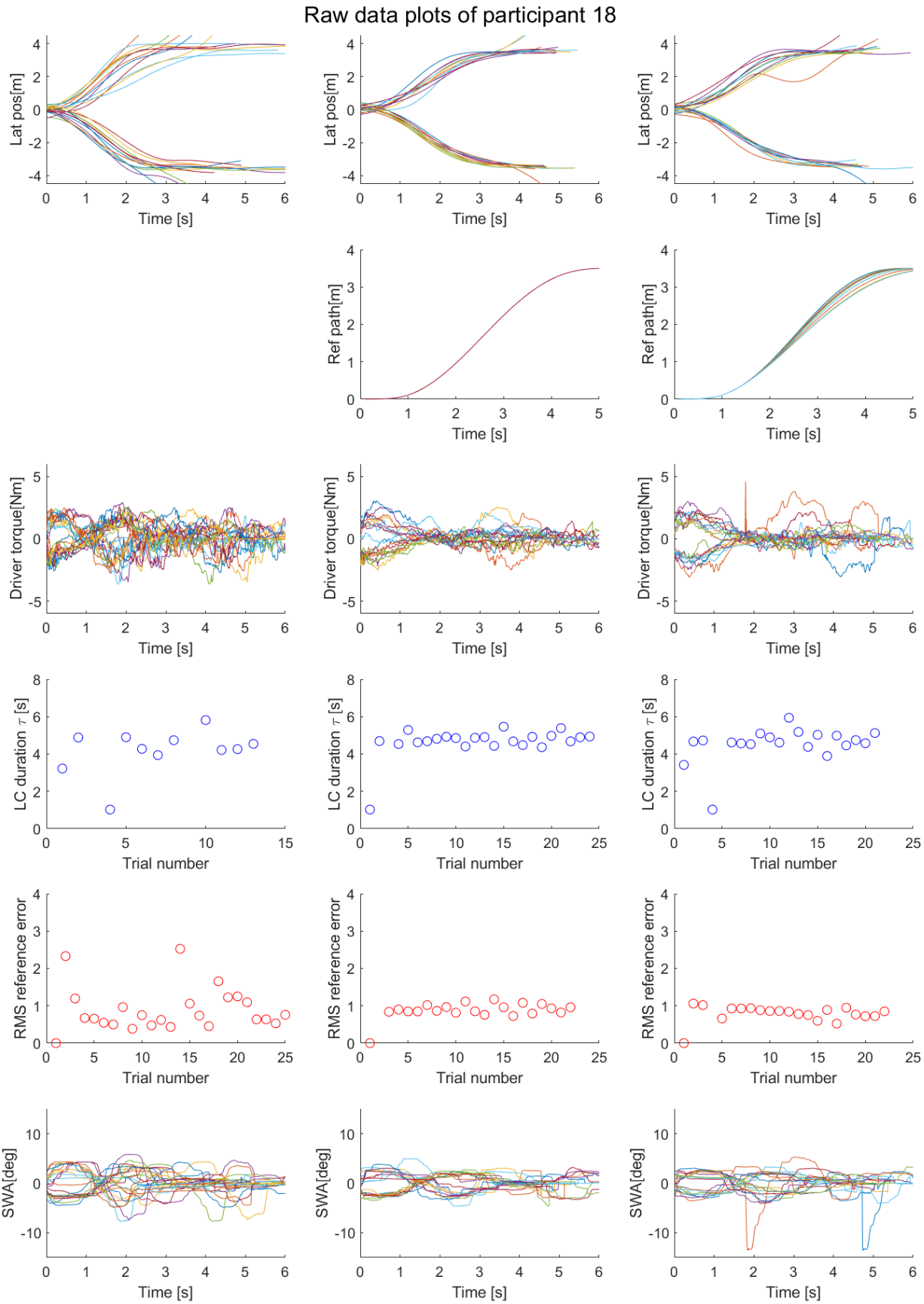
Raw data plots of participant 18
Lat pos[m]
Time [s]
Ref path[m]
Driver torque[Nm]
LC duration τ [s]
Trial number
RMS reference error
SWA[deg]

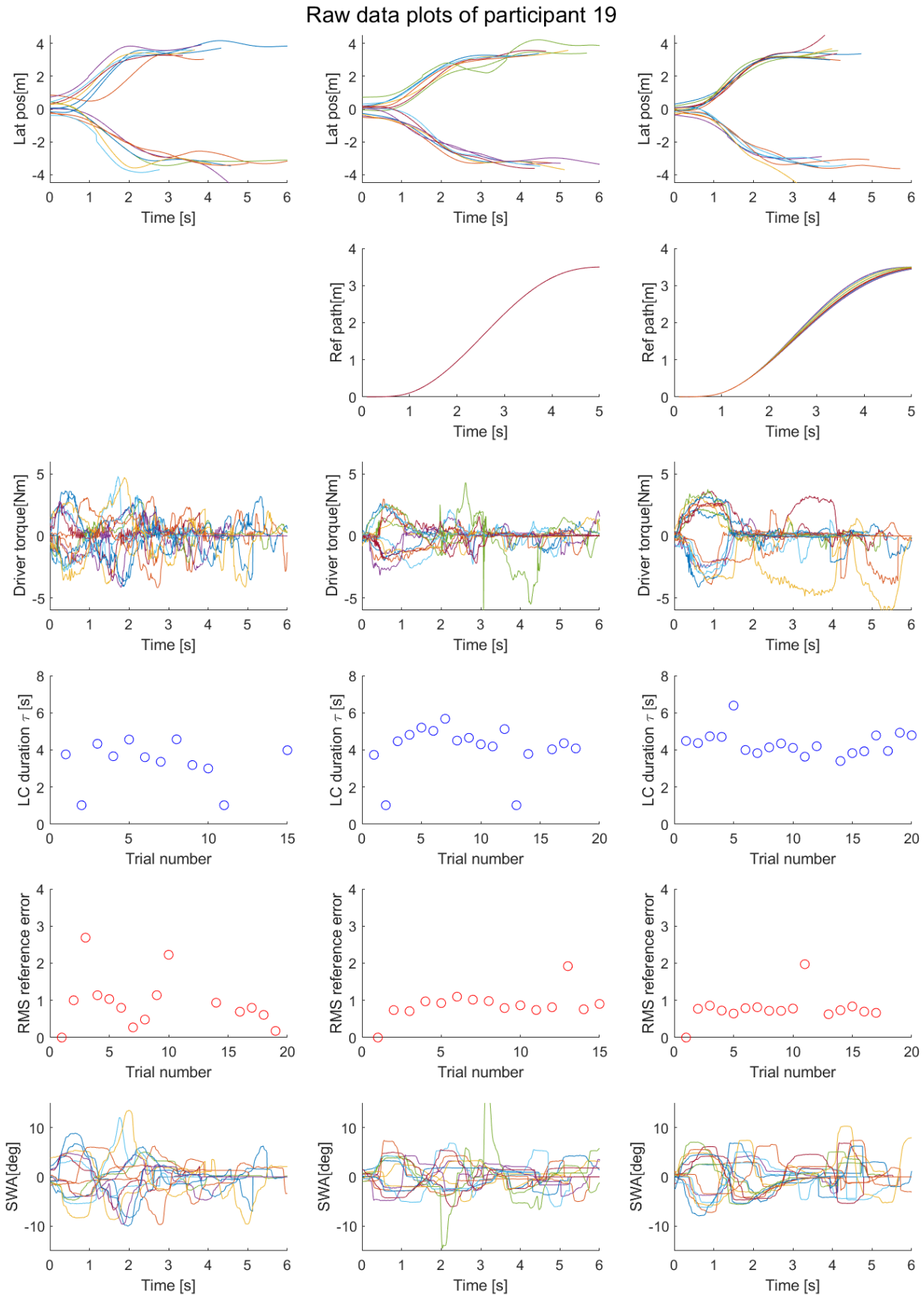
Raw data plots of participant 19
Lat pos[m]
Time [s]
Ref path[m]
Driver torque[Nm]
LC duration τ [s]
Trial number
RMS reference error
SWA[deg]

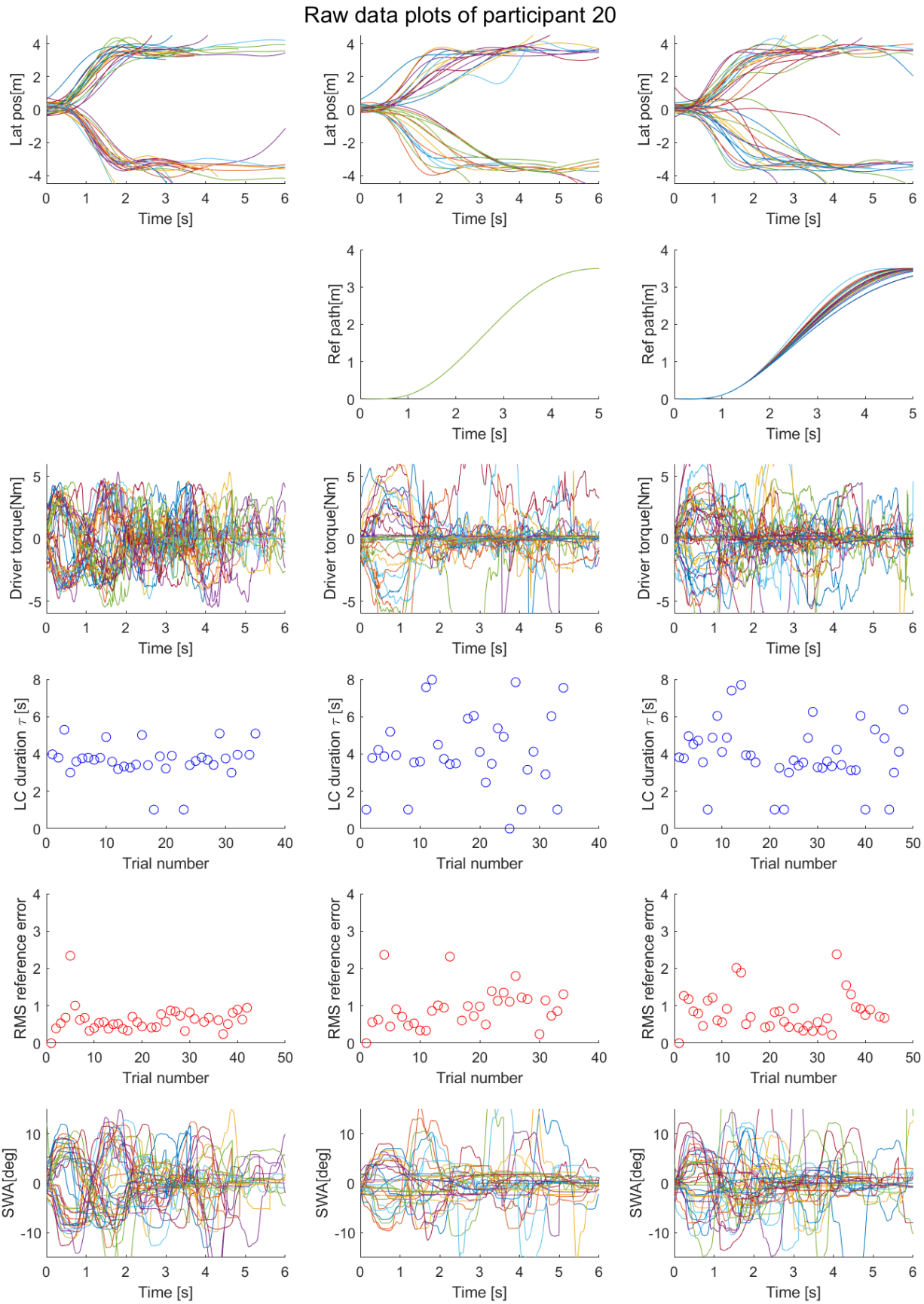
Raw data plots of participant 20
Lat pos[m]
Time [s]
Ref path[m]
Driver torque[Nm]
LC duration τ [s]
Trial number
RMS reference error
SWA[deg]

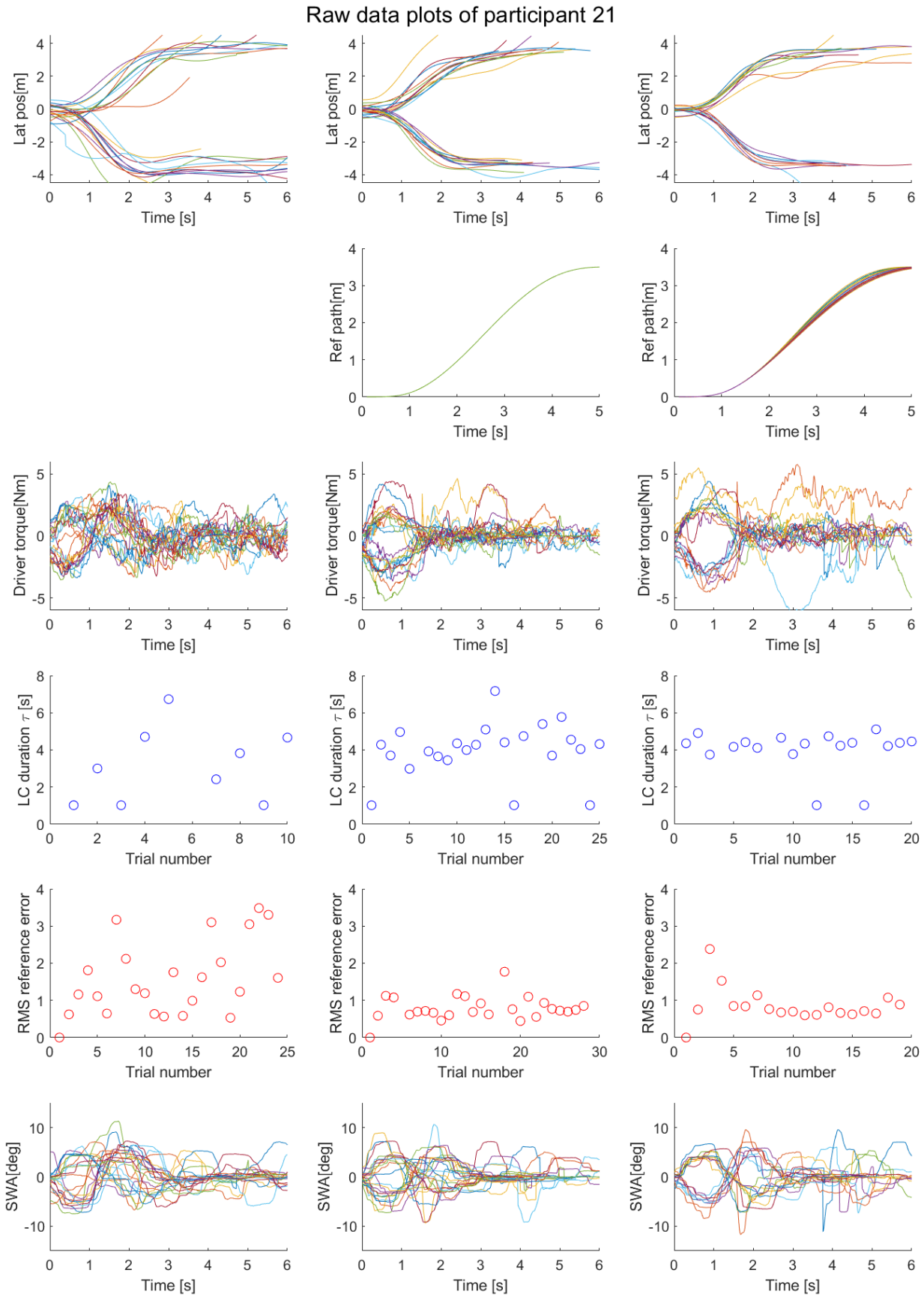
Raw data plots of participant 21
Lat pos[m]
Time [s]
Ref path[m]
Driver torque[Nm]
LC duration τ [s]
Trial number
RMS reference error
SWA[deg]

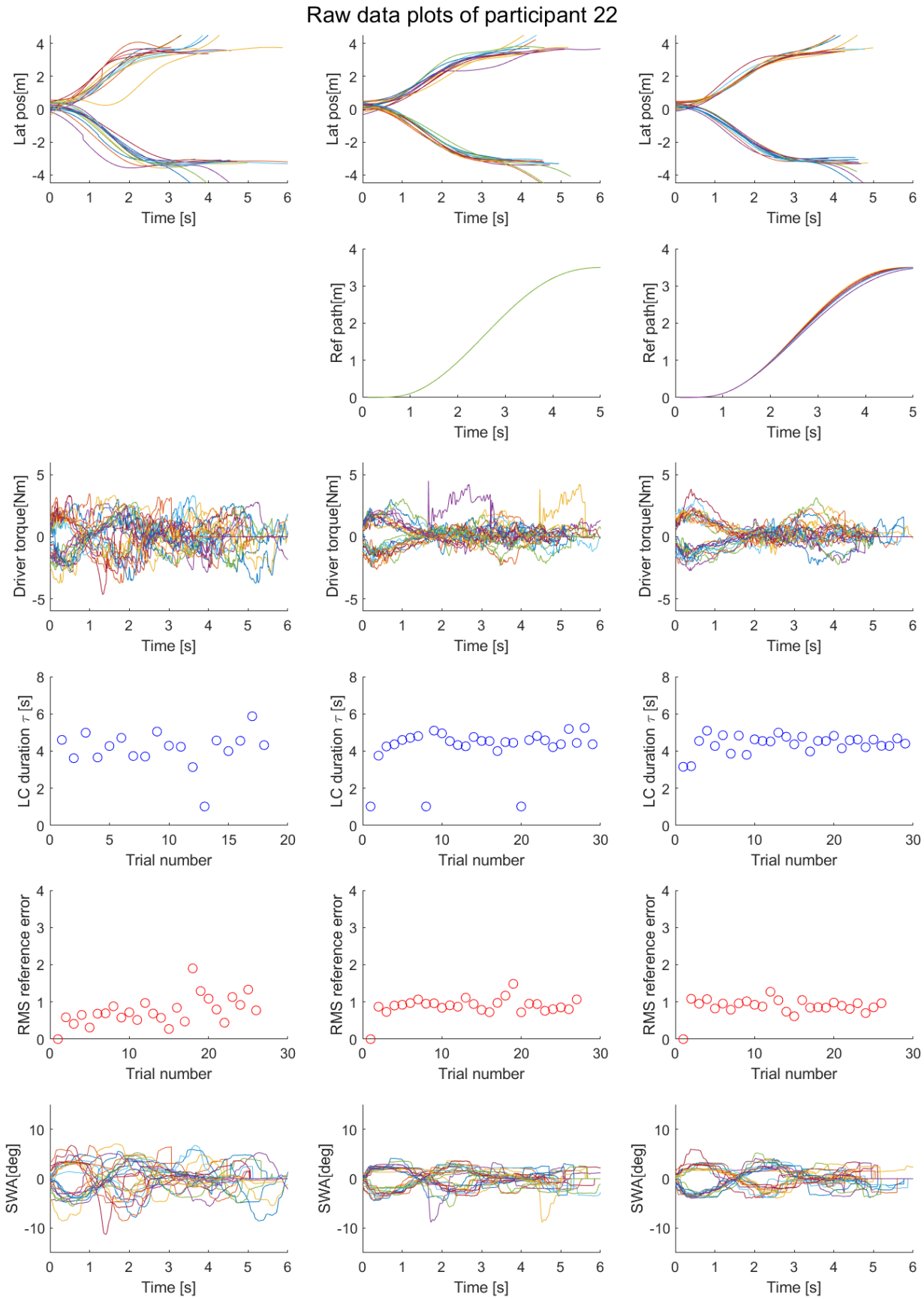
Raw data plots of participant 22
Lat pos[m]
Time [s]
Ref path[m]
Driver torque[Nm]
LC duration τ [s]
Trial number
RMS reference error
SWA[deg]

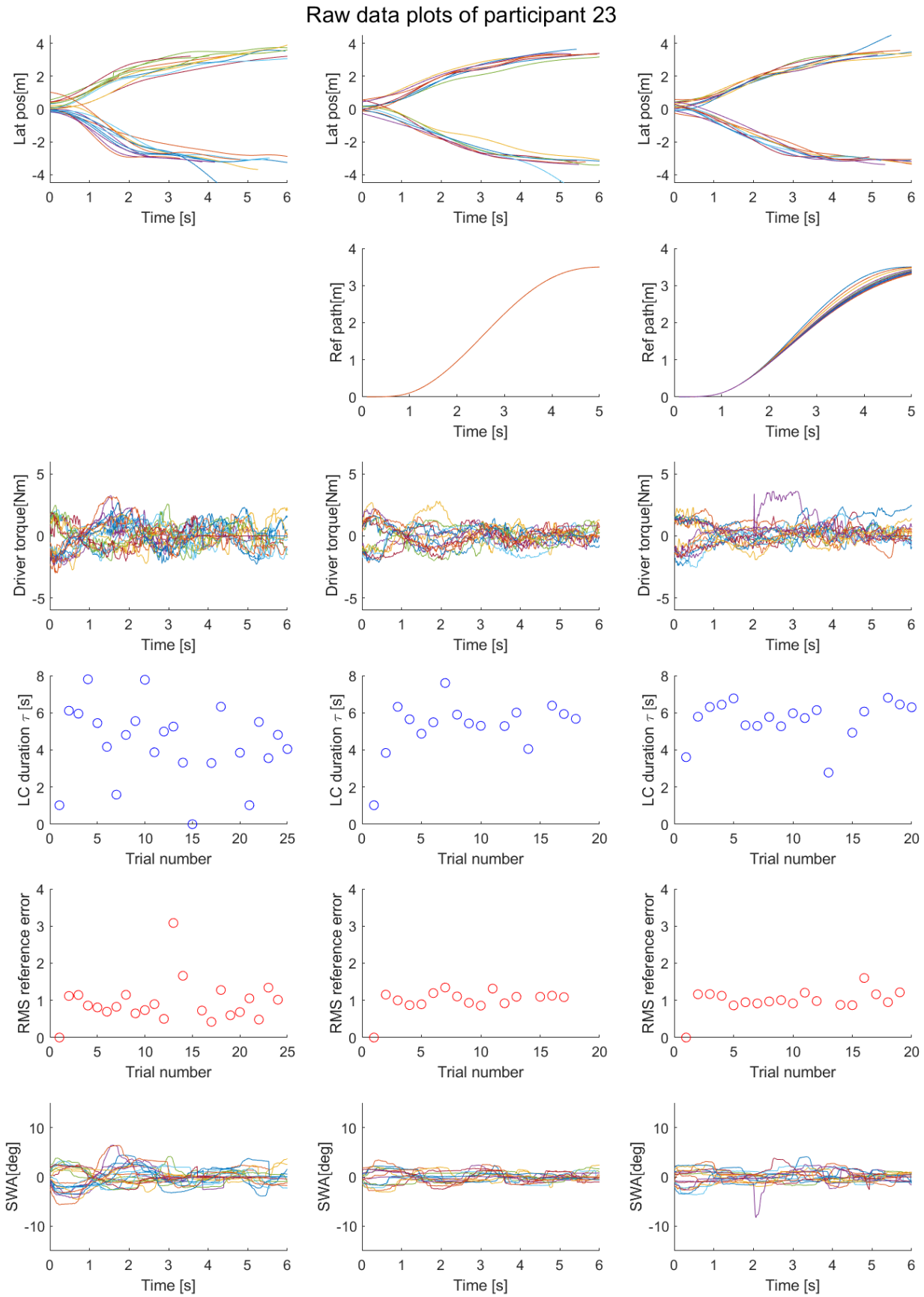
Raw data plots of participant 23
Lat pos[m]
Time [s]
Ref path[m]
Driver torque[Nm]
LC duration τ [s]
Trial number
RMS reference error
SWA[deg]

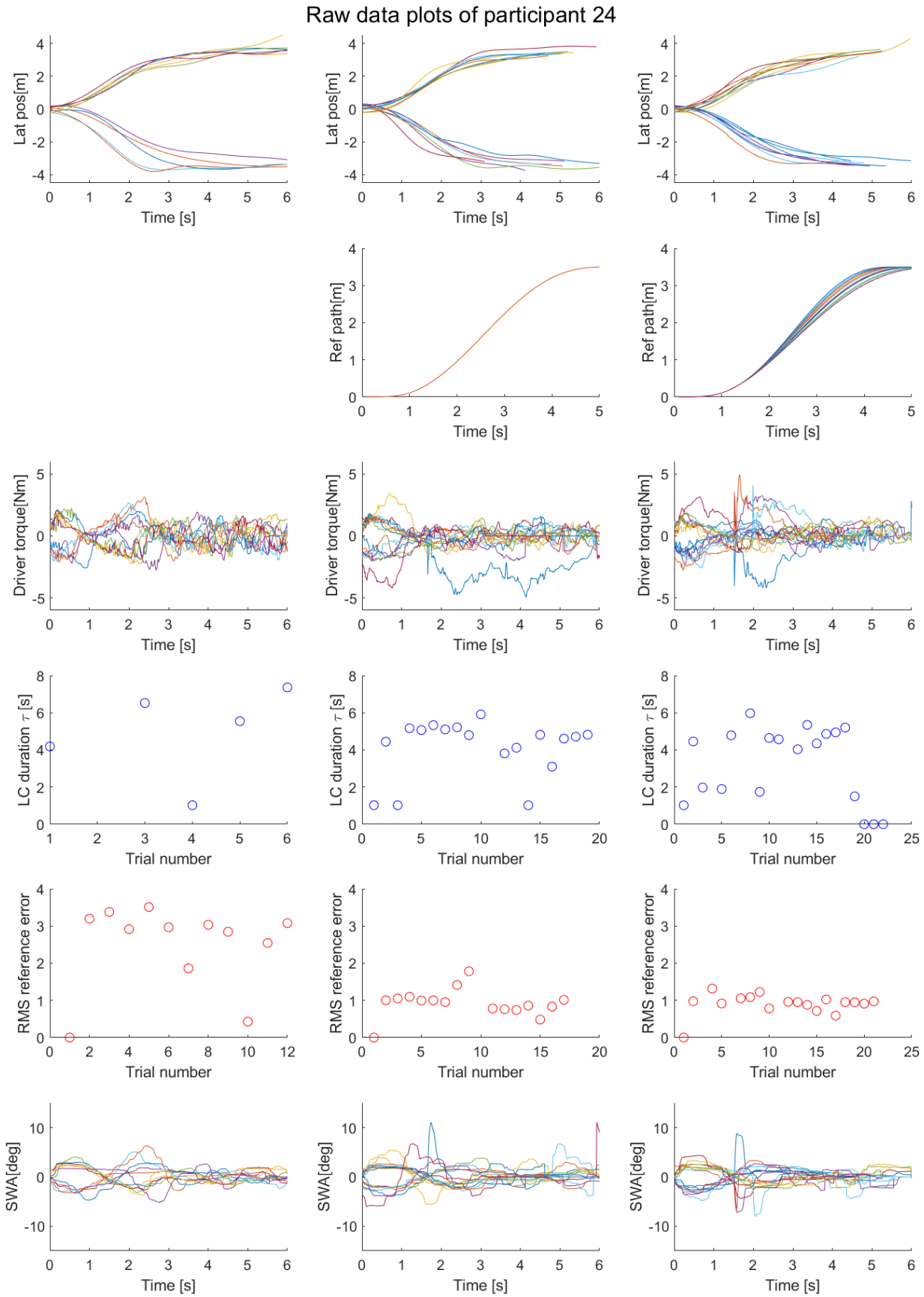
Raw data plots of participant 24
Lat pos[m]
Time [s]
Ref path[m]
Driver torque[Nm]
LC duration τ [s]
Trial number
RMS reference error
SWA[deg]

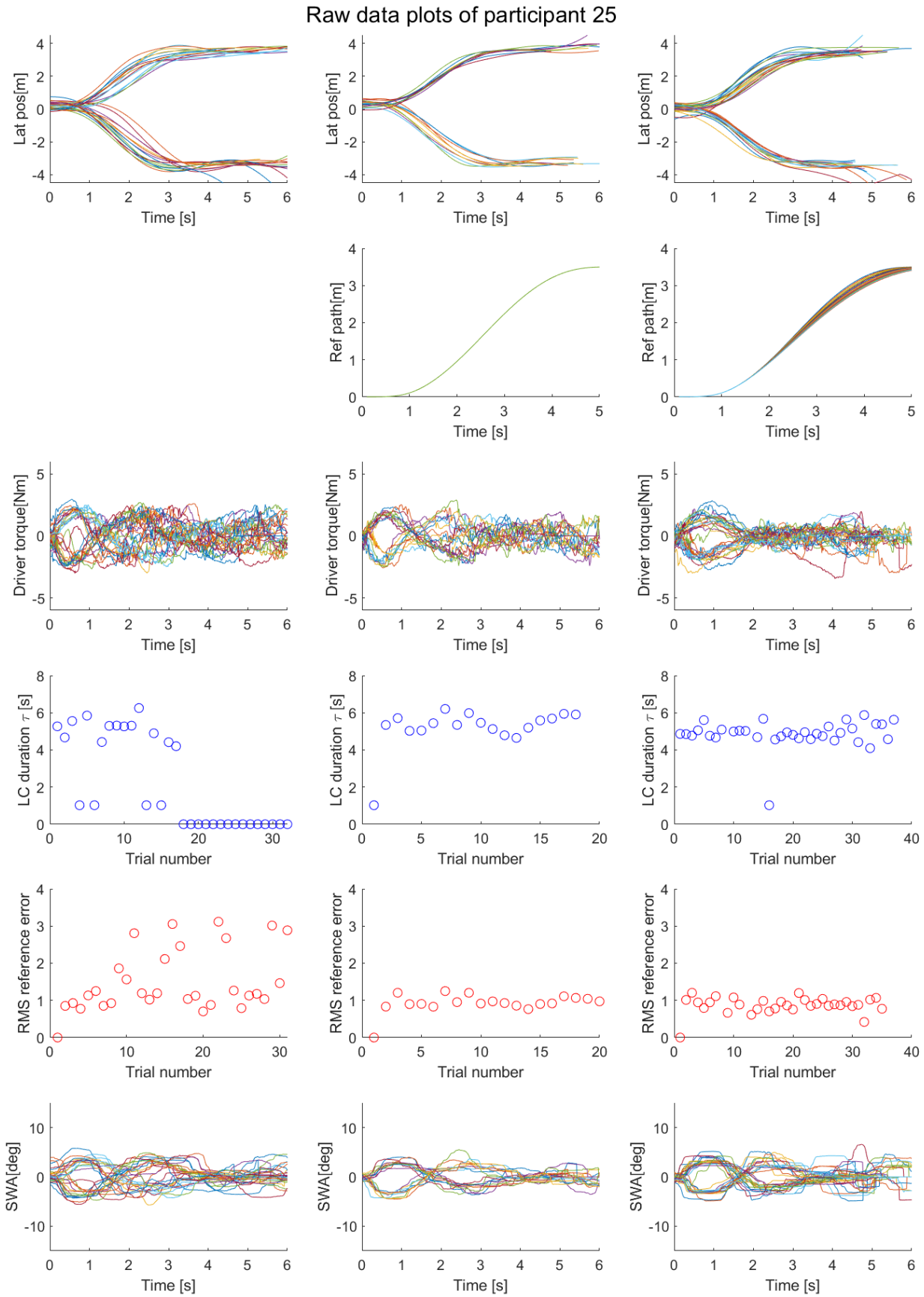
Raw data plots of participant 25
Lat pos[m]
Time [s]
Ref path[m]
Driver torque[Nm]
LC duration τ [s]
Trial number
RMS reference error
SWA[deg]

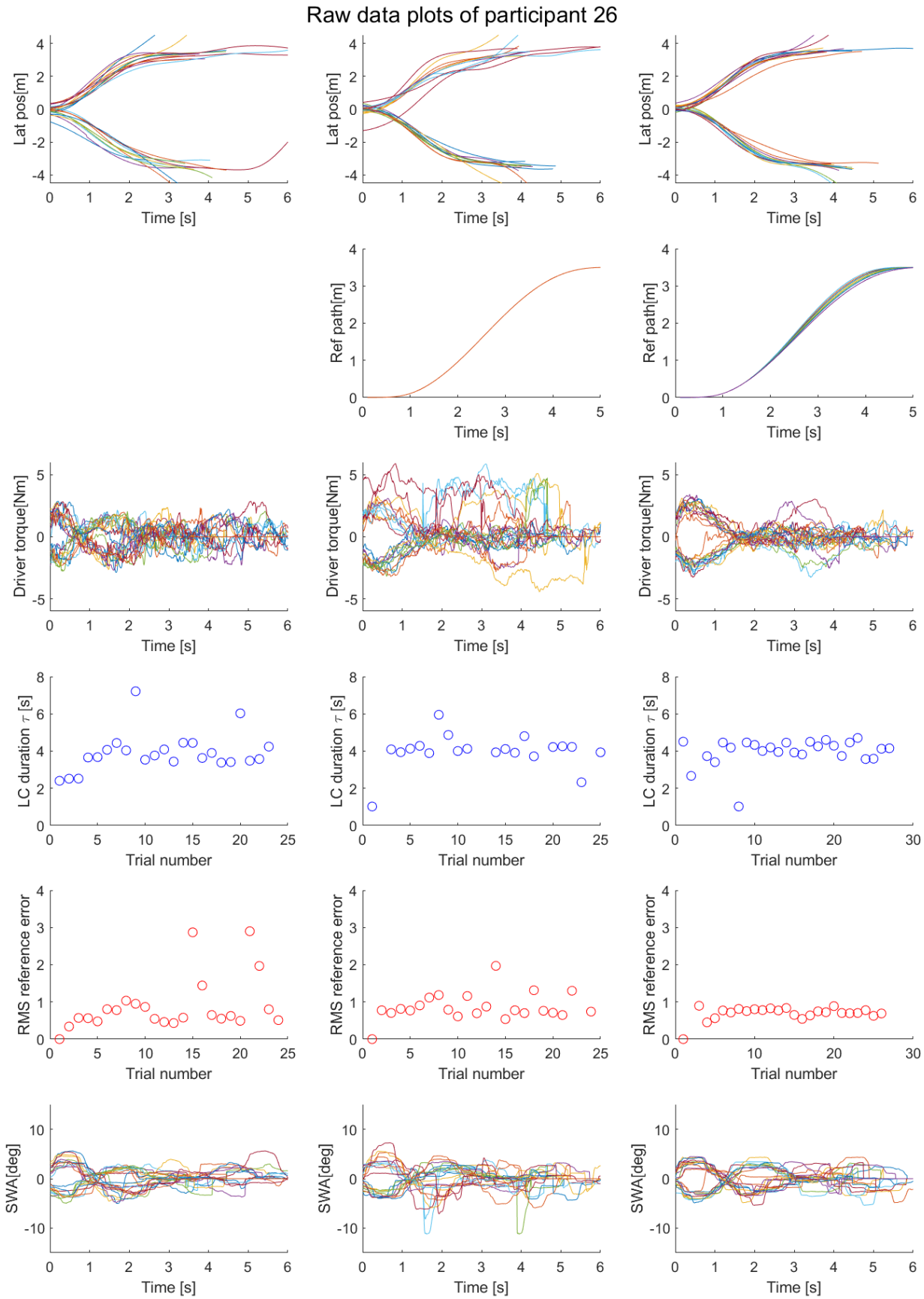
Raw data plots of participant 26
Lat pos[m]
Time [s]
Ref path[m]
Driver torque[Nm]
LC duration τ [s]
Trial number
RMS reference error
SWA[deg]

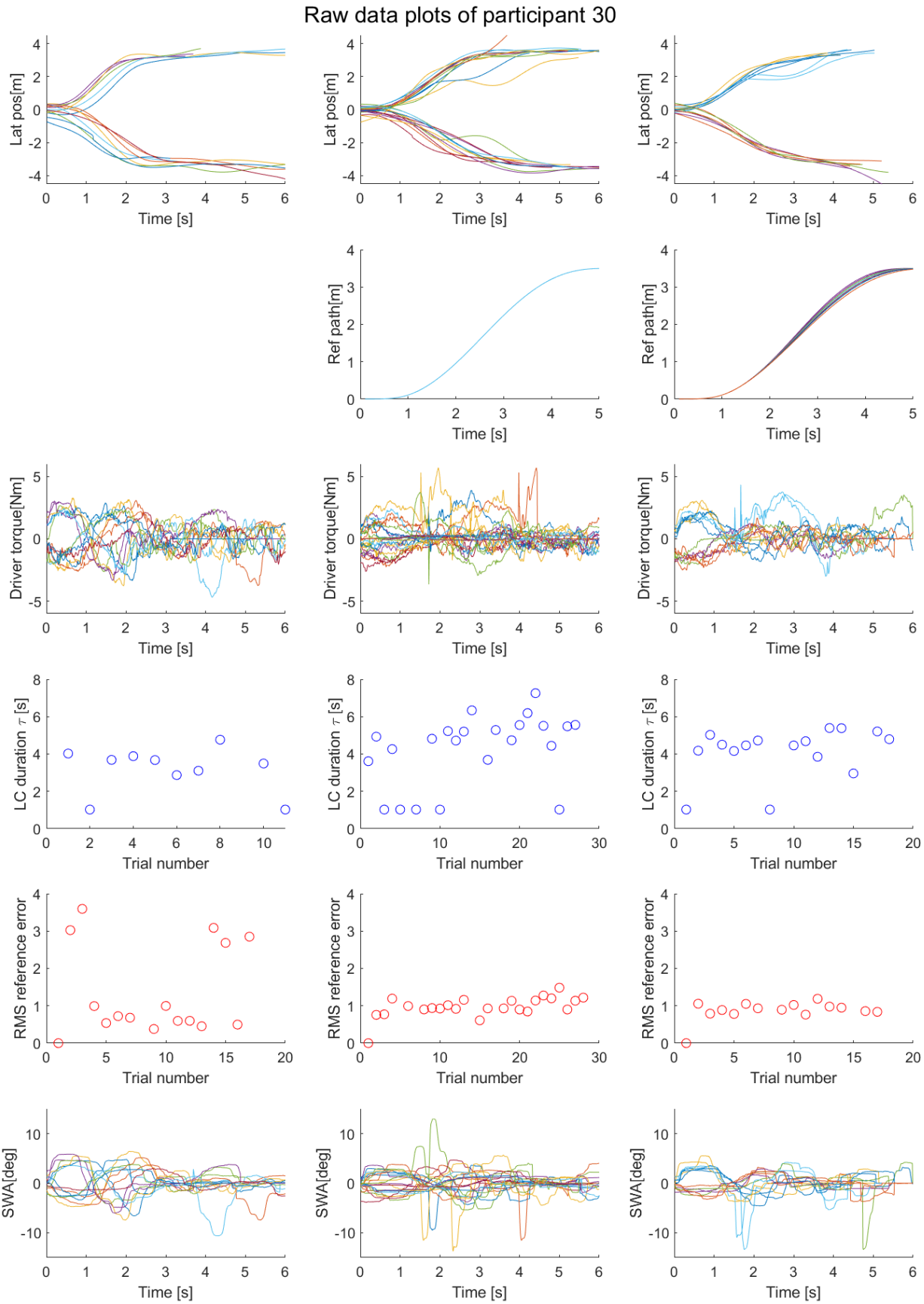
Raw data plots of participant 30
Lat pos[m]
Time [s]
Ref path[m]
Driver torque[Nm]
LC duration τ [s]
Trial number
RMS reference error
SWA[deg]

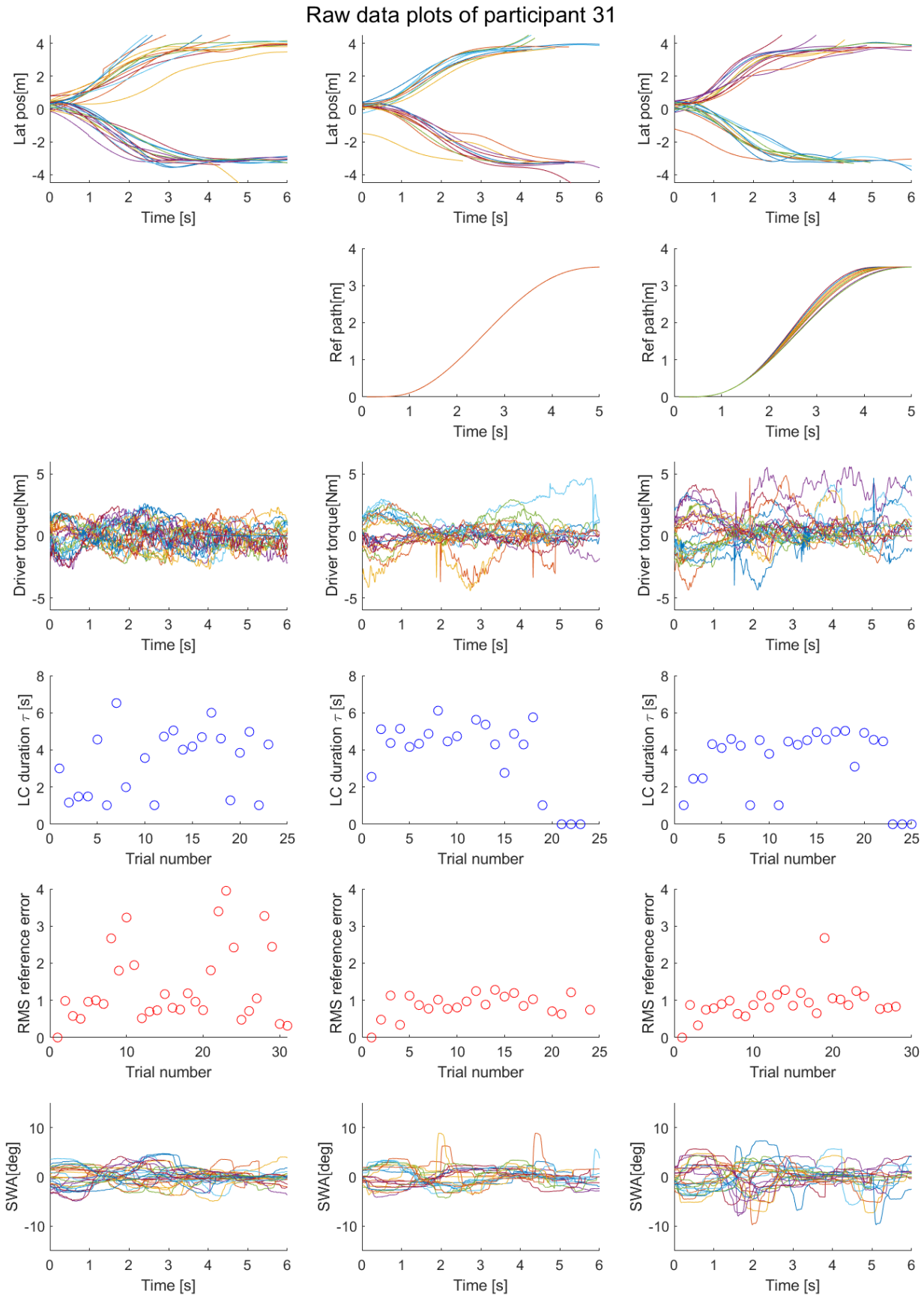
Raw data plots of participant 31
Lat pos[m]
Time [s]
Ref path[m]
Driver torque[Nm]
LC duration τ [s]
Trial number
RMS reference error
SWA[deg]

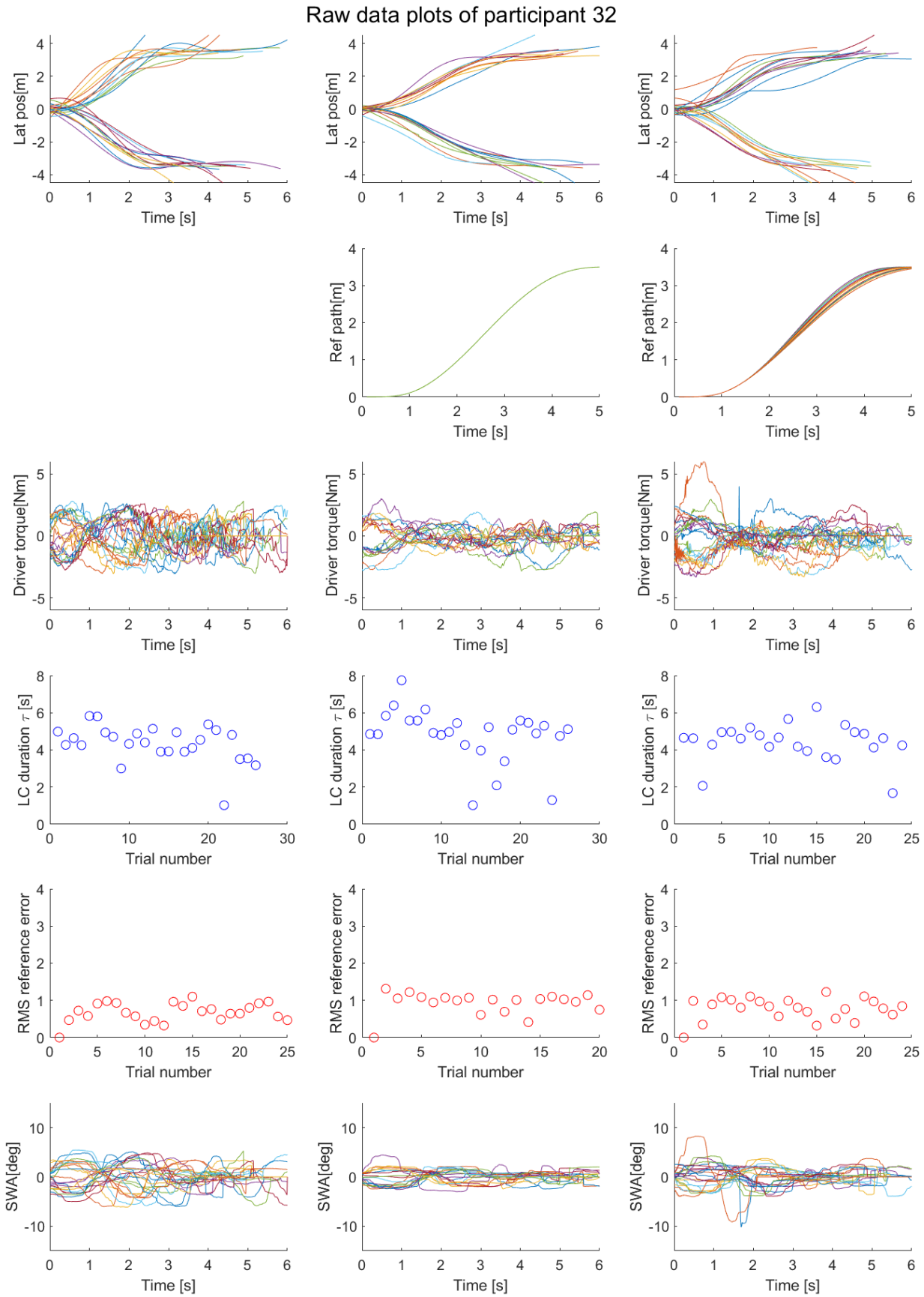
Raw data plots of participant 32
Lat pos[m]
Time [s]
Ref path[m]
Driver torque[Nm]
LC duration τ [s]
Trial number
RMS reference error
SWA[deg]

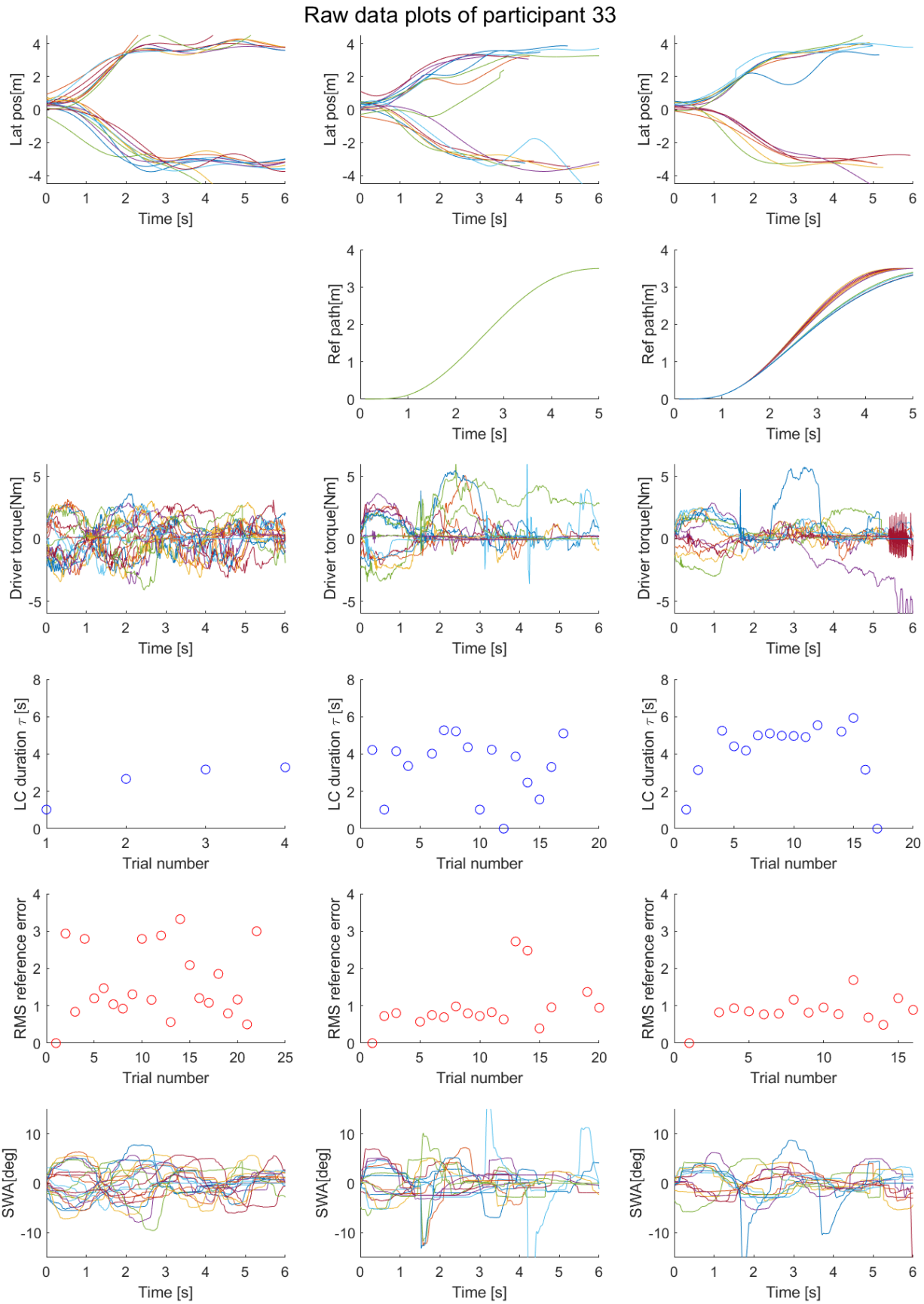
Raw data plots of participant 33
Lat pos[m]
Time [s]
Ref path[m]
Driver torque[Nm]
LC duration τ [s]
Trial number
RMS reference error
SWA[deg]

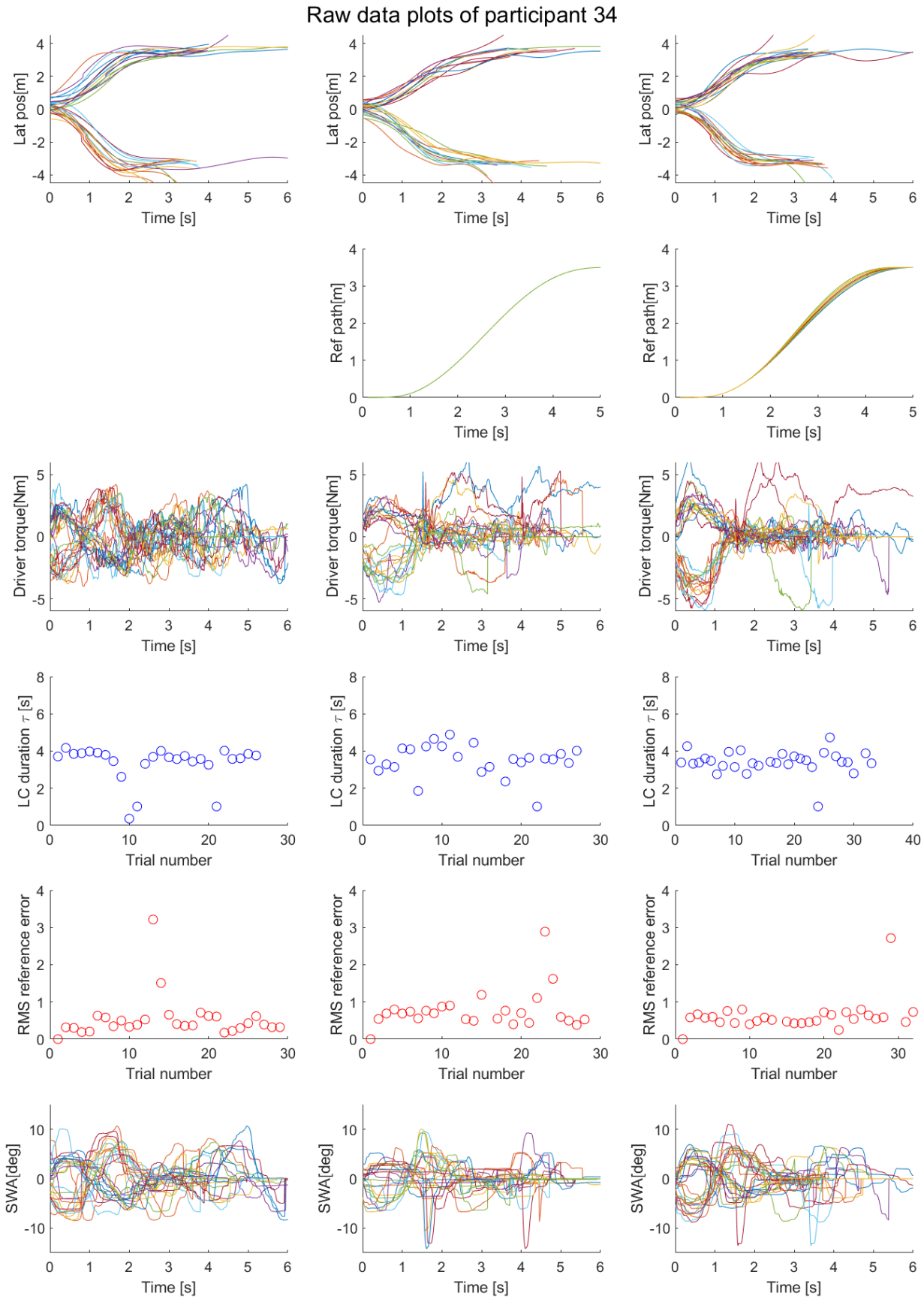
Raw data plots of participant 34
Lat pos[m]
Time [s]
Ref path[m]
Driver torque[Nm]
LC duration τ [s]
Trial number
RMS reference error
SWA[deg]

Appendix C

Thesis Timeline

Thesis Timeline

Nico James van Leeuwen

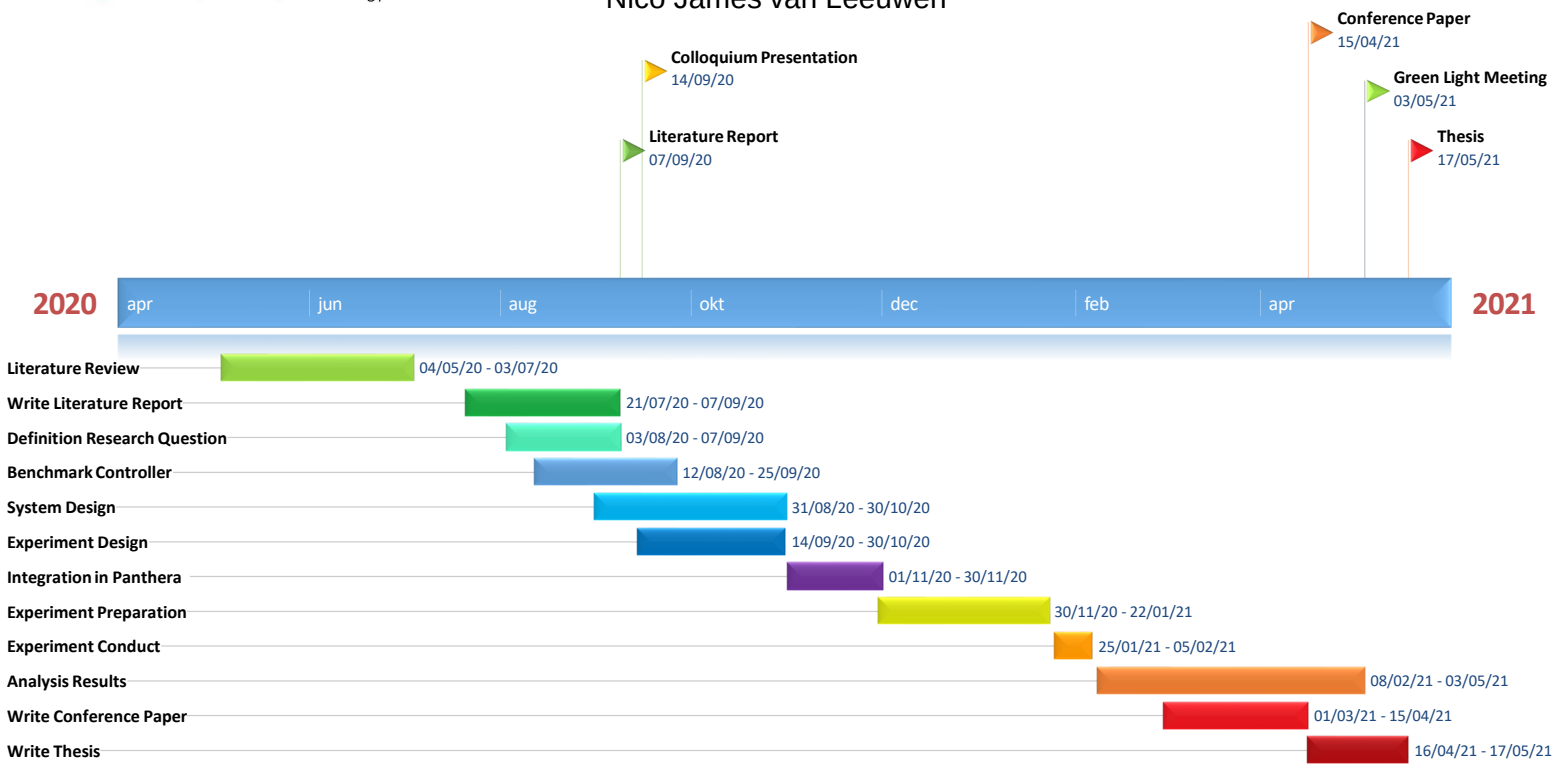

Appendix D

Experiment Participant Forms

D-1 Demographics Questionnaire

Demographics Questionnaire:

Lane change assistance analysis on a motion-based driving simulator

Please answer the questions truthfully to the best of your ability

What is your age? _____

What is your gender? _____

For how many years do you own a driver's license? _____

How many hours do you drive per week on average? _____

Do you have prior experience driving with cruise control? **YES** ☐ **NO** ☐

If yes, how many hours of driving per week on average? _____

Do you have prior experience driving with lane keeping assist? **YES** ☐ **NO** ☐

If yes, how many hours of driving per week on average? _____

Do you have prior experience driving on a driving simulator? **YES** ☐ **NO** ☐

If yes, how many hours of driving per week on average? _____

D-2 Van der Laan Questionnaire for User Acceptance

Acceptance Questionnaire:

Lane change assistance analysis on a motion-based driving simulator

Please tick the appropriate boxes

What is your judgement about the first system you have driven with?

USEFUL	☐ ☐ ☐ ☐ ☐	USELESS
PLEASANT	☐ ☐ ☐ ☐ ☐	UNPLEASANT
BAD	☐ ☐ ☐ ☐ ☐	GOOD
NICE	☐ ☐ ☐ ☐ ☐	ANNOYING
EFFECTIVE	☐ ☐ ☐ ☐ ☐	SUPERFLUOUS
IRRITATING	☐ ☐ ☐ ☐ ☐	LIKEABLE
ASSISTING	☐ ☐ ☐ ☐ ☐	WORTHLESS
UNDESIRABLE	☐ ☐ ☐ ☐ ☐	DESIRABLE
RAISING AWARENESS	☐ ☐ ☐ ☐ ☐	SLEEP-INDUCING

Please tick the appropriate boxes

What is your judgement about the second system you have driven with?

USEFUL	☐ ☐ ☐ ☐ ☐	USELESS
PLEASANT	☐ ☐ ☐ ☐ ☐	UNPLEASANT
BAD	☐ ☐ ☐ ☐ ☐	GOOD
NICE	☐ ☐ ☐ ☐ ☐	ANNOYING
EFFECTIVE	☐ ☐ ☐ ☐ ☐	SUPERFLUOUS
IRRITATING	☐ ☐ ☐ ☐ ☐	LIKEABLE
ASSISTING	☐ ☐ ☐ ☐ ☐	WORTHLESS
UNDESIRABLE	☐ ☐ ☐ ☐ ☐	DESIRABLE
RAISING AWARENESS	☐ ☐ ☐ ☐ ☐	SLEEP-INDUCING

Please tick the appropriate boxes

What is your judgement about the third system you have driven with?

USEFUL	☐ ☐ ☐ ☐ ☐	USELESS
PLEASANT	☐ ☐ ☐ ☐ ☐	UNPLEASANT
BAD	☐ ☐ ☐ ☐ ☐	GOOD
NICE	☐ ☐ ☐ ☐ ☐	ANNOYING
EFFECTIVE	☐ ☐ ☐ ☐ ☐	SUPERFLUOUS
IRRITATING	☐ ☐ ☐ ☐ ☐	LIKEABLE
ASSISTING	☐ ☐ ☐ ☐ ☐	WORTHLESS
UNDESIRABLE	☐ ☐ ☐ ☐ ☐	DESIRABLE
RAISING AWARENESS	☐ ☐ ☐ ☐ ☐	SLEEP-INDUCING

D-3 Informed Consent Form

1 Research Group

1.1 Researchers in charge of the project

Nico van Leeuwen[1]	Master Student	Delft University of Technology
Christiaan Koppel[2]	Project Engineer	Cruden B.V.
Barys Shyrokau[1]	Assistant Professor	Delft University of Technology
David Abbink[1]	Full Professor	Delft University of Technology

1.2 Organizations

1. Department of Cognitive Robotics; Faculty of Mechanical, Maritime and Materials Engineering; Delft University of Technology; Delft, the Netherlands
2. Cruden B.V.; Amsterdam, the Netherlands

---

2 This document

This informed consent form has two parts:

- **Information sheet,** pages 1-6
- **Consent form,** page 7

Before agreeing to participate in this study, you are asked to read this document carefully. The information sheet describes the purpose, procedures, and risks of this study. After reading the information sheet, feel free to ask questions about any part that seems unclear or sections that you do not understand. You should feel comfortable to speak to all of the researchers involved to answer any questions you may have at any time. After you have read this information sheet and all your question are answered and any concerns are discussed, you can decide if you would like to be involved. At the end of this document, we would like to ask you to sign a written consent form to confirm your agreement to participate. Your signature is required for participation.

---

3 Purpose of the research

Advanced Driver Assistance Systems (ADAS) are currently being deployed in the majority of new vehicles. One of these systems is Lane Keeping Assistance (LKA), which helps the driver to stay in the current lane when driving on the highway. This system lowers the workload of the driver and decreases unintentional lane and road departures. However, when the driver wishes to change lanes to overtake another vehicle, the LKA system can not provide assistance and therefore the driver is expected to retake full control of the vehicle. This requires a large increase of workload and subsequently reduces safety and driving comfort. Therefore an extension of this system is proposed to assist the driver during a lane change maneuver: This Lane Change Assistance (LCA) system will provide haptic feedback through steering torque. Since a lane

change maneuver is subject to large intra- and inter-driver variability, the proposed system will adapt to the personal preferences of the driver. The purpose of this research is to determine the effectiveness of the proposed system's capability to reduce workload during lane change maneuvers. Furthermore, the effect of the adaptive quality of the system on intention conflict between the system and the driver will be investigated. The knowledge obtained during this simulator study could be used to create lane change assistance systems for vehicles of the future.

---

4 Participation

4.1 Location of the experiment

Participation will involve completing a driving experiment on the automotive simulator at Cruden B.V. Global Headquarters, Pedro de Medinalaan 25, 1086 XP Amsterdam, the Netherlands.

4.2 Eligibility criteria

You are invited to participate in this project if:

- You are 18 years or older.
- You have a car driving license.
- You have normal or corrected-to-normal vision (i.e. glasses or contact lenses).
- You have not experienced severe (simulator) motion sickness in the past.
- You do not have heart, back or neck issues.
- You have not been diagnosed with epilepsy.
- You are not pregnant.
- You have not recently had surgery.
- You are not physically disabled.
- You are not under the influence of drugs, alcohol or prescription substances that may compromise the comfort when operating a motion-based driving simulator.

The researchers reserve the right at any time to refuse or excuse any participant who no longer meets the study requirements or who are behaving in an unnecessarily unsafe manner.

4.3 Voluntary participation

Your participation in this project is completely voluntary. We welcome you to contact us to ask any questions and to discuss your possible involvement in the project, you have the right to refuse participation at any moment. If you do agree to participate you have the right to withdraw from the project at any moment without comment or penalty.

5 Procedure

The research consists of a driving experiment on a motion-based automotive simulator. The experiment will retrieve lane change data with the aim of analysing the effectiveness of the proposed lane change assistance system. The driving data will be logged by the driving simulator.

5.1 Prior to the experiment

Prior to the experiment, the informed consent form will be sent to you. When you visit the location of the experiment, the study details will be explained to you and you will be asked to sign the informed consent form. After this a demographics questionnaire will be completed for the statistical analysis of the results. Finally, a safety instruction for operating the driving simulator will be given.

5.2 Practice session on simulator

The experiment will start with some practice to familiarise yourself with the simulator, the virtual environment and the procedure of starting an experiment. The practice session takes around 5 minutes and you are encouraged to drive both fast and slow to get a feeling of the dynamics of the simulated vehicle.

5.3 Experiment

You will be asked to perform three driving sessions of approximately ten minutes in a highway scenario. Between the sessions, there will be a short break. You will be requested to execute an n-back working memory task whilst driving. During driving, interaction with surrounding traffic will be simulated. The simulated vehicle is a generic sedan car and is controlled in the same way as a normal car. A dashboard with speedometer is available as well as two side view mirrors and one rear view mirror.

5.3.1 Controls

In addition to common controls such as steering wheel, accelerator and brake pedal, the vehicle in the driving simulator will have the functionality of cruise control. You will be requested to maintain a velocity of 100 km/h throughout the session by using the cruise control functionality. Please drive as you normally would and use the steering wheel for keeping the car in the lane, as well as for changing lanes when overtaking slower vehicles. You are urged to use the turning signal when changing lanes in both directions.

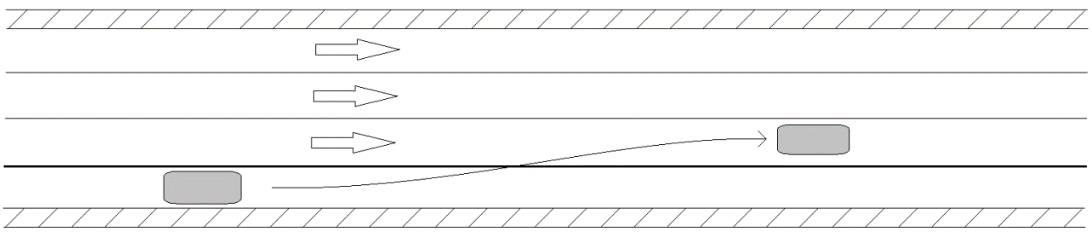

5.3.2 Scenario

Each driving session will start from standstill on the emergency lane on the right side of a three-lane highway. You will be asked to accelerate to 100km/h and and merge into the rightmost driving lane by changing one lane to the left. During the experiment other road users will be driving on the road. You are asked to treat them as you would treat normal road users. The scenario consists of multiple driving situations on a highway in which overtaking a slow lead vehicle is desirable. You are asked to overtake this slow lead vehicle as you normally would, in a safe manner. You are asked to return to the right lane after overtaking.

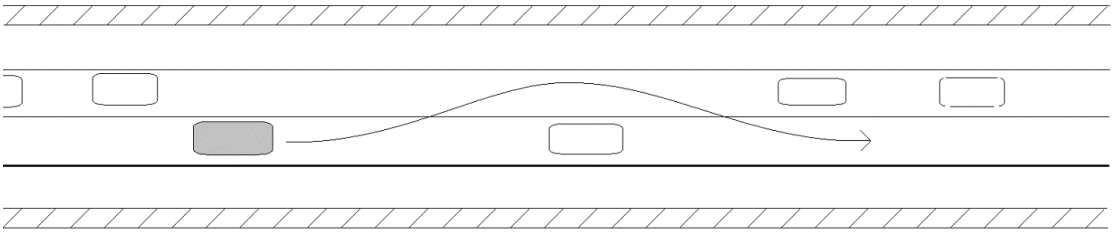

5.4 Duration

The total time commitment will amount to approximately 45 minutes and consists of signing the consent form, driving in the simulator practice session, executing the experiment including breaks and completing questionnaires.

5.5 COVID-19 precautions

To minimize the risk of COVID-19 infection for the participant and operator of the experiment, both are required to wear a face mask before and after the experiment. During the experiment, a safe distance of at least 3 meter is guaranteed. To minimize the risk of transmission amongst participants, all materials used during the experiment will be disinfected after each participant and a time buffer will be planned between participants to ensure they will not overlap. The participant and the operator will be the only two people present on the location of the experiment.

---

6 Expected benefits

It is not expected that the project directly benefits you. However, your participation in this study will add to our understanding of Advanced Driver Assistance Systems (ADAS) and the interaction of these systems with human drivers. In this way your participation will assist in developing new approaches to improve driver safety and comfort.

---

7 Risks associated with participation

Participants may experience simulator motion sickness. In case a participant experiences such sickness, the experiment can be stopped at any time. An emergency switch is available to both the operator and the participant, which will stop the simulation immediately.

Participants are instructed to wear their seat belt during the entire simulation. The seat belt can be unbuckled when the simulation has stopped and the operator has given permission to do so. Unbuckling of the seat belt during simulation will shut down the simulation.

Taking place on the simulator requires you to climb up a small staircase, which might result in an accidental fall. The participant may only enter the simulator when the simulator is shut-down, to avoid tripping due to motion of the simulator. During the experiment, an operator ensures safe conduct of operation of the driving simulator. If the operator notices unsafe or unwanted behavior of the simulator or participant, the experiment may be terminated prematurely.

Losing control of the vehicle can result in a collision with the guard rail or other objects. However, the guard rail and surrounding vehicles are non-solid objects, so a participant can drive through them without physically experiencing a collision. Riding through a non-solid object can be an emotionally uncomfortable experience.

---

8 Privacy and confidentiality

All comments and responses are anonymous and will be treated confidentially. The names of individual persons are not required in any of the responses. Publications or presentations of the results will not include any information that could identify you.

Any data collected as part of this project will be stored securely as per TU Delft's Research Data Management policy. Only the researchers involved in the project will have access to this information. Please note that non-identifiable data from this project may be used as comparative data in future projects or stored on an open access database for secondary analysis.

---

9 Responsibility

The researchers, funding bodies or institutions involved do not bear any responsibility for possible inconveniences or damages during travel to or from the location of the experimental activity.

---

10 Questions about the project

If you wish to ask questions about the project or require further information, please contact one of the researchers below:

Researcher	**E-mail**	**Phone**
Nico van Leeuwen	N.J.vanLeeuwen@student.tudelft.nl	+31(0)6 4002 0373
Christiaan Koppel	C.Koppel@cruden.com	
Barys Shyrokau	B.Shyrokau@tudelft.nl	
David Abbink	D.A.Abbink@tudelft.nl	

---

11 Ethical approval and complaints

This study has been approved by the Human Research Ethics Committee (HREC). If needed, verification of approval can be obtained by writing to the mail or e-mail address of the HREC, noted at the end of this section. If you have any concerns or complaints about the ethical conduct of the project, any of the abovementioned involved researchers can be contacted. In case this does not resolve your concern you may contact the HREC, which is not connected with the research project and can facilitate a solution to your concern in an impartial manner. Name of the experiment according to the Ethics Approval Application: *Lane change assistance analysis on a motion-based driving simulator*.

Contact Details HREC:
P.O. Box 5015
2600 GA Delft
The Netherlands

HREC@tudelft.nl

Consent Form for:

Lane change assistance analysis on a motion-based driving simulator

Please tick the appropriate boxes

Taking part in the study	**YES**	**NO**
I have read and understood the study information dated Friday 22nd January, 2021, or it has been read to me. I have been able to ask questions about the study and my questions have been answered to my satisfaction.	☐	☐
I consent voluntarily to be a participant in this study and understand that I can refuse to answer questions and I can withdraw from the study at any time, without having to give a reason.	☐	☐
I understand that taking part in the study involves the logging of driving data and the completing of questionnaires.	☐	☐
Risks associated with participating in the study		
I understand that taking part in the study involves the following risks: motion sickness due to movement of the simulator. Emotional discomfort due to the possibility of experiencing a collision scenario.	☐	☐
Use of the information in the study		
I understand that information I provide can be used for presentation in scientific and driving simulator seminars and conferences and published as master theses, PhD theses and articles in scientific journals.	☐	☐
I understand that personal information collected about me that can identify me will not be shared beyond the researchers.	☐	☐
Future use and reuse of the information by others		
I give permission for the driving simulator data that I provide to be archived in TU Delft repository so it can be used for future research and learning	☐	☐

Name of participant	Signature	Date

I have accurately read out the information sheet to the potential participant and, to the best of my ability, ensured that the participant understands to what they are voluntary consenting.

Nico van Leeuwen

Name of researcher	Signature	Date

Appendix E

Driving Simulator Conference Paper

Analysis of a trial-by-trial adaptive lane change assistance system on a motion-based simulator

Nico James van Leeuwen[1], Barys Shyrokau[1], Christiaan Koppel[2] and David Abbink[1]

(1) Delft University of Technology, Mekelweg 2, 2628 CD Delft, The Netherlands, e-mail: N.J.vanLeeuwen@student.tudelft.nl; B.Shyrokau@tudelft.nl; D.A.Abbink@tudelft.nl

(2) Cruden B.V., Pedro de Medinalaan 25, 1086 XP Amsterdam, The Netherlands, e-mail: C.Koppel@cruden.com

Abstract - *This study proposes a haptic Lane Keeping Assistance (LKA) system that adapts its provided reference trajectory to accommodate lane changes. This system enables continuous support in the lateral control task during highway driving. Two different system configurations of this Lane Change Assistance (LCA) are investigated. One is a generalized LCA and one is an adaptive LCA that learns personalized lane change trajectories through trial-by-trial adaptation to preferred lane change duration. The effects of these systems with respect to mental workload, collaborative performance and user acceptance are investigated. This is done during an experiment with three different driving sessions, consisting of a manual session and two sessions in which either the generalized or adaptive LCA is active. The experiments are executed on a 6 DoF motion-based simulator with 34 participants, driving in a simulated three-lane highway environment with a scripted traffic scenario. To measure mental workload, an auditory cognitive secondary N-back task is introduced. The results show that the introduction of a generalized LCA or adaptive LCA does not have significant influence on mental workload compared to the manual driving session. When the adaptive LCA is introduced, collaborative performance is enhanced and user acceptance is increased compared to the generalized LCA.*

Keywords: *lane change assistance, trial-by-trial adaptation, haptic shared control, mental workload, simulator*

Introduction

To enable a transition from SAE automation level 2 to level 3, it is important to consider integration of longitudinal and lateral assistance systems. German road statistics of 2017 *(Statistisches Bundesamt, 2018)* show that lane changing is the third largest cause of fatal accidents after speeding and incorrect road use. However, current Lane Keeping Assist (LKA) systems do not provide support during lane changes. Lane keeping functionality is switched off when the indicator light is engaged. Therefore, this paper proposes an LKA system with integrated lane changing capability to enable continuous lateral support during highway driving.

The increasing amount of installed ADAS systems require an effective and safe cooperation between these systems and the human driver. Haptic Shared Control (HSC) is a commonly encountered solution to balance the control authority between ADAS and drivers *(Lazcano, et al., 2021)*. To increase collaborative performance *(Dintel, et al., 2020)* and enhance user acceptance *(Chen and Wang, 2018)*, adaptation to a driver's personal preferences is desirable.

This can be done by implicit or explicit personalization, adapting either to observed user data or explicitly stated preference settings, respectively *(Hasenjager and Wersing, 2018)*. Implicit personalization is expected to be more effective, since up to 67% of drivers have been shown to incorrectly identify their own driving style when explicitly stating their preferred driving style *(Basu, et al., 2017)*.

Driving behaviour varies widely between drivers, known as inter-driver variability, but also within a driver, known as intra-driver variability *(Koppel, et al., 2019)*. Continuous adaptation is preferred rather than static personalization, since it is shown that there is a significant intra-driver modeling uncertainty when observing driving behaviour during two hours of lane keeping *(Chen and Ulsoy, 2001)*.

In this study, a Lane Change Assistance (LCA) system is developed that adapts its lane change reference trajectory to the moving average of previous lane change durations. This is implemented by means of trial-by-trial adaptation, which has successfully personalized trajectories for haptic assistance during a non-driving task *(De Jonge, et al., 2016)*.

The effect of this adaptation in an LCA system is investigated by comparing it to manual driving and driving with a generalized LCA, which is based on an average observed value for the lane change duration. The research question is formulated as follows: *Does trial-by-trial adaptation to individual preferences of a haptic feedback lane change assistance system reduce mental workload of a lane change maneuver?*

This results in the following two hypotheses:

1. A lane change assistance system reduces the mental workload of drivers during highway driving.
2. Trial-by-trial adaptation of a lane change assistance system increases collaborative performance of the lateral control task.

LCA system design

The novel adaptive LCA system is designed by integrating the concept of trial-by-trial adaptation in an LCA system. The planned reference path is adapted to the duration of previous Lane Change (LC) maneuvers. The reference path is generated by a double fifth order polynomial path planning algorithm and subsequently fed to a path-following Linear Quadratic Regulator (LQR) controller. The state-space equations of the lateral controller are formulated using a bicycle model and driver model, the resulting gains are scheduled with longitudinal velocity. All the subsystems and their interactions are schematically shown in Fig. 1.

Trial-by-Trial Adaptation

Intra-driver variability has been shown to be larger than inter-driver variability during long driving sessions *(Chen and Ulsoy, 2001)*. Therefore, an adaptive system using current driving information is preferred rather than a learning-based personalized system that statically characterizes ones driving style based on historical data. Since continuous adaptation encountered in literature does not include calculation of kinematic feasibility, the method of trial-by-trial adaptation is preferred to enable this safety feature. Furthermore, it is shown that trial-by-trial adaptation reduces control effort and torque conflict without degrading the performance in a non-driving task *(De Jonge, et al., 2016)*. Therefore, this method is chosen for implementation in the proposed LCA system to reduce the amount of mental workload that drivers experience during an LC maneuver.

The trial-by-trial adaption is based on the duration of previous LC maneuvers and is applied to the planned reference path of the LCA system. The LC duration resulting from the collaborative driving behaviour of the human driver and LCA system are registered by the LCA logic, stored and used to compute a moving average over 10 trials. This computed value is subsequently used to the determine the desired LC duration for the reference path planning of the next LC maneuver. The registration of an LC maneuver is done by the LCA logic, which is initiated by the trigger of the indicator light and is considered completed when the absolute value of both the lateral error $Y - Y_{des}$ and lateral preview error ΔY are within the lateral margin of 1 meter from the target lane center. The lane change is aborted when the indicator light is switched off before crossing the lane boundary, after which the lane keeping functionality is continued in the original lane.

Haptic Shared Control

The HSC architecture is designed according to the virtual spring model *(Ghasemi, Jayakumar, and Gillespie, 2019)*, which is expressed in Eq. 2. The HSC stiffness k_{hsc} is tuned for collaborative performance and user acceptance to a value of $k_{hsc} = 0.25$. The HSC interface of the steering wheel is used to combine the inputs of the driver and the LCA system as follows. First of all, the front wheel steering angle δ_{fc} resulting from the LQR controller is multiplied by the steering ratio i_{st} to obtain the steering wheel angle desired by the controller θ_c, as shown in Eq.1. Subsequently, the measured steering input of the driver in the loop θ_d is subtracted to determine the steering wheel angle error θ_{er}. This angle is multiplied by the HSC stiffness to obtain the assistance torque T_{LCA}. This LCA torque is added to the torque from the multibody vehicle model T_{mod} to obtain the total torque T_{tot}, shown in Eq. 3, that is sent to the control loader of the simulator's steering column.

$$\theta_c = \delta_{fc} \cdot i_{st} \tag{1}$$

$$T_{lca} = k_{hsc} \cdot \theta_{er} = k_{hsc}(\theta_c - \theta_d) \tag{2}$$

$$T_{tot} = T_{mod} + T_{lca} \tag{3}$$

Path Planning

The most commonly used method to plan the path of an LC maneuver is a fifth order polynomial. However, with a conventional fifth order polynomial replanning of the path is not possible. This could potentially lead to unsafe situations, therefore an adjustment is needed to enable the possibility to abort an LC maneuver after initiation *(Zheng, et al., 2019)*. Furthermore, a human driver uses a higher lateral acceleration for steering out of the initial lane than for steering back into the target lane *(Sporrer, et al., 1998)*. This asymmetric human-like behavior cannot be replicated by using a single quintic polynomial. By combining two different quintic polynomials, the asymmetric path can be generated to represent human LC maneuvers more accurately. Therefore a double quintic polynomial *(Heil, Lange, and Cramer, 2016)* is implemented to determine the reference path for the path following controller previously described.

$$\begin{aligned} s_1(t) &= c_0 + c_1 \cdot t + c_2 \cdot t^2 + c_3 \cdot t^3 + c_4 \cdot t^4 + c_5 \cdot t^5 \\ s_2(t) &= c_6 + c_7 \cdot t + c_8 \cdot t^2 + c_9 \cdot t^3 + c_{10} \cdot t^4 + c_{11} \cdot t^5 \end{aligned} \tag{4}$$

By determining the maximum desired lateral acceleration of $a_{max} = 1\ m/s^2$, the maximum desired lateral jerk of $j_{max} = 1.5\ m/s^3$ and the lane width of $w = 3.5\ m$, the two polynomials are solved with the symbolic toolbox of Matlab.

$$\begin{aligned} t_{a_{max}}(s_1) &= -\frac{2 \cdot c_4 \pm \sqrt{4 \cdot c_4^2 - 10 \cdot c_3 \cdot c_5}}{10 \cdot c_5} \\ t_{j_{max}}(s_1) &= -\frac{c_4}{5 \cdot c_5} \end{aligned} \tag{5}$$

The coefficients can be solved using Eq. 5 for s_1 and s_2 under assumption that the maneuver is initiated without lateral acceleration, velocity or deviation from the lane centre. Continuity is guaranteed by enforcing that the initial values of the second polynomial s_2 are equal to the final values of the first polynomial s_1. Since the LCA is integrated with an LKA and to minimize the influence of the initiation on the results, the manual trigger of the indicator light is used to switch from the lane keeping to lane changing functionality.

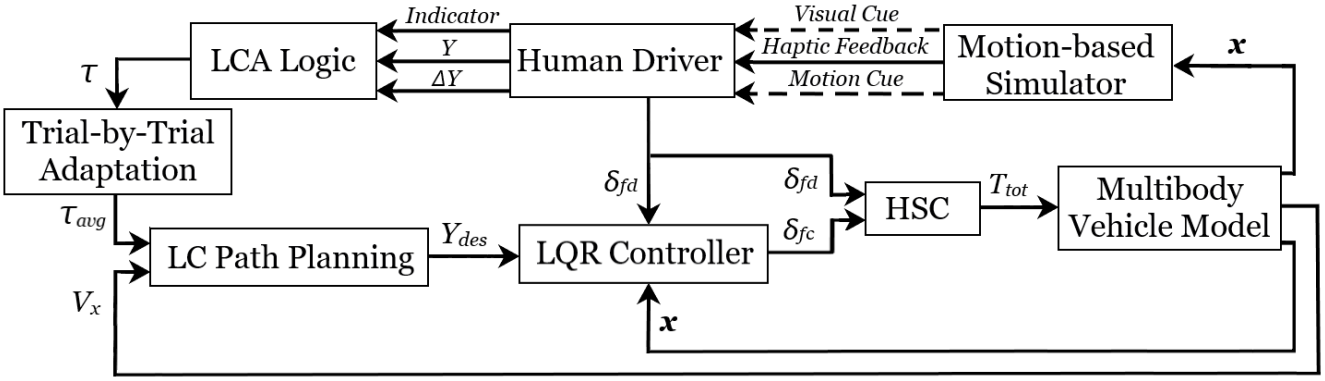

Figure 1: Schematic of the Lane Change Assistance system

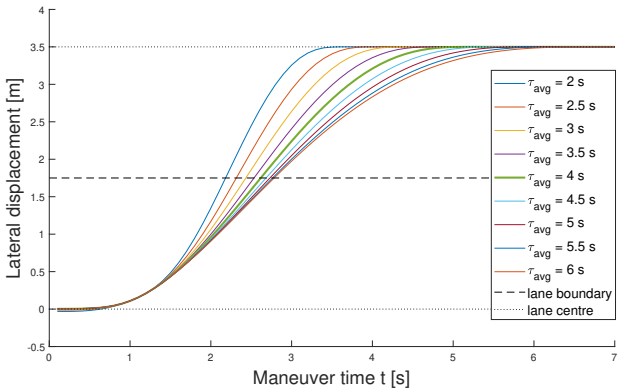

Figure 2: LC maneuver path planning for values of lane change duration τ_{avg} that were obtained from 27 participants

To ensure a smooth transition between the two polynomials, especially in the case of replanning, a hyperbolic tangent blending function with a one-sided blending time $t_b = 0.5$ seconds is used, as expressed in Eq.6. LC maneuver paths are computed for lane change duration values between $\tau = 1$ and $\tau = 10$ seconds and stored in a lookup table to minimize computational power during simulation. The computed reference paths are visualised in Fig. 2 for the range of values between $\tau_{avg} = 2$ and $\tau_{avg} = 6$ seconds that were encountered during the experiment. The fixed value $\tau_{avg} = 4$ that is used as lane change duration for the generalized LCA is highlighted.

$$s(t) = \frac{1 - tanh(\frac{(t-\tau_{s_1})}{t_b})}{2} \cdot s_1(t) + \frac{1 + tanh(\frac{(t-\tau_{s_1})}{t_b})}{2} \cdot s_2(t) \tag{6}$$

Controller Design

A state feedback controller was selected to perform path-following, demonstrating similar performance to state-of-the-art path-followers in highway driving conditions. *(Lu, et al., 2018)*. The LCA system uses a gain-scheduling state feedback LQR controller. State vector $\boldsymbol{x}$ containing 7 states is used to determine the additional steering angle δ_{fc} that the controller should provide to the front wheels of the vehicle, which is shown in Eq. 7 - 9.

$$\delta_{fc} = \boldsymbol{k}(V_x) \cdot \boldsymbol{x} \tag{7}$$

$$\boldsymbol{x} = [V_y \quad \dot{\psi} \quad \psi \quad Y \quad \delta_{fd} \quad \dot{\delta}_{fd} \quad \Delta Y_p] \tag{8}$$

$$\Delta Y_p = Y_p - Y - t_p \cdot V_x \cdot \psi \tag{9}$$

The definition of lateral preview error ΔY_p is visualized by the schematic in Fig. 3.

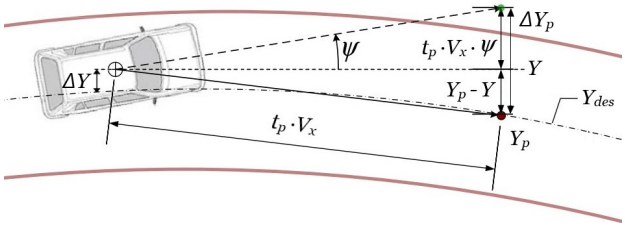

Figure 3: Schematic of the preview model adapted from *(Wang, et al., 2017)*

By considering multiple objectives including path-tracking error, driver's physical and mental workloads and control effort in the LQR controller, the cost function described in Eq. 10 is minimized. J_1 represents the cost for lateral preview error, J_2 and J_3 represent the driver's mental and physical workload, respectively, and J_4 represents the control effort of the LCA system. To minimize computational power during simulation, the closed-loop control gains are calculated offline for a range of longitudinal velocities and integrated in the model by using a lookup table. The control equations are formulated to schedule the gain based on longitudinal velocity. These control equations and the corresponding simplified vehicle and driver model are formulated in Eq.13 - 29 of the Appendix.

$$J = J_1 + J_2 + J_3 + J_4$$
$$J = \int_0^\infty (q_1 \cdot \Delta Y_p^2 + q_2 \cdot \delta_{fd}^2 + q_3 \cdot \dot{\delta}_{fd}^2 + R \cdot \delta_{fc}^2) dt \tag{10}$$

Experiment Design

Figure 4: A lane change maneuver during the experiment in the highway scenario on the 6 DoF motion-based simulator

To determine the effect of the adaptive LCA and the generalized LCA on mental workload, collaborative performance and user acceptance, experiments with human participants in the loop are executed on a motion-based driving simulator. This six DoF driving simulator utilizes a projected view of 210 degrees horizontally and 50 degrees vertically, two exterior rear-view mirrors, one interior rear-view mirror and a dashboard depicting all relevant dials.

The vehicle model used for the simulation in the experiment is a 13 DoF dSpace multibody Automotive Simulation Model (ASM) with the parametrization of a generic sedan. The vehicle is equipped with cruise control, which is set at 100 km/h and can be adjusted by the driver when necessary. A traffic scenario with 30 recurring entities is scripted such that the vehicles in the right lane drive at 90 km/h, in the middle lane 95 km/h and in the left lane 105 km/h. The participants are instructed to adjust the longitudinal velocity as infrequently as possible and return to the right lane after overtaking, such that a high amount of LC maneuvers is encouraged.

Table 1: Participant groups for driving sequence of different systems

Group	Session 1	Session 2	Session 3
A	Manual	Generalized	Adaptive
B	Generalized	Adaptive	Manual
C	Adaptive	Manual	Generalized

The experiment consists of 3 different sessions of 10 minutes on the driving simulator. A baseline measurement is recorded in a manual driving session, in which the driver has full lateral control and receives no assistance. Another session is driven with the generalized LCA system, for which the average value of a lane change duration τ was determined to be 4 seconds in a pilot study. A third session is driven with the adaptive LCA system, in which the lane change duration is determined by the LCA logic and implemented in the assistance by means of trial-by-trial adaptation. These three sessions are shuffled in sequence by using the Latin squares method to mitigate both learning effect and fatigue of the participants. The resulting three groups are classified as group A, group B and group C, which are shown in Tab. 1. The drivers are not informed which assistance system is active during the sessions.

Table 2: Demographic parameters of the 27 participants

Parameter	Mean	σ	Unit
Participant age	36.8	15.6	years
Driver's license	17.8	16.2	years
Average driving	4.52	3.90	hours/week
CC driving	2.18	3.22	hours/week
LKA driving	0.50	1.95	hours/week
Simulator driving	0.29	0.57	hours/week

The experiments were executed with 34 participants in total, of which five measurements contained corrupted data. To ensure equal distribution over the three groups described in Tab. 1, two participants were eliminated randomly to obtain 9 participants per group, thus 27 in total. The demographics parameters of the 27 participants that are used for the analysis of the results are shown in Tab. 2. The measurements were rearranged such that the results can be presented per system configuration.

For all presented results a linear mixed-effect model regression analysis is applied to obtain information about the statistical significance of the metrics. In this way, the individual participants were regarded as a random effect with no a-priori expectations. Since the data is obtained with repeated measurements of an individual participant with different system configurations, repeated-measures analysis of variance (ANOVA) is more suitable than a one-way or two-way ANOVA. However, mixed-effect modeling is more robust against systematic inter-driver variability than repeated-measures ANOVA *(Van Dongen, et al., 2004)*. Since inter-driver variability is expected to be an important influence, linear mixed-effect model regression analysis is used to determine the statistical significance of the results.

Metrics

Mental workload is measured during the complete duration of the experiment by means of an auditory N-back task *(Layden, 2018)*, which is introduced as a cognitive secondary task. In this task participants are asked to respond by tapping a touchscreen when the audio fragment of a recorded letter is identical to the one played back N trials before. N is chosen to be one, considering the substantial workload required for the driving task. The resulting score is expressed as Discrimination Index (DI), which is calculated by using the hit rate H and false-positive rate F, as shown in Eq. 11.

$$DI = 0.5 + sign(H - F) \cdot \frac{(H - F)^2 + abs(H - F))}{(4 \cdot max(H, F) - 4 \cdot H \cdot F)}$$
$$H = \frac{\#hits}{\#signal\ trials} \qquad F = \frac{\#false\ positives}{\#noise\ trials} \tag{11}$$

Steering Reversal Rate (SRR) can be used as complement or alternative to lane position metrics to quantify lateral control performance *(Markkula and Engström, 2006)*. Since a cognitive secondary task is introduced in this study, the corresponding parameters are specified to obtain the highest sensitivity for this scenario.

The steering wheel angle signal θ is filtered with a second order Butterworth filter with a 3dB cut-off frequency of 0.6 Hz to obtain θ_{filt}. If the difference in θ_{filt} of the current and previous time step is larger than the gap value $\theta_{gap} = 0.1\ deg$, it is registered as a reversal. These are expressed in SRR as reversals per minute. The SRR metric is also computed for the LC maneuvers only, by cutting out the lane change sections of the steering wheel angle signal.

To express the user acceptance of the participants, a subjective van der Laan questionnaire is used, in which the generalized and adaptive LCA system configurations are rated with respect to the manual driving session. The participants are requested to score the system configurations on 9 different aspects of the system, leading to both a usefulness score (USE) and a satisfaction score (SAT) *(Van Der Laan, Heino, and De Waard, 1997)*. It is stated that Cronbach's coefficient of reliability α should be higher that 0.65 for the results to be valid, which is the case for both results. No prior knowledge about the LCA systems is given to the participants, therefore the results are regarded as unbiased.

Results

The means and statistical significance of the objective metrics for each system configuration are presented in Tab. 3. The means, statistical significance and Cronbach's coefficient of reliability α for the subjective metrics are shown in Tab. 4. The results are displayed graphically in Fig. 5-8 by a combination of boxplots and individual participant results, connected by lines between the different system configurations.

Table 3: Resulting means of objective metrics and statistical significance of mixed-effect linear regression

Metric	MAN	GEN	ADA	F	p
DI	0.808	0.810	0.810	0.216	0.806
SRR	34.67	33.22	32.34	9.390	<0.001
LC-SRR	56.48	54.03	53.55	2.961	0.058

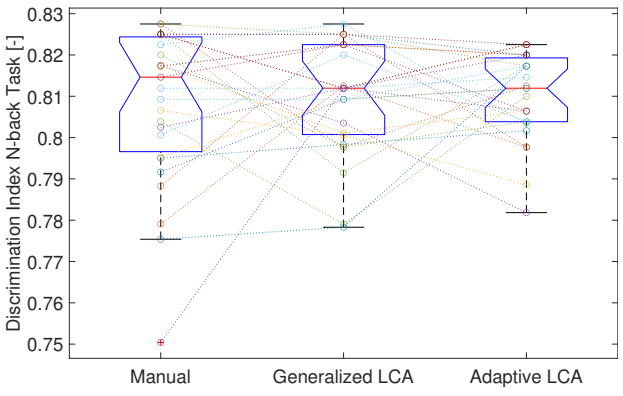

Figure 5: Mental workload measured by the cognitive N-back task per system configuration for 27 participants

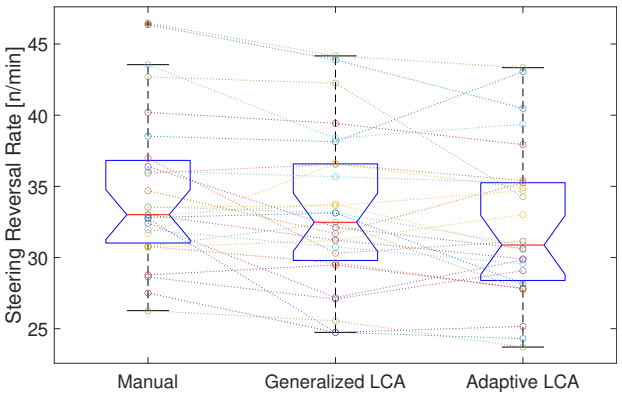

Figure 6: Steering reversal rate during complete driving session per system configuration for 27 participants

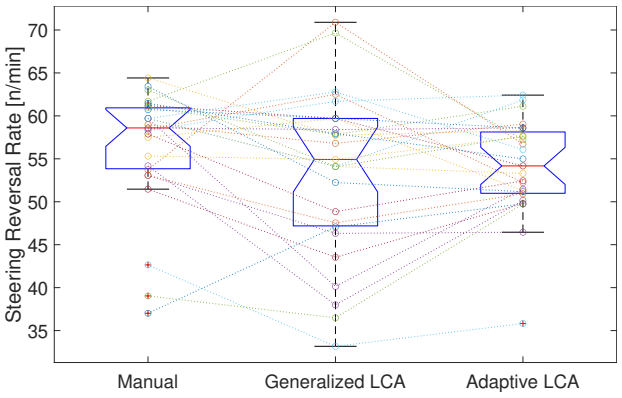

Figure 7: Steering reversal rate during lane change maneuvers per system configuration for 27 participants

Table 4: Resulting means of subjective metrics and statistical significance of mixed-effect linear regression

Metric	GEN	ADA	α	F	p
USE	3.444	4.407	0.901	7.773	0.007
SAT	1.889	2.667	0.765	2.338	0.132

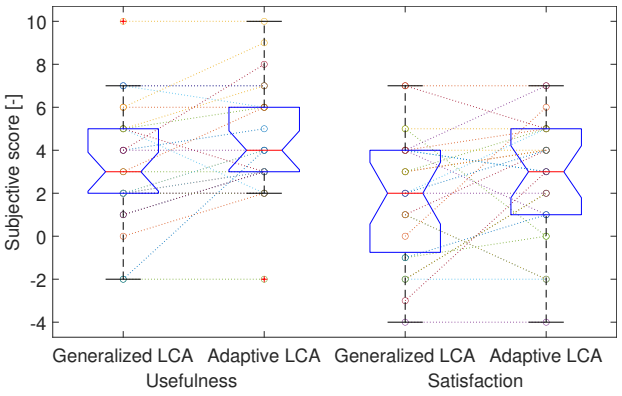

Figure 8: Subjective usefulness and satisfaction score per system configuration for 27 participants

Discussion

The mean of mental workload required for driving decreases slightly by introducing an LCA system. This can be seen in the slight increase of the measured DI from the auditory N-back task in Tab. 3. However, due to the limited amount of change in mean compared to the variance, the mixed effect linear regression analysis of variance shows that these results cannot be regarded as significant. However, it can be seen in Fig. 5 that the variance of workload reduces by introducing a generalized LCA system and reduces further when introducing an adaptive LCA system.

Collaborative performance and SRR are inversely related, since the control performance is considered to be reduced when many steering corrections have to be made. As can be seen from Tab. 3 and Fig. 6, the SRR decreases when the LCA system is introduced and further decreases when the adaptive LCA is introduced. Therefore, the collaborative lateral control performance is increased by introducing a generalized LCA and further increased when introducing an adaptive LCA system.

Furthermore, it can be seen from Fig. 7 that the variance of SRR during LC maneuvers is much larger with the generalized LCA than with adaptive LCA. This indicates that the inter-driver variability of collaborative performance is reduced by introducing the trial-by-trial adaptation functionality.

User acceptance is expressed in a USE and SAT score, resulting from the subjective questionnaire. As can be seen from the Tab. 4, the usefulness score is increased significantly from generalized to adaptive LCA system with a p-value smaller than 0.01. The satisfaction score also increases, however from the mixed effect linear regression analysis of variance it can be concluded that this is not significant. Furthermore it can be seen from Fig. 8 that the mean of the usefulness score is higher for both LCA system configurations compared to the mean of the satisfaction score of the same system configuration.

Conclusion

The hypotheses of this study were stated as follows:

1. A lane change assistance system reduces the mental workload of drivers during highway driving.
2. Trial-by-trial adaptation of a lane change assistance system increases collaborative performance of the lateral control task.

The first hypothesis is rejected, since there is no significant change in mental workload, measured by the discrimination index of the cognitive secondary N-back task, when the generalized or adaptive LCA system is introduced.

The second hypothesis is accepted, since the collaborative performance, measured by the steering reversal rate, is increased significantly when introducing trial-by-trial adaptation to lane change duration in the adaptive LCA compared to the generalized LCA.

Furthermore, inter-driver variability of collaborative performance is reduced by introducing trial-by-trial adaptation to lane change duration in the adaptive LCA compared to the generalized LCA. In addition to this, the user acceptance is increased by introducing the adaptive LCA system, of which the subjective usefulness score is increased significantly.

Recommendations

During this study, several observations are made of aspects that could be improved upon in future studies. First of all, to achieve a fully integrate longitudinal and lateral functionality of lane change assistance, implementation of HSC on a longitudinal control interface such as the acceleration or brake pedal would be preferable. By doing this, excessive braking or acceleration to complete a safe lane change could be made redundant. For the purpose of this study, longitudinal control is supported by means of cruise control instead of adaptive cruise control to stimulate lane changing rather than car-following behaviour. However, it was observed during the experiments that the longitudinal control task required a lot of workload capacity in situations with high traffic density. Therefore it is expected that this has distorted the measurements, especially in terms of mental workload. By integrating longitudinal control, the functionalities of these systems could be optimized to complement one another.

Furthermore, if this longitudinal HSC interface is integrated, distance and relative velocity to a lead vehicle could be used as a trigger or advice for a lane change. An additional prerequisite would be to integrate sensors such as blind spot sensors to observe vehicles in the parallel lanes. In this way, the safety and comfort of the LC maneuver could be evaluated, thus largely improving the user acceptance of the system.

It is highly recommended to adjust the lane change detection algorithm to facilitate a more universal detection of lane change intention. For this study, it was chosen to embed a safety feature in this detection by aborting a lane change if the indicator light is switched off before crossing the lane boundary. However, aborted LC maneuvers were almost never encountered during the experiments, whereas many people switched off the indicator light before crossing the lane boundary during an intentional LC maneuver. Furthermore, an LC maneuver of two lanes in once could not be identified as such if the indicator light was not switched off in between. This led to a large number of conflicts between the LCA logic and the driver, which are defined as instances that the lane change intention is incorrectly observed by the LCA system. These conflicts could be mitigated by enlarging the time duration in which the lane boundary has to be crossed or implement a completely different LCA logic. It is expect that this will further enhancing user acceptance and ensure safe collaborative driving behaviour.

To improve upon the learning speed of the adaptive LCA system, data of a practice session could be used to obtain initial values for the preferred lane change duration of a person. Also, further research could be done to the effect of adaptation to driver parameters other than lane change duration, such as preferred lateral acceleration.

$$A = \begin{bmatrix} 2\frac{(C_f+C_r)}{m\cdot V_x} & -\frac{V_x+(2\cdot(C_r\cdot l_r - Cf\cdot l_f))}{m\cdot V_x} & 0 & 0 & 2\frac{C_f}{m} & 0 & 0 \\ 2\frac{C_r\cdot l_r - C_f\cdot l_f}{I_z\cdot V_x} & -2\frac{C_f\cdot l_f^2 + C_r\cdot l_r^2}{I_z\cdot V_x} & 0 & 0 & 2\frac{C_f\cdot l_f}{I_z} & 0 & 0 \\ 0 & 1 & 0 & 0 & 0 & 0 & 0 \\ 1 & 0 & V_x & 0 & 0 & 0 & 0 \\ 0 & 0 & 0 & 0 & 0 & 1 & 0 \\ 0 & 0 & -\frac{R_g\cdot G_h\cdot t_p\cdot V_x}{a_0\cdot T_d^2} & -\frac{R_g\cdot G_h}{a_0\cdot T_d^2} & -\frac{1}{a_0\cdot T_d^2} & -\frac{1}{a_0\cdot T_d} & 0 \\ 0 & 0 & -t_p\cdot V_x & -1 & 0 & 0 & 0 \end{bmatrix} \quad (12)$$

Appendix

In this appendix, the design of the gain-scheduling state feedback LQR controller used for the LCA system is discussed and the are corresponding control equations are formulated.

Control Equations

$$B = \begin{bmatrix} 0 & 0 & 0 & 0 & 0 & \frac{R_g\cdot G_h}{a_0\cdot T_d^2} & 0 \end{bmatrix} \quad (13)$$

$$C = \begin{bmatrix} 0 & 0 & -t_p\cdot V_x & -1 & 0 & 0 & 0 \\ 0 & 0 & 0 & 0 & 1 & 0 & 0 \\ 0 & 0 & 0 & 0 & 0 & 1 & 0 \end{bmatrix} \quad (14)$$

$$D = \begin{bmatrix} 1 & 0 & 0 \end{bmatrix}^T \quad (15)$$

$$Q_d = \begin{bmatrix} q_1 & 0 & 0 \\ 0 & q_2 & 0 \\ 0 & 0 & q_3 \end{bmatrix} \quad (16)$$

$$Q = (C^T \cdot Q_d \cdot C) + (D^T \cdot Q_d \cdot D) \quad (17)$$

$$a_0 = \frac{\tau_{lag}\cdot\tau_{delay}}{T_d^2} \quad (18)$$

$$T_d = (\tau_{lag} + \tau_{delay}) \quad (19)$$

The state-space system to be solved is the simplified form seen in Eq. 20, since the system matrices $\boldsymbol{C}$ and $\boldsymbol{D}$ are incorporated in state weighting matrix $\boldsymbol{Q}$.

$$\dot{\boldsymbol{x}} = \boldsymbol{A}(V_x)\boldsymbol{x} + \boldsymbol{B}(V_x)\boldsymbol{u} \quad (20)$$

The closed-loop control gain vector $\boldsymbol{k}(V_x)$ is determined by solving the Ricatti equation for the state-space system with corresponding state weighting matrix $\boldsymbol{Q}$ and control weighting matrix $\boldsymbol{R}$. The gain vector $\boldsymbol{k}(V_x)$ is solved for each longitudinal velocity $V_x = 0 - 120km/h$ and stored in the matrix $\boldsymbol{K}$. After obtaining the interpolated gain vector corresponding to the longitudinal velocity from the lookup-table, it is multiplied by the state vector to determine the additional front wheel steering angle to be added by the controller. This can be expressed as shown in Eq. 21.

$$\begin{aligned} \delta_f &= \delta_{fc} + \delta_{fd} \\ \delta_{fc} &= \boldsymbol{k}(V_x)\cdot\boldsymbol{x} \end{aligned} \quad (21)$$

Simplified Vehicle Model

The simplified vehicle model used for the controller design is a 2-DoF bicycle model. The parameters of this vehicle model are based on the generic sedan multibody vehicle ASM that is used for the simulation in the experiment. The values of the corresponding parameters are shown in Tab. 5.

The lateral and yaw dynamics of the simplified vehicle model are expressed in Eq. 22- 24.

$$m\dot{V}_y = -mV_x\dot{\psi} + F_{yf}\cos\delta_f + F_{yr} \quad (22)$$

$$I_z\ddot{\psi} = l_f F_{yf}\cos\delta_f - l_r F_{yr} \quad (23)$$

$$\dot{Y} = V_x\sin\psi + V_y\cos\psi \quad (24)$$

The equations used to determine the front and rear lateral tire forces are shown in Eq. 25, using the formulas for front and rear slip angle shown in Eq.26

$$F_{yf} = -2C_f\alpha_f \qquad F_{yr} = -2C_r\alpha_r \quad (25)$$

$$\alpha_f = \beta + l_f\frac{\dot{\psi}}{V_x} - \delta_f \qquad \alpha_r = \beta - l_r\frac{\dot{\psi}}{V_x} \quad (26)$$

Table 5: Simplified Vehicle Model Parameters

Symbol	Parameter	Value	Unit
l_f	Distance from CoG to front axle	1.185	m
l_r	Distance from CoG to rear axle	1.665	m
m	Full vehicle mass	1500	kg
I_z	Inertia moment around z-axis	2450	$kg\cdot m^2$
R_g	Steering gear ratio	1/18	-
C_f	Front cornering stiffness per wheel	103130	N/rad
C_r	Rear cornering stiffness per wheel	73854	N/rad

Driver Model

The steering behaviour of the driver model is expressed as a transfer function from lateral preview error ΔY to the driver's front wheel steering angle δ_{fd} and is shown in Eq. 27. The calculation of the lateral preview error ΔY is shown in Eq. 28. The parameters used in both equations are specified in Tab. 6 and are based on the benchmark controller *(Wang, et al., 2017)*.

$$\delta_{fd}(s) = \frac{G_h\,(1+\tau_{lead}\cdot s)\,e^{-\tau_{delay}\cdot s}}{1+\tau_{lag}\cdot s}\Delta Y(s) \quad (27)$$

$$\Delta Y(s) = Y_{des}(s)\cdot e^{\tau_{prev}\cdot s} - Y(s) - V_x\cdot\tau_{prev}\cdot\psi(s) \quad (28)$$

Previous studies have shown that human preview times vary between 0.5 and 2 seconds and that preview time is inversely correlated with the road curvature as is shown in Eq. 29 *(Yang, et al., 2020)*.

$$t_p = \lambda(\rho)\frac{L_{pn}}{V_x} + [1-\lambda(\rho)]\frac{L_{pf}}{V_x} \quad (29)$$

Table 6: Driver Model Parameters

Symbol	Parameter	Value	Unit
G_h	Proportional Gain	0.8	-
τ_{lead}	Lead time constant	0.12	s
τ_{delay}	Delay time constant	0.05	s
τ_{lag}	Lag time constant	0.09	s
τ_{prev}	Preview time constant	2	s

Preview time t_p is expressed as function of the road curvature λ and near and far preview point L_{pn} and L_{pf}, respectively. The far preview point L_{pf} is defined as 40 meter for a velocity of 20 m/s and the road curvature of the highway in the experiment is zero. Since preview distance increases linearly with longitudinal speed $L = t_p \cdot V_x$ *(Schnelle, et al., 2017)*, the resulting preview time is $t_p = 2$ seconds. Therefore it is chosen to use this value for the preview time constant τ_{prev} opposed to the original value of $\tau_{prev} = 0.68$ seconds for a double lane change maneuver found in the benchmark driver model *(Wang, et al., 2017)*.

References

Basu, C., Yang, Q., Hungerman, D., Singhal, M., and Dragan, A. D., 2017. Do You Want Your Autonomous Car to Drive Like You? *ACM/IEEE International Conference on Human-Robot Interaction*, Part F1271, pp. 417–425. ISSN: 21672148. https://doi.org/10.1145/2909824.3020250. arXiv: 1802.01636.

Chen, L.-k. and Ulsoy, A. G., 2001. Identification of a Driver Steering Model and Model Uncertainty from Driving Simulator Data. *Journal of Dynamic Systems, Measurement, and Control*, 123. https://doi.org/10.1115/1.1409554.

Chen, Y. and Wang, J., 2018. Personalized Vehicle Path Following Based on Robust Gain-scheduling Control in Lane-changing and Left-turning Maneuvers. *Proceedings of the American Control Conference*, 2018-June, pp. 4784–4789. ISSN: 07431619. https://doi.org/10.23919/ACC.2018.8431065.

De Jonge, A. W., Wildenbeest, J. G., Boessenkool, H., and Abbink, D. A., 2016. The Effect of Trial-by-Trial Adaptation on Conflicts in Haptic Shared Control for Free-Air Teleoperation Tasks. *IEEE Transactions on Haptics*, 9(1), pp. 111–120. ISSN: 19391412. https://doi.org/10.1109/TOH.2015.2477302.

Dintel, K. M. V., Petermeijer, S. M., Vries, E. J. H. D., and Abbink, D. A., 2020. Transitioning back from SAE-L3 autonomy - comparing traded and shared control. In: *The Driving Simulation Conference Europe 2020 VR*.

Ghasemi, A. H., Jayakumar, P., and Gillespie, R. B., 2019. Shared control architectures for vehicle steering. *Cognition, Technology and Work*, 21(4), pp. 699–709. ISSN: 14355566. https://doi.org/10.1007/s10111-019-00560-9.

Hasenjager, M. and Wersing, H., 2018. Personalization in advanced driver assistance systems and autonomous vehicles: A review. *IEEE Conference on Intelligent Transportation Systems, Proceedings, ITSC*, 2018-March, pp. 1–7. https://doi.org/10.1109/ITSC.2017.8317803.

Heil, T., Lange, A., and Cramer, S., 2016. Adaptive and efficient lane change path planning for automated vehicles. *IEEE Conference on Intelligent Transportation Systems, Proceedings, ITSC*, pp. 479–484. https://doi.org/10.1109/ITSC.2016.7795598.

Koppel, C. N., Petermeijer, S. M., Doornik, J. van, and Abbink, D. A., Sept. 4, 2019. Lane change manoeuvre analysis: inter- and intra-driver variability in lane change behaviour. In: *Proceedings of the Driving Simulation Conference 2019 Europe VR*. Driving Simulation Association. Strasbourg, France, pp. 127–134. ISBN: 978-2-85782-749-8.

Layden, E. A., 2018. *N-Back for Matlab*. The University of Chicago.

Lazcano, A. M. R., Niu, T., Carrera Akutain, X., Cole, D., and Shyrokau, B., 2021. MPC-based Haptic Shared Steering System: A Driver Modelling Approach for Symbiotic Driving. *IEEE/ASME Transactions on Mechatronics*. https://doi.org/10.1109/TMECH.2021.3063902.

Lu, Z., Shyrokau, B., Boulkroune, B., Van Aalst, S., and Happee, R., 2018. Performance benchmark of state-of-the-art lateral path-following controllers. In: *Proceedings - 2018 IEEE 15th International Workshop on Advanced Motion Control (AMC 2018)*, pp. 541–546. https://doi.org/10.1109/AMC.2019.8371151.

Markkula, G and Engström, J, 2006. A Steering Wheel Reversal Rate Metric for Assessing Effects of Visual and Cognitive Secondary Task Load. In: *13th ITS World Congress*. https://doi.org/10.1177/0018720817690639.

Schnelle, S., Wang, J., Su, H., and Jagacinski, R., 2017. A Driver Steering Model with Personalized Desired Path Generation. *IEEE Transactions on Systems, Man, and Cybernetics: Systems*, 47(1), pp. 111–120. ISSN: 10834427. https://doi.org/10.1109/TSMC.2016.2529582.

Sporrer, A., Prell, G., Buck, J., and Schaible, S., 1998. Realsimulation von Spurwechselvorgängen im Straßenverkehr. *Verkehrsunfall und Fahrzeugtechnik*, 36(3), pp. 69–76. ISSN: 0724-2050.

Statistisches Bundesamt, 2018. Unfallentwicklung auf deutschen Straßen 2017, p. 46. Available at: ¡https://www.destatis.de/DE/Presse/Pressekonferenzen/2018/Verkehrsunfaelle-2017/pressebroschuere-unfallentwicklung.pdf?__blob=publicationFile¿.

Van Der Laan, J. D., Heino, A., and De Waard, D., 1997. A simple procedure for the assessment of acceptance of advanced transport telematics. *Transportation Research Part C: Emerging Technologies*, 5(1), pp. 1–10. ISSN: 0968-090X. https://doi.org/10.1016/S0968-090X(96)00025-3.

Van Dongen, H. P., Olofsen, E., Dinges, D. F., and Maislin, G., 2004. Mixed-Model Regression Analysis and Dealing with Interindividual Differences. In: *Numerical Computer Methods, Part E*. Vol. 384. Methods in Enzymology. Academic Press, pp. 139–171. https://doi.org/10.1016/S0076-6879(04)84010-2.

Wang, J., Zhang, G., Wang, R., Schnelle, S. C., and Wang, J., 2017. A Gain-Scheduling Driver Assistance Trajectory-Following Algorithm Considering Different Driver Steering Characteristics. *IEEE Transactions on Intelligent Transportation Systems*, 18(5), pp. 1097–1108. ISSN: 15249050. https://doi.org/10.1109/TITS.2016.2598792.

Yang, K., Liu, Y., Na, X., He, X., Liu, Y., Wu, J., Nakano, S., and Ji, X., 2020. Preview-scheduled steering assistance control for co-piloting vehicle: a human-like methodology. *Vehicle System Dynamics*, 58(4), pp. 518–544. ISSN: 17445159. https://doi.org/10.1080/00423114.2019.1590607.

Zheng, H., Zhou, J., Shao, Q., and Wang, Y., 2019. Investigation of a longitudinal and lateral lane-changing motion planning model for intelligent vehicles in dynamical driving environments. *IEEE Access*, 7, pp. 44783–44802. ISSN: 21693536. https://doi.org/10.1109/ACCESS.2019.2909273.

Bibliography

[1] H. Kim, Y. Hwang, D. Yoon, and C. H. Park, "An analysis of driver's workload in the lane change behavior," in *International Conference on ICT Convergence*, pp. 242–247, 2013.

[2] T. Toledo and D. Zohar, "Modeling duration of lane changes," *Transportation Research Record*, no. 1999, pp. 71–78, 2007.

[3] J. Wang, G. Zhang, R. Wang, S. C. Schnelle, and J. Wang, "A Gain-Scheduling Driver Assistance Trajectory-Following Algorithm Considering Different Driver Steering Characteristics," *IEEE Transactions on Intelligent Transportation Systems*, vol. 18, no. 5, pp. 1097–1108, 2017.

[4] J. B. Hurwitz and D. J. Wheatley, "Using driver performance measures to estimate workload," *Proceedings of the Human Factors and Ergonomics Society Annual Meeting*, vol. 46, no. 22, pp. 1804–1808, 2002.

[5] B. Mehler, B. Reimer, J. F. Coughlin, and J. A. Dusek, "Impact of incremental increases in cognitive workload on physiological arousal and performance in young adult drivers," *Transportation Research Record*, vol. 2138, no. 1, pp. 6–12, 2009.

[6] SAE, *Taxonomy and Definitions for Terms Related to Driving Automation Systems for On-Road Motor Vehicles*, 2021.

[7] A. M. R. Lazcano, T. Niu, X. Carrera Akutain, D. Cole, and B. Shyrokau, "Mpc-based haptic shared steering system: A driver modelling approach for symbiotic driving," *IEEE/ASME Transactions on Mechatronics*, 2021.

[8] K. M. van Dintel, S. M. Petermeijer, E. J. H. de Vries, and D. A. Abbink, "Transitioning back from SAE-L3 autonomy - comparing traded and shared control," in *The Driving Simulation Conference Europe 2020 VR*, 2020.

[9] Y. Chen and J. Wang, "Personalized Vehicle Path Following Based on Robust Gain-scheduling Control in Lane-changing and Left-turning Maneuvers," *Proceedings of the American Control Conference*, vol. 2018-June, pp. 4784–4789, 2018.

[10] M. Hasenjager and H. Wersing, "Personalization in advanced driver assistance systems and autonomous vehicles: A review," *IEEE Conference on Intelligent Transportation Systems, Proceedings, ITSC*, vol. 2018-March, pp. 1–7, 2018.

[11] C. Basu, Q. Yang, D. Hungerman, M. Singhal, and A. D. Dragan, "Do You Want Your Autonomous Car to Drive Like You?," *ACM/IEEE International Conference on Human-Robot Interaction*, vol. Part F1271, pp. 417–425, 2017.

[12] C. N. Koppel, S. M. Petermeijer, J. van Doornik, and D. A. Abbink, "Lane change manoeuvre analysis: inter- and intra-driver variability in lane change behaviour," in *Proceedings of the Driving Simulation Conference 2019 Europe VR*, pp. 127–134, Driving Simulation Association, 2019.

[13] L. K. Chen and A. G. Ulsoy, "Identification of a Driver Steering Model and Model Uncertainty from Driving Simulator Data," *Journal of Dynamic Systems, Measurement, and Control*, vol. 123, 2001.

[14] A. W. De Jonge, J. G. Wildenbeest, H. Boessenkool, and D. A. Abbink, "The Effect of Trial-by-Trial Adaptation on Conflicts in Haptic Shared Control for Free-Air Teleoperation Tasks," *IEEE Transactions on Haptics*, vol. 9, no. 1, pp. 111–120, 2016.

[15] A. H. Ghasemi, P. Jayakumar, and R. B. Gillespie, "Shared control architectures for vehicle steering," *Cognition, Technology and Work*, vol. 21, no. 4, pp. 699–709, 2019.

[16] H. Zheng, J. Zhou, Q. Shao, and Y. Wang, "Investigation of a longitudinal and lateral lane-changing motion planning model for intelligent vehicles in dynamical driving environments," *IEEE Access*, vol. 7, pp. 44783–44802, 2019.

[17] A. Sporrer, G. Prell, J. Buck, and S. Schaible, "Realsimulation von Spurwechselvorgängen im Straßenverkehr," *Verkehrsunfall und Fahrzeugtechnik*, vol. 36, no. 3, pp. 69–76, 1998.

[18] T. Heil, A. Lange, and S. Cramer, "Adaptive and efficient lane change path planning for automated vehicles," *IEEE Conference on Intelligent Transportation Systems, Proceedings, ITSC*, pp. 479–484, 2016.

[19] Y. Xing, C. Lv, H. Wang, H. Wang, Y. Ai, D. Cao, E. Velenis, and F.-Y. Wang, "Driver lane change intention inference for intelligent vehicles: Framework, survey, and challenges," *IEEE Transactions on Vehicular Technology*, vol. 68, no. 5, pp. 4377–4390, 2019.

[20] Z. Lu, B. Shyrokau, B. Boulkroune, S. van Aalst, and R. Happee, "Performance benchmark of state-of-the-art lateral path-following controllers," in *Proceedings - 2018 IEEE 15th International Workshop on Advanced Motion Control (AMC 2018)*, pp. 541–546, 2018.

[21] E. A. Layden, "N-Back for Matlab," 2018.

[22] S. M. Jaeggi, M. Buschkuehl, W. J. Perrig, and B. Meier, "The concurrent validity of the n-back task as a working memory measure," *Memory*, vol. 18, no. 4, pp. 394–412, 2010.

[23] G. Markkula and J. Engström, "A steering wheel reversal rate metric for assessing effects of visual and cognitive secondary task load," in *13th ITS World Congress*, 2006.

[24] Y. Kuo, C. Seidler, B. Schick, and D. Nissing, "Workload evaluation of effects of a lane keeping assistance system with physiological and performance measures," *Proceedings of the Human Factors and Ergonomics Society Europe Chapter 2018 Annual Conference*, vol. 4959, no. 2001, 2020.

[25] O. Carsten, N. Merat, W. Janssen, E. Johansson, M. Fowkes, and K. Brookhuis, "HASTE: Final Report," Tech. Rep. HASTE-D6, Transport Research and Innovation Monitoring and Information System, 2005.

[26] J. D. Van Der Laan, A. Heino, and D. De Waard, "A simple procedure for the assessment of acceptance of advanced transport telematics," *Transportation Research Part C: Emerging Technologies*, vol. 5, no. 1, pp. 1–10, 1997.

[27] H. P. Van Dongen, E. Olofsen, D. F. Dinges, and G. Maislin, "Mixed-model regression analysis and dealing with interindividual differences," in *Numerical Computer Methods, Part E*, vol. 384 of *Methods in Enzymology*, pp. 139–171, Academic Press, 2004.

[28] C. J. Patten, A. Kircher, J. Östlund, L. Nilsson, and O. Svenson, "Driver experience and cognitive workload in different traffic environments," *Accident Analysis Prevention*, vol. 38, no. 5, pp. 887–894, 2006.

[29] J. R. McLean and E. R. Hoffmann, "Steering reversals as a measure of driver performance and steering task difficulty," *Human Factors*, vol. 17, no. 3, pp. 248–256, 1975.

[30] G. Knappe, A. Keinath, K. Bengler, C. Meinecke, and F. Alexander, "Driving simulators as an evaluation tool - assessment of the influence of field of view and secondary tasks on lane keeping and steering performance," *Proceedings of the International Technical Conference on the Enhanced Safety of Vehicles*, pp. 1–11, 2007.

[31] S. Lefevre, A. Carvalho, Y. Gao, E. Tseng, and F. Borrelli, "Driver models for personalized driving assistance," *Vehicle System Dynamics*, vol. 53, 2015.

[32] B. Zhu, S. Yan, J. Zhao, and W. Deng, "Personalized Lane-Change Assistance System With Driver Behavior Identification," *IEEE Transactions on Vehicular Technology*, vol. 67, no. 11, pp. 10293–10306, 2018.

[33] J. Wang, L. Zhang, D. Zhang, and K. Li, "An adaptive longitudinal driving assistance system based on driver characteristics," *IEEE Transactions on Intelligent Transportation Systems*, vol. 14, no. 1, pp. 1–12, 2013.

[34] R. Dang, J. Wang, S. E. Li, and K. Li, "Coordinated Adaptive Cruise Control System With Lane-Change Assistance," *IEEE Transactions on Intelligent Transportation Systems*, vol. 16, no. 5, pp. 2373–2383, 2015.

[35] J. M. Fleming, C. K. Allison, X. Yan, R. Lot, and N. A. Stanton, "Adaptive driver modelling in adas to improve user acceptance: A study using naturalistic data," *Safety Science*, vol. 119, pp. 76–83, 2019.

[36] L. Saleh, P. Chevrel, F. Claveau, J. F. Lafay, and F. Mars, "Shared steering control between a driver and an automation: Stability in the presence of driver behavior uncertainty," *IEEE Transactions on Intelligent Transportation Systems*, vol. 14, no. 2, pp. 974–983, 2013.